

Oil & Natural Gas Technology

DOE Award No.: DE-FC26-06NT42877

Semiannual Progress Report

**HYDRATE RESEARCH ACTIVITIES THAT BOTH SUPPORT AND
DERIVE FROM THE MONITORING STATION/SEA-FLOOR
OBSERVATORY,
MISSISSIPPI CANYON 118, NORTHERN GULF OF MEXICO**

Submitted by:

CENTER FOR MARINE RESOURCES AND ENVIRONMENTAL TECHNOLOGY
111 BREVARD HALL, UNIVERSITY, MS 38677

Principal Author: Carol Lutken, PI

Prepared for:
United States Department of Energy
National Energy Technology Laboratory

March, 2011



Office of Fossil Energy

**HYDRATE RESEARCH ACTIVITIES THAT BOTH SUPPORT AND
DERIVE FROM THE MONITORING STATION/SEA-FLOOR
OBSERVATORY,
MISSISSIPPI CANYON 118, NORTHERN GULF OF MEXICO**

SEMIANNUAL PROGRESS REPORT
1 JULY, 2010 THROUGH 31 DECEMBER, 2010

PREPARED BY THE MANAGEMENT TEAM
Carol Blanton Lutken and Dianne R. Welch
CENTER FOR MARINE RESOURCES AND ENVIRONMENTAL TECHNOLOGY
111 BREVARD HALL, UNIVERSITY, MS 38677
(CONTACT: CAROL LUTKEN)

MARCH, 2011

DOE AWARD NUMBER DE-FC26-06NT42877

**FOLLOWING DOE AWARD NUMBERS
DE-FC26-00NT40920 and DE-FC26-02NT41628**

This report was prepared with the support of the United States Department of Energy, under award No. DE-FC26-06NT42877. However, any opinions, findings, conclusions, or recommendations expressed herein are those of the authors and do not necessarily reflect the views of the DOE. DOE Award Number DE-FC26-06NT42877 is managed by the U.S. Department of Energy's National Energy Technology Laboratory.

PHASE 1 Subcontractors and Tasks for FY 2006:

Paul Higley, Specialty Devices, Inc., 2905 Capital Street, Wylie, TX 75098

Task 1: Design and Construction of four Horizontal Line Arrays

Bob A. Hardage, Bureau of Economic Geology, John A. and Katherine G.

Jackson School of Geosciences, University of Texas at Austin, University Station, Box X, Austin, TX 78713

Task 2: Seismic Data Processing at the Gas Hydrate Sea-floor Observatory: MC118.

Jeffrey Chanton, Department of Oceanography, Florida State University, Tallahassee, FL 32306

Task 3: Coupling of Continuous Geochemical and Sea-floor Acoustic Measurements

Peter Gerstoft, Marine Physical Laboratory, University of California at San Diego, 9500 Gilman Drive, La Jolla, CA 92093

Task 4: Noise-Based Gas Hydrates Monitoring.

PHASE 2 Subcontractors and Tasks for FY 2008:

Camelia Knapp, Department of Geological Sciences, University of South Carolina 701 Sumter Street, Columbia, SC 29208.

TASK 2: Processing and Interpretation of TGS-NOPEC Industry Seismic Data and Integration with Existing Surface-Source/Deep-Receiver (SSDR) High Resolution Seismic Data at MC118, Gulf of Mexico.

Bob A. Hardage, Bureau of Economic Geology, John A. and Katherine G.

Jackson School of Geosciences, the University of Texas at Austin, University Station, Box X, Austin, TX 78713-8924.

TASK 3: Seismic Data Processing at the Gas Hydrate Sea-Floor Observatory: MC118.

Laura Lapham and Jeff Chanton, Department of Oceanography, Florida State University, Tallahassee, Florida, 32306-4320.

TASK 4: Geochemical investigations at MC 118: Pore fluid time series and gas hydrate stability.

John Noakes, Scott Noakes, and Chuanlun Zhang, The University of Georgia, Athens, Georgia, and Tim Short, SRI International, St. Petersburg, Florida.

TASK 5: Automated Biological/Chemical Monitoring System (ABCMS) for Offshore Oceanographic Carbon Dynamic Studies.

Rudy Rogers, Department of Chemical Engineering, Mississippi State University, PO Drawer 9595, Mississippi State, MS 39762.

TASK 6: Microbial techniques to extract carbon from stored hydrocarbon gases.

Ira Leifer, Marine Science Institute, University of California at Santa Barbara, Bldg. 2, Room 3357, Santa Barbara, CA 93103-5080.

TASK 7: Scoping study using Spatio-Temporal Measurement of Seep Emissions by Multibeam Sonar at MC118.

Paul Higley, Specialty Devices, Inc., 2905 Capital Street, Wylie, TX 75098
TASK 8: Validate high-frequency scatter on SDR data by acquisition of targeted cores and velocity profiles at MC118 Hydrate Mound.

Sabodh Garg, Science Applications International Corporation, 10260 Point Campus Drive, MS A-3, San Diego, CA 92121.

TASK 9: Recipient shall model carbonate/hydrate mound in Mississippi Canyon 118 using modified version of (THROBS).

PHASE 3 Subcontractors and Tasks for FY 2009:

Camelia Knapp and James H. Knapp, Department of Geological Sciences, University of South Carolina 701 Sumter Street, Columbia, SC 29208.

TASK 2: Geological and Geophysical Baseline Characterization of Gas Hydrates at MC118, Gulf of Mexico.

Bob A. Hardage, Bureau of Economic Geology, John A. and Katherine G. Jackson School of Geosciences, the University of Texas at Austin, University Station, Box X, Austin, TX 78713-8924.

TASK 3: Near seafloor geology at MC118 using converted shear-waves from 4C seafloor sensor data.

Laura Lapham and Jeff Chanton, Department of Oceanography, Florida State University, Tallahassee, Florida, 32306-4320.

TASK 4: Geochemical investigations at MC 118: Pore fluid time series and gas hydrate stability.

John Noakes, Scott Noakes, and Chuanlun Zhang, The University of Georgia, Athens, Georgia, and Tim Short, SRI International, St. Petersburg, Florida.

TASK 5: Automated Biological/Chemical Monitoring System (ABCMS) for Offshore Oceanographic Carbon Dynamic Studies.

Ira Leifer, Marine Science Institute, University of California at Santa Barbara, Bldg. 2, Room 3357, Santa Barbara, CA 93103-5080.

TASK 6: Quantification of Seep Emissions by Multibeam Sonar at MC118.

Sabodh Garg, Science Applications International Corporation, 10260 Point Campus Drive, MS A-3, San Diego, CA 92121.

TASK 7: Modeling a carbonate/hydrate mound in Mississippi Canyon 118 using modified version of (THROBS).

PHASE 4 Subcontractors and Tasks for FY 2010

Leonardo Macelloni, Carol Lutken and Ken Sleeper, Mississippi Mineral Resources Institute, University of Mississippi, University, MS, 38677.

TASK 2: Integration of Multiple Methods of Geological and Geophysical investigations to advance Shallow Subsurface Characterization at MC118.

Sabodh Garg, Science Applications International Corporation, 10260 Point
Campus Drive, MS A-3, San Diego, CA 92121.

TASK 3: Modeling a carbonate/hydrate mound in Mississippi Canyon 118
using modified version of (THROBS).

Laura Lapham and Jeff Chanton, Department of Oceanography, Florida State
University, Tallahassee, Florida, 32306-4320.

TASK 4: Geochemical investigations at MC 118: Pore fluid time series and
gas hydrate stability.

John Noakes, Scott Noakes, and Chuanlun Zhang, The University of Georgia,
Athens, Georgia, and Tim Short, SRI International, St. Petersburg, Florida.

TASK 5: Automated Biological/Chemical Monitoring System (ABCMS) for
Offshore Oceanographic Carbon Dynamic Studies.

Ira Leifer, Marine Science Institute, University of California at Santa Barbara,
Bldg. 2, Room 3357, Santa Barbara, CA 93103-5080.

TASK 6: Quantification of Seep Emissions by Multibeam Sonar at
MC118.

TABLE OF CONTENTS

PAGE

DISCLAIMER.....	ii
PHASE 1 Subcontractors and Tasks for FY 2006.....	iii
PHASE 2 Subcontractors and Tasks for FY 2008.....	iii
PHASE 3 Subcontractors and Tasks for FY 2009.....	iv
PHASE 4 Subcontractors and Tasks for FY 2010.....	iv
TABLE OF CONTENTS.....	vi
LIST OF GRAPHICAL MATERIALS.....	vi
INTRODUCTION.....	1
EXECUTIVE SUMMARY.....	1
EXPERIMENTAL/RESULTS AND DISCUSSION.....	11
PHASE 1.....	11
PHASE 2.....	15
PHASE 3.....	26
CONCLUSIONS.....	83
LIST OF ACRONYMS AND ABBREVIATIONS.....	83
COST STATUS.....	86
MILESTONE STATUS.....	94
ACCOMPLISHMENTS.....	96
PROBLEMS/DELAYS.....	96
PRODUCTS.....	97
REFERENCES.....	97
RECENT PUBLICATIONS BY CONSORTIUM MEMBERS.....	97

LIST OF GRAPHICAL MATERIALS

Figure 1. Location of Mississippi Canyon Block 118 in the Gulf of Mexico.....	2
Figure 2. Monitoring Station/Sea-floor Observatory seafloor hardware with funding sources.....	3
Figure 3. Bathymetry at MC118 as revealed in reprocessed multibeam data.....	4
Figure 4. The ROVARD. Left - being prepared for deployment. Note chimney, lower left, enclosing instruments; peepers lower right. Above, right - close-up of peepers, pore-fluid collecting devices, attached to the ROVARD. Lower right - ROVARD, with CSAs, on the seafloor at MC118.....	7
Figure 5. The Sleeping Dragon, above, is composed of outcropping gas hydrate as well as carbonate and supports ice worms, bacterial mat and other chemosynthetic organisms (center and bottom enlargements).....	9
Figure 6. Woolsey Mound with locations of instruments and additional landmarks currently on the seafloor: CSA ROVARD, PFA-1, PFA-2, GPA, IDP, POD, BBLA, sonar reflector, Markers 6, 7, 9, Noakesville, The Sleeping Dragon and documented outcropping gas hydrates.....	10
Figure 7. 3AM SSD Recovery - Dive 37 HLA POD and IDP Inspection Dive.....	12

Figure 8. HLA Deployment Attempt.....	13
Figure 9. Commercial kinetic inhibitors (Ohtake, 2005).....	19
Figure 10. Structure of peptidoglycan (Beveridge and Murray, 1980; Vollmeret al., 2008).....	20
Figure 11. Gas-hydrate inhibition by N-acetylglucosamine.....	21
Figure 12. CMP (red plus symbol) location map for WesternGeco 3D seismic volume stacking velocities with MC118 boundaries (blue dashed box): a) CMP locations of 3D seismic volume with stacking velocity profiles, b) the 22 InLine locations that coincide with the stacking velocity locations.....	28
Figure 13. WesternGeco 3D seismic stacked data vertical sections: a) In-Line: Rel-397; b) In-Line: Rel-497; c) In-Line: Rel-597; d) In-Line: Rel-597.....	29
Figure 14. WesternGeco 3D seismic stacked data, time slices: a) 1500 ms ; b) 2000 ms; c) 2500 ms; d) 3000 ms.....	30
Figure 15. Model runs, (a) compressional velocity with alpha equal to 0.8, (b) shear velocity with alpha equal to 0.2.....	34
Figure 16. Model configurations for gas hydrates in unconsolidated sediment, (a) pore-fluid model - gas hydrate homogeneously distributed throughout the pore space, (b) rock matrix model - gas hydrate is part of the rock matrix and contributes to its stiffness.....	35
Figure 17. Proposed jumbo piston core locations on shaded bathymetry of Woolsey Mound and surrounding area.....	37
Figure 18. Sites PC-1, PC-3, and PC-7: Left to right and top to bottom; a) bathymetry and transect location, b) SSSR north-south transect, c) SSSR east-west transect, d) close-up CHIRP transect.....	38
Figure 19. Sites PC-4 and PC-6: Left to right and top to bottom; a) bathymetry and transect location, b) SSSR east-west transect, c) SSSR north-south transect, d) close-up of CHIRP transect.....	39
Figure 20. Sites PC-2 and PC-8: Left to right and top to bottom; a) bathymetry and transect location, b) SSSR east-west transect, c) SSSR north-south transect, d) close-up of CHIRP transect.....	40
Figure 21. Comparison of (equilibrium pressure / temperature) relationship for a salt-free system with Structure II hydrate and with a feedgas composition of 96% CH₄, 3% C₂H₆ and 1% C₃H₈ (mole fractions), according to algebraic fits (red symbols) of Mann et al. (1989), and to the CSMHYD program (blue symbols) of Sloan (1998).....	49
Figure 22. Influence of feed-gas composition, brine salinity and temperature upon equilibrium pressure where three hydrocarbon-containing phases (gaseous, aqueous and solid hydrate) may coexist.....	52
Figure 23. Influence of feed-gas composition, brine salinity and temperature upon solid hydrate CH₄ content relative to other hydrocarbons.....	53
Figure 24. Influence of feed-gas composition, brine salinity and temperature upon solid hydrate C₃H₈ content relative to C₂H₆.....	54
Figure 25. Our group has clarified the distinction between hydrate dissociation and dissolution.....	65

Figure 26. Seafloor pictures of mini-PFAs. Both were deployed with ROV Doc Ricketts (MBARI) and retrieved with ROV ROPOS. A) Barkley Canyon and B) Bubbly Gulch.....67

Figure 27. Location of mini-PFAs offshore Vancouver Island. The stars indicate the two sites, Barkley Canyon and Bubbly Gulch.....68

Figure 28: Time-series data for two samplers within the mini-PFA deployed at Barkley Canyon. A) methane concentrations and stable isotopes 1cm from hydrate surface. B) sulfate and chloride concentrations 1cm from hydrate surface. C) methane concentrations and stable isotopes 3cm from hydrate surface. D) Sulfate and chloride concentrations 3cm from hydrate surface. Complete interpretation of data is pending.....69

Figure 29. Photo-comparison of “sleeping dragon” at MC 118 between 2006 (photo courtesy of GOMHRC and the Johnson SeaLink and 2010 (photo courtesy of Chuck Fisher and the Lophelia II cruise).....71

Figure 30. Results of Dissolution Experiments Comparing Dissolution Rates of StrI and StrII hydrates. In panel A are the results of two (replicated) experiments measuring the dissolution rate of methane (strI) hydrate in the lab. Panel B gives the results for strII (mixed-gas) hydrate. Dissolution of strI and strII hydrates over time are similar.....72

Figure 31. Effect of Oil on hydrate dissolution.....73

Figure 32. Filter assembly mounted on distilled water pumping station.....75

Figure 33. Lander assembly.....76

Figure 34. Photo of benthic lander.....78

TABLES:

TABLE 1. Refined Coordinate Locations for Jumbo Piston Core targets.....36

TABLE 2. CSMHYD results57

TABLE 3. Dissolution rates of natural and artificial hydrate.....73

INTRODUCTION / PROJECT SUMMARY

The Gulf of Mexico-Hydrate Research Consortium (GOM-HRC) is in its tenth year of developing a sea-floor station to monitor a mound where hydrates outcrop on the sea floor. The plan for the Monitoring Station/Sea Floor Observatory (MS/SFO) is that it be a multi-sensor station that provides more-or-less continuous monitoring of the near-seabed hydrocarbon system, within the hydrate stability zone (HSZ) of the northern Gulf of Mexico (GOM). The goal of the GOM-HRC is to oversee the development and emplacement of such a facility to provide a better understanding of this complex hydrocarbon system, particularly hydrate formation and dissociation, fluid venting to the water column, and associated microbial and/or chemosynthetic communities. Models developed from these studies should provide researchers with an improved understanding of gas hydrates and associated free gas as: 1) a geo-hazard to conventional deep oil and gas activities; 2) a future energy resource of considerable significance; and 3) a source of hydrocarbon gases, venting to the water column and eventually the atmosphere, with global climate implications.

Initial funding for the MS/SFO was received from the Department of Interior (DOI) Minerals Management Service (MMS, now the Bureau of Ocean Energy, Management, and Enforcement, BOEMRE) in FY1998. Funding from the Department of Energy (DOE) National Energy Technology Laboratory (NETL) began in FY2000 and from the Department of Commerce (DOC) National Oceanographic and Atmospheric Administration's National Undersea Research Program (NOAA-NURP) in 2002 via their National Institute for Undersea Science and Technology (NIUST). Some ten industries and fifteen universities, the United States Geological Survey (USGS), the US Navy, Naval Meteorology and Oceanography Command, Naval Research Laboratory (NRL) and NOAA's National Data Buoy Center are involved at various levels of participation. Funded investigations include a range of physical, chemical, and microbiological studies. Studies of the benthic fauna will be added in the next cycle of research studies.

EXECUTIVE SUMMARY

In 1999, a consortium was assembled for the purpose of consolidating both laboratory and field efforts of leaders in gas hydrates research in the Gulf of Mexico. The Consortium, established at and administered by the University of Mississippi's Center for Marine Resources and Environmental Technology (CMRET), has, as its primary objective, the design and emplacement of a remote monitoring station on the sea-floor in the northern Gulf of Mexico. The primary purpose of the station is to monitor activity in an area where gas hydrates are known to be present at, or just below, the sea-floor. In order to meet this goal, the Consortium has developed and assembled components for a station that will monitor physical and chemical parameters of the sea water, sea-floor sediments, and shallow subsea-floor sediments on a more-or-less continuous basis over an extended period of time. The study of chemosynthetic communities and their interactions with geologic processes is a component of the plan for the Observatory; results will provide an assessment of environmental health in the area of the station including the effects of deep sea activities on world atmosphere and, therefore, weather.

Central to the establishment of the Consortium is the need to coordinate activities, avoid redundancies and promote effective and efficient communication among researchers. Complementary expertise, both scientific and technical, has been assembled; collaborative research and coordinated research methods have grown out of the Consortium and design and construction of most instrumentation for the sea-floor station are essentially complete.

Following much scientific research, consideration and discussion, the Consortium selected Mississippi Canyon 118 (MC118) as the site of the MS/SFO. Criteria for selection included evidence of gas hydrates on the sea-floor, active venting and availability. MMS placed a research restriction on the unleased block so Observatory research might continue even if the block should subsequently be leased, as is now the case. CMRET regularly conducts research cruises to MC118 to enable investigations of the site and to test, deploy, and recover instruments/components of the SFO.

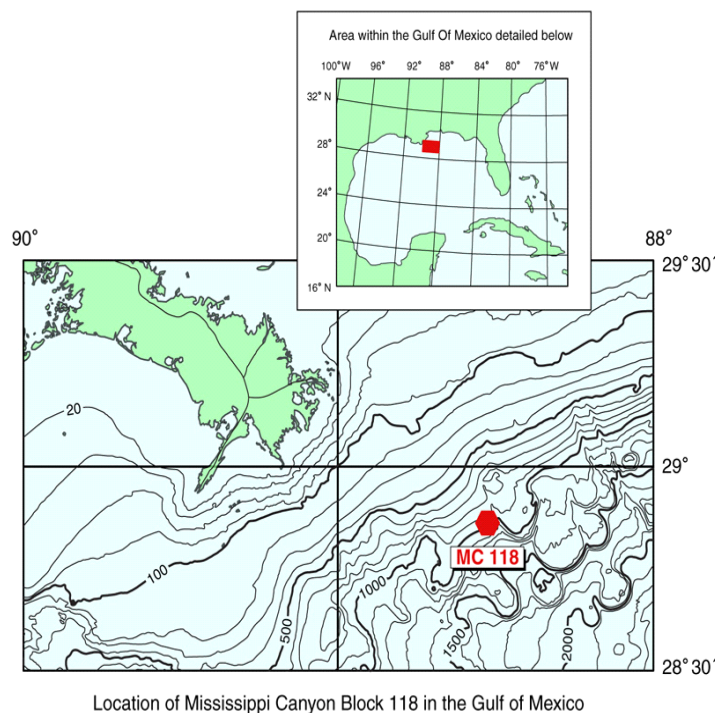


Figure 1. Location of Mississippi Canyon Block 118 in the Gulf of Mexico.

Initial components of the observatory were deployed at MC118 in May of 2005. In spite of a variety of delays, including the effects of several severe hurricanes, follow-up surveys and deployments, continue to take place.

The centerpiece of the observatory (Figure 2) is a series of vertical and horizontal line arrays of sensors (VLA, HLAs) designed to detect shifts in the hydrate stability zone (HSZ). The VLA is to be moored to the sea floor and extend approximately 200 meters into the water column. Sensors in the VLA include hydrophones to record water-borne acoustic energy (and measure sound speed in the lower water column), thermistors to measure water temperature, tilt meters to sense deviations from the vertical induced by water currents, and compasses to indicate the directions in which deviations occur. The

horizontal water-bottom arrays consist of hydrophones laid upon, and pressed into, the soft sediment of the sea-floor, and arranged into a cross with four 500m-long arms: two perpendicular arrays, the length of each approximating the water depth at the observatory site. This seismic array design will enable the use of natural surface noise (*via* hydrophone) and microseism noise from salt movement (*via* accelerometer). The goal is to use these passive seismic sources for long-term monitoring of structural and hydrocarbon fluid dynamics in a way analogous to conventional reservoir monitoring. The system will be incorporated into the SFO at the hydrate mound/salt dome complex at MC118, providing the capability of long-term, continuous seismic monitoring that is marine mammal friendly through the elimination of the traditional seismic energy source.

The sea-floor arrangement of arrays will be accomplished by means of the Station Service Device (SSD), the remotely operated vehicle (ROV) especially designed to service the Observatory. The SSD has been used to effect deployments and recoveries and will be used in array deployment to unspool cable and to make underwater connections. It is anticipated that accelerometers will be implanted in the vicinity of the HLAs in the future, making it possible to image the HSZ to greater depths and to see interstitial space occupied by gas (shown by hydrophone data and which does not travel through gas). The MMS-funded sled will be used as a seismic source of compressional and shear waves for calibrating the accelerometers.

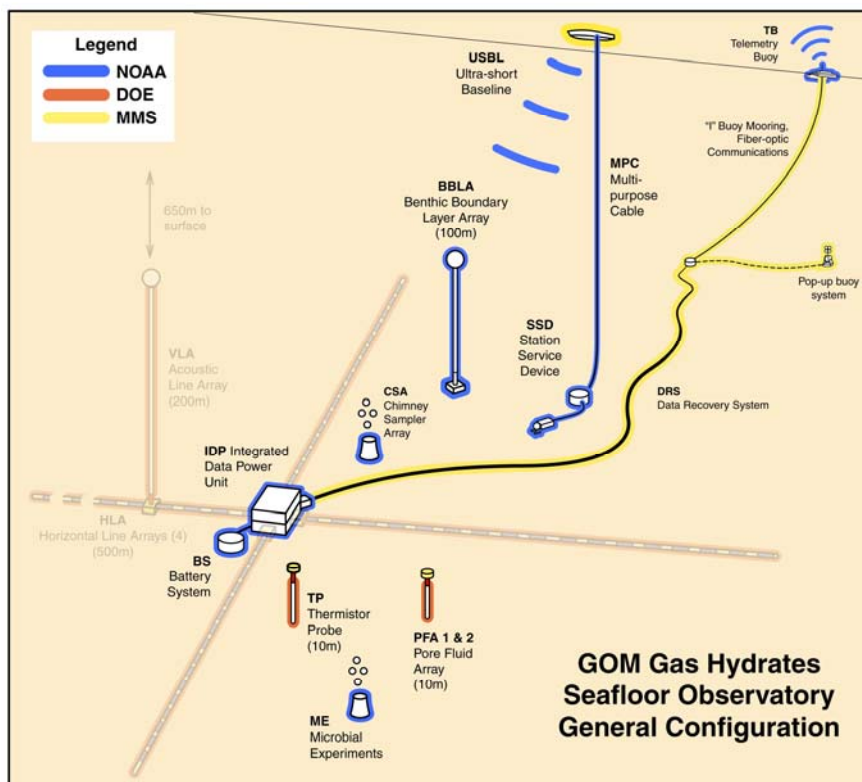


Figure 2. Monitoring Station/Sea-floor Observatory hardware with funding sources. Components already deployed are highlighted. The Vertical Line Array, Benthic Boundary Layer Array, Chimney Sampler Array and additional experiments have been deployed to collect data in test mode, recovered, data analyzed and adjustments made in preparation for permanent deployment.

The MMS-funded Sea-Floor Probe (SFP) has been used several times to retrieve core samples from MC118. These samples are used in the effort to select sites appropriate for deployment of microbial experiments and thermistor and geochemical probes. Images recovered during a C&C Technologies autonomous underwater vehicle (AUV) survey in 2005, have been reprocessed and the results (Figure 3) used in analyses and selection of sites for further study. The NIUST AUV, *Eagle Ray*, has been used to resurvey MC118 (multibeam) and the photomosaic-capable AUV, *Mola Mola*, is scheduled to survey the site in 2011.

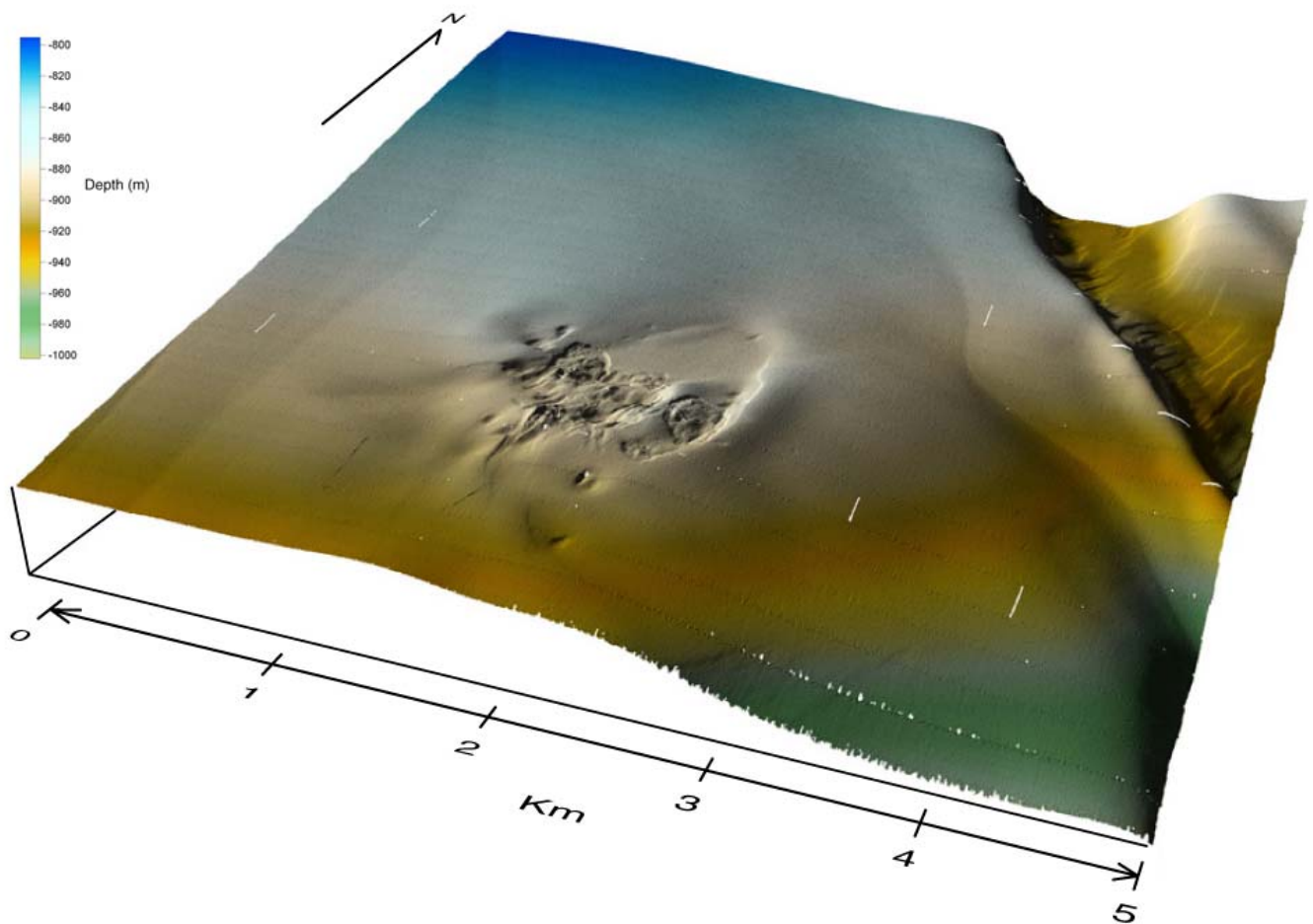


Figure 3. Bathymetry at MC118 as revealed in reprocessed multibeam data. The mound complex includes three crater complexes: a northwestern complex, a southwestern complex and a southeastern complex.

A complete surface-source/deep-receiver (SSDR) survey of the mound at MC118 has been made. The resultant 109 profiles of very high resolution seismic data have undergone processing to create a 3-D model of the mound, including the application of Empirical Mode Decomposition described by Battista et al. (2007).

Experiments designed to assess water-column geochemistry, microbial communities and activities, hydrate host materials, and composition of pore-fluids have been designed, built and tests run at MC118. Sediments collected from Mississippi Canyon have been studied for effects of parameters possibly involved in hydrate formation. Laboratory analyses show that smectite clays promote hydrate formation when basic platelets slough off the clay mass. These small platelets act as nuclei for hydrate formation. Experiments show an increasing importance of microbial activities surrounding active vents in promoting the formation and stability of seafloor gas hydrates. Most recently (see Phase 2, Task 6, below) experimental analyses of MC118 microbial consortia have shown the intriguing finding that *microbial cell wall material inhibits hydrate formation*, a necessary occurrence for the bacterial cell's survival, as it prevents hydrate formation-heats from being liberated directly onto cell surfaces. Microbes inhibit hydrate formation, thus enhancing their ability to survive the extreme conditions of the deep sea HSZ.

Seismic data-processing software has been developed at Exploration Geophysics Laboratory (EGL) of the Texas Bureau of Economic Geology (BEG) that is structured to optimize P-P and P-SV image resolution in the immediate vicinity of 4C seafloor-based seismic sensors. Acquiring shear data from the vicinity of Woolsey Mound comprises the subject of a revision in the statement of work for the CMRET and Consortium. Since the CGGVeritas nodes have never materialized (in 2 years), a decision was made, by mutual consent, to terminate the FY09 subcontract to the BEG. The ocean bottom seismometers and capability to collect the 4C data exist at Woods Hole Oceanographic Institution and we are pursuing a replacement subcontract with them that should result in the acquisition of suitable data for the BEG to process and analyze. The 4C experiment designed to test this software and to enhance what is known of the shear characteristics of the subseafloor at MC118 is scheduled to take place on a CMRET March-April cruise to MC118.

Interpretation of the MC118 TGS 3D seismic volume provides evidence of successive temporal movement on a series of at least three main faults genetically related to an underlying salt body. The subsurface structural, stratigraphic, thermal, and fluid flow architecture of MC118, like that of many regions in the Gulf of Mexico, is dominated by the presence of salt. The hydrate mound system at MC118 is situated above one of two major salt bodies beneath the block, and appears to have evolved in close association with the crestal fault system developed above and around a dome-shaped salt body. From the 3D seismic volume, some of the preliminary observations provide evidence that (1) the salt moves upward as it is loaded by sediments, (2) major faults nucleate off of the salt body, (3) the salt flank and the associated faults provide vertical migration pathways for deep basin fluids, and (4) the crestal structure is dominated by a radiating system of arcuate faults.

Preliminary conclusions of this work are that the gas hydrate system at MC118 appears to be controlled by the presence of two temporally and kinematically distinct salt bodies present in the subsurface; the salt-related fault systems provide likely migration pathways for the thermogenic hydrocarbons; locations, orientations, and geometries of crestal faults developed above the salt bodies appear to correlate with the surface structural and microbial activities as well as with the gas hydrate mounds observed on the seafloor.

Current site characterization efforts center about evaluating the TGS dataset to make quantitative estimates of the lithologic influence on gas hydrate seismic response by implementing recently developed rock physics models for saturated gas hydrates. Modeled results for seismic velocities as a function of gas hydrate saturation are followed by computation of seismic velocities as a function of depth for synthetic porosity profiles. Models for seismic velocities as a function of free gas volumetric fraction are also made.

A new 12 second seismic dataset has been acquired from Western Geco and, following analyses will provide a time dimension to the subsurface analyses of the block. Integration of these industry data sets with the high resolution SDR and chirp is providing amazing insights into the shallow subsurface geology and structure as well as the seafloor at MC118. This information is critically important to the site-selection processes for the Jumbo Piston and heat-flow cruises, to be conducted in 2011.

Time-series geochemical experiments at MC118 have been seriously impacted by the failure of the SSD to recover the Seafloor Probe (SFP) boxes. However, alternative-site experiments and laboratory analyses have produced new information on the formation and dissolution rates – and controls on these rates – of gas hydrates. Additional geochemical instruments have been acquired or constructed and are enabling Consortium researchers to add to the ever-growing store of chemical data relating to Woolsey Mound.

Although not prescribed in this contract, changes in geochemistry and water chemistry related to the catastrophic oil spill at MC252 are being included in monitoring at the Observatory site. With obvious – and not-so-obvious – impact possibilities on our work, we feel obliged to do our own monitoring of these parameters at MC118. Results appear in the subcontractors' reports but they agree that hydrocarbon plumes did exist at depth, where we have not detected them in the past. However, September follow-up monitoring indicates that they have dissipated. Rather, oil-rich bottom-cover was seen on several dives of the SSD and testing of samples recovered via the SSD push-coring capabilities are being evaluated/fingerprinted to determine the source of the hydrocarbons.

The marine lander survey system was not deployed this year and although the sonar rotator was taken to sea, failure of the pressure housing prevented its being deployed. FY09 improvements have been completed on the former and a pressure test scheduled for late January. It is scheduled for an August/October deployment with the SRI mass spectrometer, the same instrument used with great success to detect the methane plumes deriving from the Deep Water Horizon spill.

Work on the model of hydrate stability at MC118 has progressed to the point that the equation of state has been used in simulated runs. The Equation of State has been developed to include the multigas hydrates present as well as their phase behaviors under conditions prevailing at MC118. This includes developing constitutive relations for the gaseous phase for ethane and propane, with profoundly different saturation pressures form methane, indirectly.

Two cruises were conducted by the GOM-HRC this fall. A September cruise to MC118 was executed to attempt to deploy an HLA using the SSD, deploy the Chimney Sampler Array (CSA) via the new ROVARD lander at a site where bacterial mat is thriving, make CTD casts and collect sediment and water samples from MC118 and

from nearer MC252, and begin the photosurvey of the site using the NIUST AUV *Mola Mola*. Just two weeks later, a follow-up cruise that was to have included additional HLA deployments, lander surveying, collection of additional samples and the redeployment of the Benthic Boundary Layer (oceanographic) Array (BBLA) was completed. During the first cruise, dives of the SSD succeeded in surveying most of the fault scarp that defines the northern boundary of the northwest crater complex at Woolsey Mound and in identifying several new habitats. We were successful in locating mat suitable for the deployment of the CSA, and in locating the Pore-fluid Array (PFA) -2 for the first time and verifying it to be in a nearly vertical orientation and with a fully penetrated probe. Push-cores were collected to get additional information from the site of the PFA and close to the CSA.

SSD communications were lost but deployment of the CSA was not hindered as the MMRI/CMRET/STRC-developed ROV Assisted Recovery Device or ROVARD (Figure 4) was employed for the mission. Pore-fluid peepers were added to the payload and all were deployed successfully, as verified on the subsequent cruise with the repaired and fully-functioning SSD. The remainder of the first cruise was devoted to *Mola* tests and CTD casts and water-sampling.

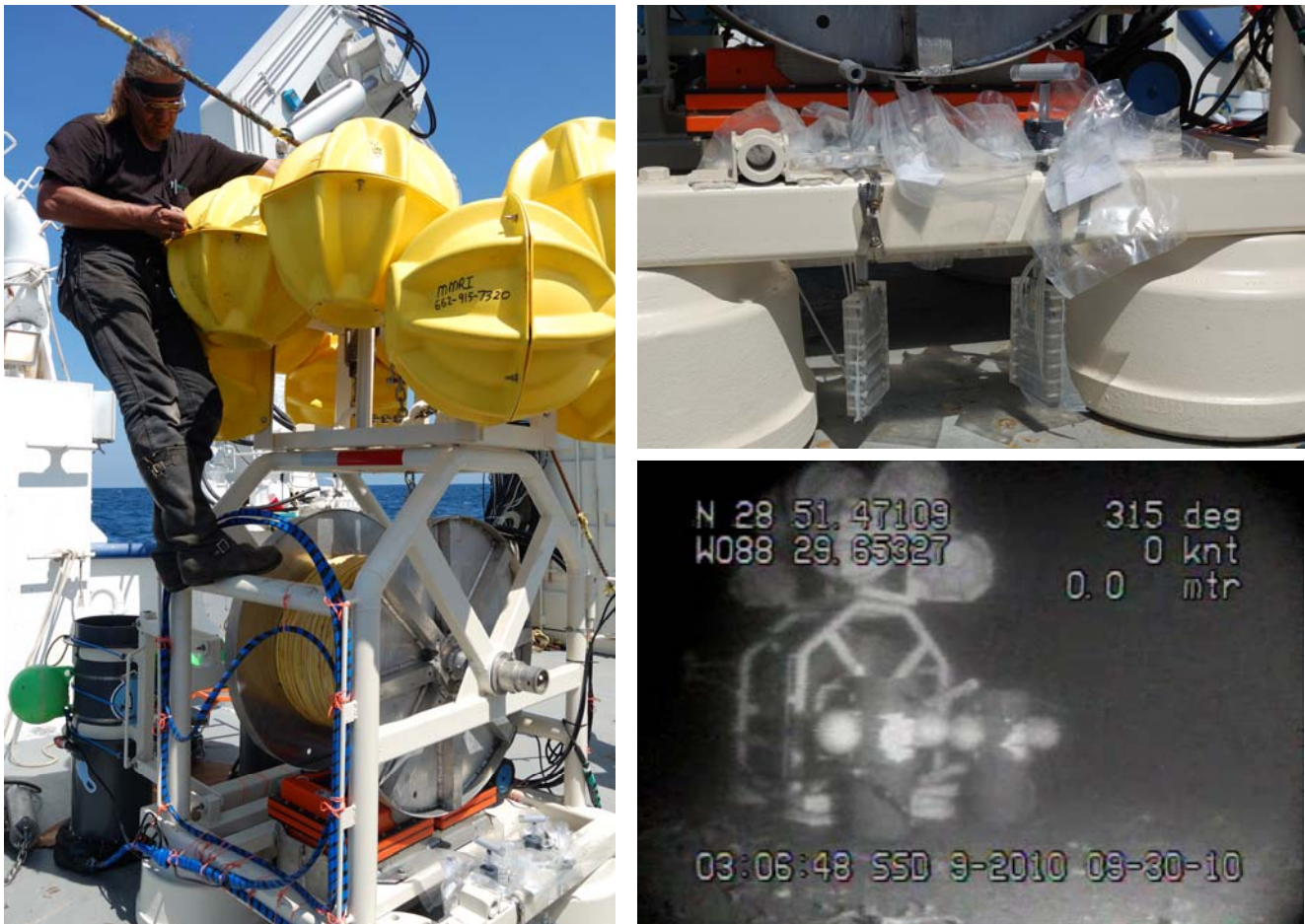


Figure 4. The ROVARD. Left - being prepared for deployment. Note chimney, lower left, enclosing instruments; peepers lower right. Above, right - close-up of peepers, pore-fluid collecting devices, attached to the ROVARD. Lower right - ROVARD, with CSAs, on the seafloor at MC118.

The CTD was enhanced with the Gandhi sensor package, a CTD package intended for real-time chemical surveys on the ROV that includes several additional sensors, most notably a METS methane sensor. A series of seacasts was completed at a location where methane plumes were detected during the June cruise. Although no indication of the existence of the plumes was detected during this cruise, water samples were retained for follow up, chemical and microbial, laboratory analysis. On the second trip, rough seas resulted in the SSD bracket being damaged and dropping the array. As the array was tethered to the SSD it was recovered but the damage to the bracket could not be repaired on the cruise so any further attempts to deploy arrays were abandoned. We were, however, successful at locating the ROVARD (Figure 4) with the SSD and used the SSD to remove and place one of the chimneys over mat. The pore-fluid Peepers, which were also deployed on the ROVARD, were observed to have been properly installed to the correct depth below the surface. The Benthic Boundary Layer Array was successfully deployed for its second multi-month deployment. A Contros sensor was added to the array for direct methane measurements to augment the Aquatrack, CDOM, and Chyl-a fluorometers and the CTD, O₂ and ORP/pH sensors. Additional tasks of the cruise included using multi-beam sonar systems to detect bubbles in the benthic zone. The Reson multi-beam system worked well (as a fish finder) but was not powerful enough to reach the bottom and issues with the pressure vessel for the seafloor founded Delta-T prevented the deployment of this instrument.

The new launch and recovery technique for the SSD – replacing the midwater weight (anchor) with weights attached to the cable – worked flawlessly on both cruises.

Still struggling to determine the cause of the communications failures in the SSD, we returned to Oxford with the vehicle and contracted an outside consultant (December) who discovered a faulty motor in the Hydrolek manipulator arm. With Hydrolek, we are determined to have a solution by the next SSD cruise.

In October, Visiting Scholar Michela Ingrassia participated in a Jason-2 cruise as the guest of PI, Chuck Fisher. Since the purpose of the cruise was to document damage to the benthic fauna in the vicinity of the Macondo oil spill, Michela was able to make significant contributions with her expertise in marine biology. Michela will study with Dr. Fisher at Penn State University during the spring semester and further the characterization of the benthos at Woolsey Mound. Figure 5 depicts the Sleeping Dragon, as it appeared in October, 2010.

An updated location map with bathymetry and instrument and landmark locations appears as Figure 6. An updated publications list accompanies this report but of particular significance is the recognition the Consortium received from the Gulf Coast Association of Geological Societies, GCAGS, for the Macelloni, et al paper, *Spatial distribution of seafloor bio-geological and geochemical processes as proxy to evaluate fluid-flux regime and time evolution of a complex carbonate/hydrates mound, northern Gulf of Mexico* that was chosen to receive the Second Place GCSSEPM / GCAGS Grover E. Murray Best Published Paper Award as one of the most outstanding papers published in this year's *GCAGS Transactions*.



Figure 5. The *Sleeping Dragon*, above, is composed of outcropping gas hydrate as well as carbonate and supports ice worms, bacterial mat and other chemosynthetic organisms (center and bottom enlargements). Images courtesy of Chuck Fisher and the *Lophelia* II cruise, co-funded by BOEMRE and NOAA.

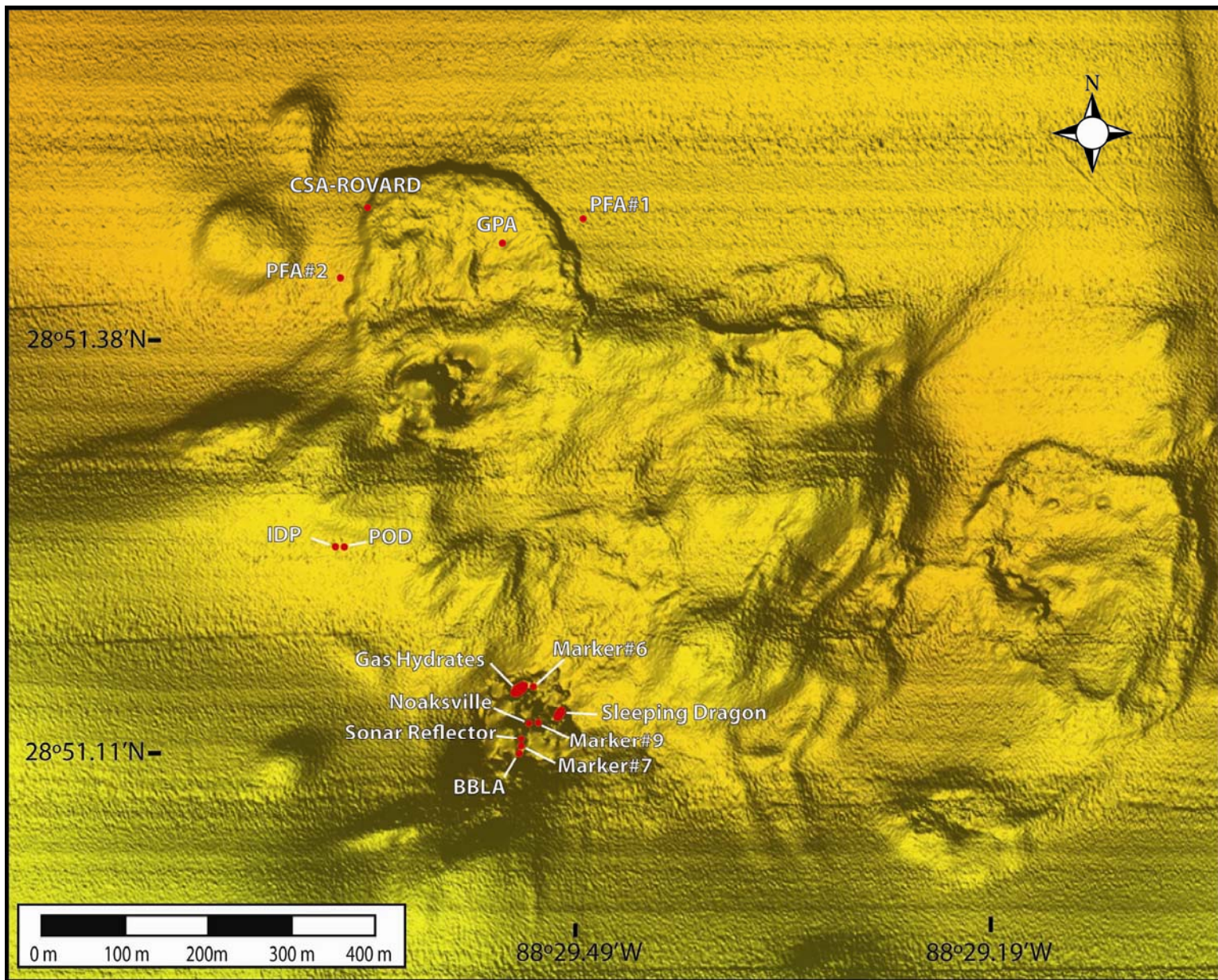


Figure 6. Woolsey Mound with locations of instruments and additional landmarks currently on the seafloor: CSA ROVARD, PFA-1, PFA-2, GPA, IDP, POD, BBLA, sonar reflector, Markers 6, 7, 9, Noakesville, The Sleeping Dragon and documented outcropping gas hydrates.

EXPERIMENTAL/ RESULTS AND DISCUSSION

PHASE 1 Tasks for FY 2006:

Task 1: Design and Construction of four Horizontal Line Arrays

Introduction

The Horizontal Line Array (HLA) design evolved with a change replacing the two arrays of 4C sensor packages to four longer all hydrophone arrays. New cable designs were developed to meet these program needs. During the last period a deployment technique was developed and all components of the deployment technique were successfully tested. This reporting period has seen an HLA array cable deployment attempt at MC118 which was defeated by weather conditions.

Background

The Horizontal Line Array (HLA) design was contracted in April 2007 with the plan to build two horizontal 4C arrays utilizing technology developed for these 4C sensors during the Borehole Line (BLA) development project. The project plan for the Horizontal Line Arrays included building 2 arrays of 4C sensors, each 400 meters long. This plan was modified to include more than 2,000 meters of arrays in the form of four all hydrophone arrays arranged as an "X" pattern of 500 meters per leg.

In addition to building these arrays, efforts have continued to develop a method to deploy these arrays. The planned deployment method has evolved based on available installation vehicles. The deployment plan for the HLAs originally was planned using a sled but has evolved into the use of the Sea Floor Observatory's SSD ROV. The preliminary concept for the deployment had all of these arrays simultaneously deployed on a HLA POD. The connections were to be made between the arrays and the Sea Floor Observatory's master data-logger, the Integrated Data Power unit (IDP) using the SSD. This plan evolved into deployment of the arrays one at a time using the SSD to carry the arrays to the sea floor. The previously planned SDI- built HLA "POD" was modified to accommodate the one at a time approach and several other devices designed to aid in this installation method.

The last reporting period included the successful testing of all parts of this deployment technique including the connection of the arrays to the central HLA POD using the SSD ROV. Also tested were the ROV mateable underwater connectors developed for the Sea Floor Observatory IDP.

Activities during this period

Two closely timed cruises occurred in September 2010. The later cruise included an inspection dive (Figure 7) to verify the location and condition of the previously deployed IDP and HLA POD assemblies at MC118. With all sea floor equipment in good condition and the operation status of the IDP checked via acoustic modem, the 1st HLA array to be deployed was assembled on the SSD ROV. Along with the HLA array, the HLA DATS "transporter", the HLA DATS, and the interconnect for the IDP were installed on

the SSD.

The deployment configuration (Figure 8) has the HLA array wound on a deployment spool which is mounted on the back of the SSD deployment cage. The array cable extends to the front of the SSD deployment cage and terminates at the HLA DATS which is mounted in its “transport” This transport carries both the DATS and the interconnect cable and connector to interface the DATS to the IDP. A set of syntactic floats on the “transporter” makes the weight in water nearly neutral.

Due to the large size of the HLA array spool and associated equipment the weather conditions need to be good to allow deployment. When the HLA array cable and its deployment spool are mounted on the back of SSD and the complete assembly is submerged, the total weight and entrained mass of the water within the array and the SSD make the assembly susceptible to rough sea conditions.

The weather did not cooperate and the dive was delayed. With the available cruise time running out, an attempt was made in less than ideal conditions. When the SSD and its HLA equipment entered the water, the boat heaved in response to a large wave. The heave was sufficient to cause the lifting line to the SSD to become slack. With the reversal of the heave the lifting line went taut and the resulting shock load was severe. This was repeated through a few ship heave cycles and the result was a fracture in the HLA Spool mounts on the SSD cage. The array pulled out of this mount and was suspended below the SSD cage as if ready to be laid on the sea floor. Unfortunately this was premature and the deployment could not be continued in this manner. The weather conditions did not improve to an acceptable level during the remainder of the cruise. The deployment of these arrays was reserved to better weather in the spring of 2011. Alternates for the array mounts will be investigated to extend the acceptable weather conditions.



Figure 7. 3AM SSD Recovery - Dive 37 HLA POD and IDP Inspection Dive

Summary

With acceptable weather conditions, the HLA arrays and the deployment equipment is ready to be deployed. An attempt will be made to extend the conditions under which the arrays can be deployed.



Figure 8. HLA Deployment Attempt

Task 2: Seismic Data Processing at the Gas Hydrate Sea-floor Observatory: MC118.

This task has been completed: software has been written, tested on data from another hydrates location and awaits data from the MS/SFO.

Task 3: Coupling of Continuous Geochemical and Sea-floor Acoustic Measurements

Phase 1 of this project is complete but the project continues under Phases 2, 3 and 4.

Task 4: Noise-Based Gas Hydrates Monitoring.

Abstract

Monitoring of gas hydrates at Mississippi Canyon 118 is possible using ambient noise as a sound source. The goal is to attempt to apply passive methods to supply information similar to that supplied by active sources, but on a continuous basis, as passive sources, such as wave-noise, are ever-present at MC118.

Introduction

By using ambient noise-based methods with dense networks, passive monitoring of gas hydrates is possible. Making use of ambient-noise cross correlation function of diffuse fields between two receivers, information can be recovered that is similar to that recovered using an active source.

Executive summary

In the second half of 2010, we have focused on analyzing array data from the East Pacific Rise. We have five papers published on this analysis in the Journal of Society of America and Geophysical Research Letters.

Hurricane monitoring

We have a paper [Zhang et al 2010] showing how we can monitor storms in the Pacific using seismics: Nonlinear wave-wave interactions generate double-frequency (DF) microseisms, which include both surface waves (mainly Rayleigh-type) and compressional (P) waves. Although it is unclear whether DF surface waves generated in deep oceans are observed on land, we show that DF P waves generated under Super Typhoon Ioke far offshore are detected by beamforming of land-based seismic array data, allowing tropical cyclones to be well-tracked seismologically. Two distinct spectral bands associated with different microseismic P -wave source locations are observed. The short-period DF band (0.16–0.35 Hz) is dominated by P waves generated in the deep ocean by local wind seas near the storm. In contrast, P waves in the long-period DF band (0.1–0.15 Hz) are weaker and generated closer to the coast of Japan from swell interactions. The accurate identification of DF P -wave microseism source areas is necessary to image Earth structure using ambient noise.

Noise cross correlation

In the second half of 2010, we have focused on noise processing of ambient noise in the East Pacific Rise (see AGU abstract). Noise cross-correlation has been used to recover surface wave Green's functions between receivers. However, most noise cross-correlation studies are restricted to land seismic stations and few studies have observed higher-mode surface waves. We apply noise cross-correlation on three-component broadband data recorded by 30 ocean bottom seismometers (OBSs) around the Gofar/Discovery/Quebrada transform faults on the Eastern Pacific Rise. On the vertical component, the cross-correlation functions (CFs) reveal clear Rayleigh wave

propagation between each station pair for both the fundamental mode in the 2-30s period band and the first-higher mode in the 2-10 s band. However, on the radial component CFs, the first-higher mode Rayleigh waves dominate within 2-10s band and the fundamental mode Rayleigh waves appear mainly in 10-20s band. On the transverse component CFs, Love waves are observed within 2-10s band. The directionality of CFs is different for the fundamental mode and the first higher-mode surface waves, and is also frequency dependent. This infers different mechanisms for each mode, probably due to ocean wave activities and ocean bottom scattering. The dispersion characteristics of the vertical component CFs are analyzed using the time-frequency analysis for group velocities and a time-variable filter technique for phase velocities. We obtain inter-station dispersion curves within 2-30s period for the fundamental mode and within 2-8s period for the first higher-mode. These dispersion curves are averaged over station pairs and used to invert for the 1-D shear wavespeed structure in the crust and uppermost mantle in the study region. The obtained 1-D velocity model shows very low shear wavespeed in the uppermost mantle (4.25 and 4.0 km/s within 10-25 km and 25-45 km depth ranges, respectively), consistent with the local geology with hot upper mantle material upwelling to the surface through the ridges of the Eastern Pacific Rise.

Abstract

H Yao, P Gouedard, P Gerstoft, J McGuire, J A Collins, R van der Hilst, Analysis of fundamental and higher mode surface waves from noise correlation near Eastern Pacific Rise, AGU fall meeting 2010.

Conclusions

Several papers demonstrate the utility of passive monitoring. The analysis shows promise of providing a true monitoring capability at MC118.

PHASE 2 Tasks for FY 2008:

TASK 1: Project Management Plan

This task is complete.

TASK 2: Processing and Interpretation of TGS-NOPEC Industry Seismic Data and Integration with Existing Surface-Source/Deep-Receiver (SSDR) High Resolution Seismic Data at MC118, Gulf of Mexico.

This task includes processing and interpreting industry seismic data collected and provided by TGS-NOPEC, Inc. Geophysical Company and integrating them with existing Surface-source/ Deep-receiver (SSDR) high resolution seismic data at from Mississippi Canyon Block 118, Gulf of Mexico (GOM), in order to image and understand the complex geologic structures at the Observatory site and how they relate to gas

hydrate formation and dissociation. This work has been focused on the (1) refinement of the structural interpretation of the TGS-NOPEC seismic data, (2) interpretation and mapping of the high-amplitude reflectors identified as possible bottom simulating reflectors (BSRs), (3) integration of this dataset with the high-resolution SDR single-channel seismic data, (4) preparation and submission of a proposal to the Integrated Ocean Drilling Program (IODP), and (5) initiation of a thorough analysis of the rock physics properties of the inferred gas hydrates at the study site.

The characterization of the subsurface geology – particularly the structure of the carbonate-hydrate mound and how it relates to and impacts hydrate formation and dissociation – has been essentially completed. Integration of the data from the nearby ARCO-1 deep well was a major accomplishment of this phase. The proposal submitted to the IODP supports this effort and has progressed to the full proposal stage but is not expected to develop into a project until 2013, at the earliest. The proposal is to drill borehole(s) to define the subsurface geology at MC118 and to provide the ability to monitor the subsurface at the site, continuously, into the future.

To date, findings of this effort support the inferences that the structure, stratigraphy and thermal and fluid-flow architecture at MC118 are dominated by salt structures, the mound having evolved in association with a crestal fault system that formed over a domed salt body. Depth conversions have been performed and horizons on TGS records correlated with picked horizons in the ARCO-1 well. AVO analysis was performed on one of the TGS inlines. The results included the identification of an interpreted accumulation of free gas beneath the base of gas hydrates. A request for an additional seismic line in raw form – one that crosses the middle of the mound - was made to substantiate this find and to determine how wide-spread the reflector might be. TGS agreed to provide the line.

USC researchers began deriving an impedance volume from the TGS seismic data to be used in porosity calculations and in calculations of gas hydrate saturations.

In their request for continued funding for this project, USC has included funds to purchase an additional, deeper, 3-D dataset from WesternGeco. Accomplishments of this phase are summarized in the Phase 3 sections.

TASK 3: Seismic Data Processing at the Gas Hydrate Sea-Floor Observatory: MC118.

Since no 4-C data have been acquired, no work has been done on this subcontract. Negotiations with Woods Hole Oceanographic Institution (WHOI) are in progress for use of their 4C nodes to collect the data for completion of this task.

TASK 4: Geochemical investigations at MC 118: Pore fluid time series and gas hydrate stability.

Additional instruments have been built and some deployed. Accomplishments of this task are covered in depth in the Phase 4 reports.

TASK 5: Automated Biological/Chemical Monitoring System (ABCMS) for Offshore Oceanographic Carbon Dynamic Studies.

The University of Georgia (UGA) and SRI International (SRI) research team have developed a unique survey instrument capable of surveying the methane rich seafloor and collecting biomass and suspended sediment samples on demand. This project is extended into Phase 4 and progress is covered more fully in that section of this report.

TASK 6: Microbial techniques to extract carbon from stored hydrocarbon gases: Exploring Extent of Microbial Involvement in Seafloor Hydrate Formations/Decompositions and Establishing that Mechanism

ABSTRACT

In the early phase of this research, Task #4 was addressed: Establish the influence of indigenous microbes on the mechanisms and kinetics of seafloor hydrate formations and dissociations. During the project, analyses of many sediments have shown that proliferate microbial activities around MC-118 hydrates play an important part in the nucleation, accumulation, and dissociation of near-surface hydrates. The reader is referred to our refereed journal articles, technical conference presentations, and dissertation/theses derived from the work—in many cases the initial discoveries in the topic.

This report pursues the second goal (Task #6): Utilize microbial techniques to extract carbon from stored hydrocarbon gases—i.e., to assist in the production of the occluded hydrocarbon gases.

We present the intriguing finding that microbial cell wall material inhibits hydrate formation—a necessary occurrence for the bacterial cell's survival, as it prevents hydrate formation—heats from being liberated directly onto cell surfaces. We find the hydrate inhibitor to be peptidoglycan, a chemical common in microbial cell walls. Our work is the first to report hydrate inhibition by bacterial cell wall material. Data were gathered showing this water-insoluble peptidoglycan polymeric compound, to be increasingly effective as an inhibitor by increasing its surface area through cell lysing.

A smaller, water-soluble, molecular component of the peptidoglycan polymer was tested and shown to retain hydrate-inhibiting properties. In tests comparing with a methanol standard, this water-soluble, glycan strand performed better in delaying gas hydrate formation (i.e., longer induction times) than similar amounts of methanol.

INTRODUCTION

Background of Hydrate Inhibitors

The inaugural natural-gas pipeline from Texas to Chicago was constructed in 1931 (Zigenhain, 1931). During its first winter of gas transport, the 24-inch diameter line immediately became clogged with an icelike material while operating at about 600 psi and 40 °F (Hammerschmidt, 1934). For roughly 50 years thereafter the main thrust, if not practically the only thrust, of gas hydrate research was directed toward preventing gas hydrates from forming in pressurized hydrocarbon lines. Methanol and glycol were

found to inhibit hydrates by shifting the thermodynamic properties of formation. Consequently, methanol injection became a standard for hydrate prevention in subsea production lines in the oilfield. For example, by 1996 some \$500 million of methanol was being injected per year (Lederhos et al., 1996). As offshore wells are drilled in increasingly deeper waters, the need for hydrate inhibition becomes more pressing, requiring methanol to the extent of 10-50% of the water content in production streams (Kelland et al., 2006; Xiao et al., 2009).

In addition to the thermodynamic inhibitors of methanol or ethylene glycol, synthetic inhibitors have been developed in recent years—namely, kinetic inhibitors and anti-agglomerates. Instead of altering the thermodynamic conditions of hydrate formation in the solution, the synthetic inhibitors increase the time for hydrates to form or cause the hydrate crystals to form along polymeric molecules at specific sites and thus delay catastrophic hydrate agglomeration for a period beyond pipeline residence time. Some of these synthetic inhibitors are effective and have been commercially used sparingly. The synthetic inhibitors are expensive.

Besides thermodynamic, kinetic, and anti-agglomerate inhibitors, other approaches have been made to the hydrate inhibition problem. Anti-freezing proteins in flounder and arctic fish, perennial rye grass, and insects have been evaluated with some success as hydrate inhibitors (Barrett, 2001; Chao et al., 1997; Gilbert et al., 2005; Gordienko et al., 2010; Gordon et al., 1962; Ramsey, 1964; Tyshenko et al., 1997; Zhang et al., 2004).

The deciding factor in using any inhibitor is cost. Therefore, methanol injection remains the primary means of inhibiting gas-hydrate formation in offshore oil and gas production, although cheaper and environmentally-friendly alternatives are still sought.

Potential Role of Inhibitors in Producing Gas from Hydrates

Future gas-hydrate research must develop a viable production technique. Seemingly insurmountable problems were overcome in developing other production methods for non-conventional natural gas (coalbed methane, shale gas, tight formations). Based on these experiences, there should be optimism that the complex problems to produce hydrate gas can be surmounted. For example, depressurization is the current favored approach (Konno et al., 2010; Mordis and Reagan, 2007; Rutqvist et al., 2009), but depressurization alone has serious limitations such as subsidence/formation-instability, incomplete production of gas from the hydrates, and ice or hydrate reforming near the wellbore. The latter fault may be a universal fault to be overcome with any hydrate-production technique.

A suitable inhibitor could possibly fit into hydrate production, either as a stand-alone process to decompose hydrates or as a process complement to prevent hydrates from reforming near the wellbore. Regardless, an inhibitor will be necessary in transporting produced gas to onshore.

Therefore, an 'ideal' hydrate inhibitor might be envisioned that has the following properties: (1) As effective as methanol, although not necessarily via the same mechanism, (2) Low cost in large quantities, and (3) Environmentally compatible, i.e., naturally occurring in the environment and biodegradable.

RESULTS AND DISCUSSION

The chemical structures of four Kinetic Inhibitors that other researchers have synthesized, tested and made commercially available (Ohtake, 2005) are presented in Figure 9. Most Kinetic Inhibitors are polymer-based (Xiao, 2009) and, in general, perform by two mechanisms: slowing crystal nucleation by lengthening induction time and/or retarding formation rate after critical cluster size is reached.

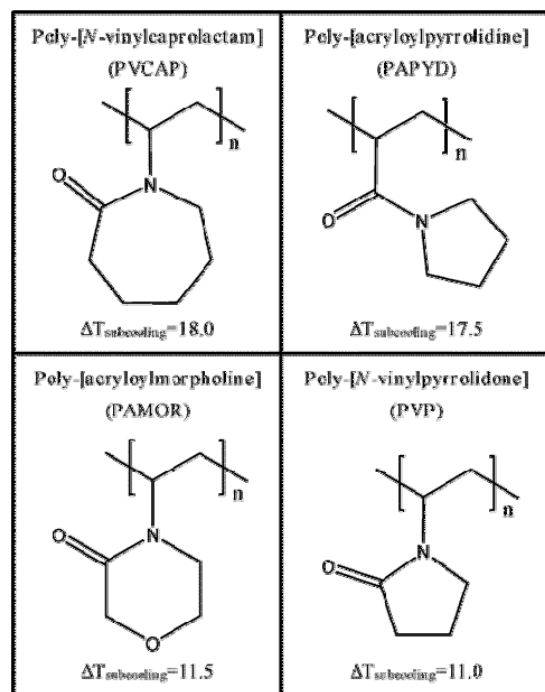


Figure 9. Commercial kinetic inhibitors (Ohtake, 2005).

The functional groups of the Kinetic Inhibitors shown in Figure 9 are a lactam ring and an amide group (-N-C=O) attached to the carbon backbone. The 5-member lactam ring is thought to cover by adsorption the pentagonal face of the hydrate crystal when the amide becomes associated with the hydrate crystal. The 7-member lactam ring is thought to cover by adsorption the hydrate-crystal's hexagonal face (Lederhos, 1996).

Compare these structures with the peptidoglycan polymer structure in bacterial cell walls. See Figure 10.

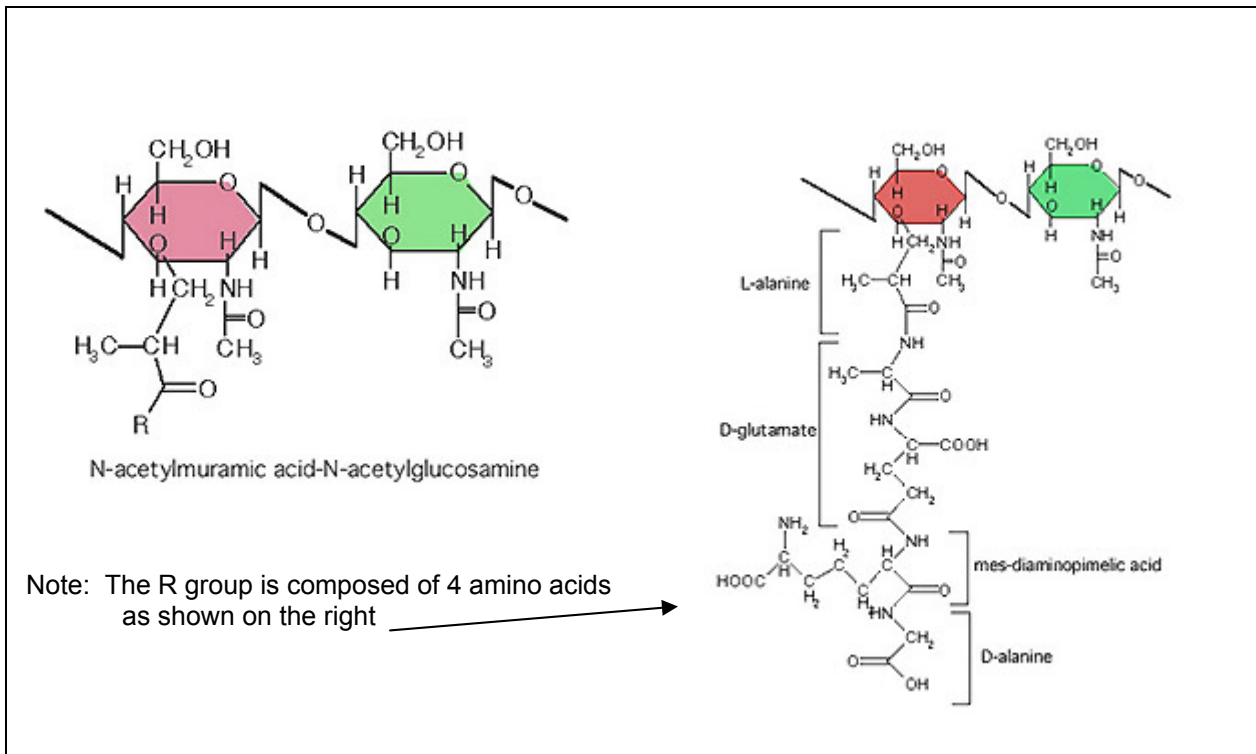


Figure 10. Structure of peptidoglycan (Beveridge and Murray, 1980; Vollmer et al., 2008).

During the work on this project in a prior report period, the water-insoluble polymers comprising the cell walls from a culture of indigenous MC-118 bacteria inhibited hydrate formation in the laboratory. When we fragmented the cells by lysing to give a much greater surface area of those same particles, hydrates were inhibited to an even greater extent.

The polymer as presented in Figure 10 is water insoluble. For some important applications to hydrate inhibition, the inhibitor should be water soluble—as is methanol. Therefore, during the current report period, tests were run to evaluate the efficacy of just the N-acetylglucosamine segment of the structure shown in Figure 10; the N-acetylglucosamine by itself is water-soluble.

In Figure 11 is shown our laboratory results on hydrate induction time.

Note: The following nomenclature applies to Figure 11:

NAGA = N-acetylglucosamine
 MeOH = Methanol
 NB = Nutrient broth

The experimental procedure involved using liquid nutrient broth, ordinarily used in culturing of cells, as the base liquid component in all tests. The reference test was fresh nutrient broth with no additive. A constant volume of the broth was placed in a stainless-steel test-cell, pressurized with a 90/6/4 methane/ethane/propane gas to a constant initial pressure of about 500 psi, and cooled with a 0.5 °C chilling bath; induction time was the time after passing the hydrate equilibrium curve to hydrate

precipitation. The indicated weights of methanol or NAGA were added individually to nutrient broth from the same batch and the test repeated for each addition.

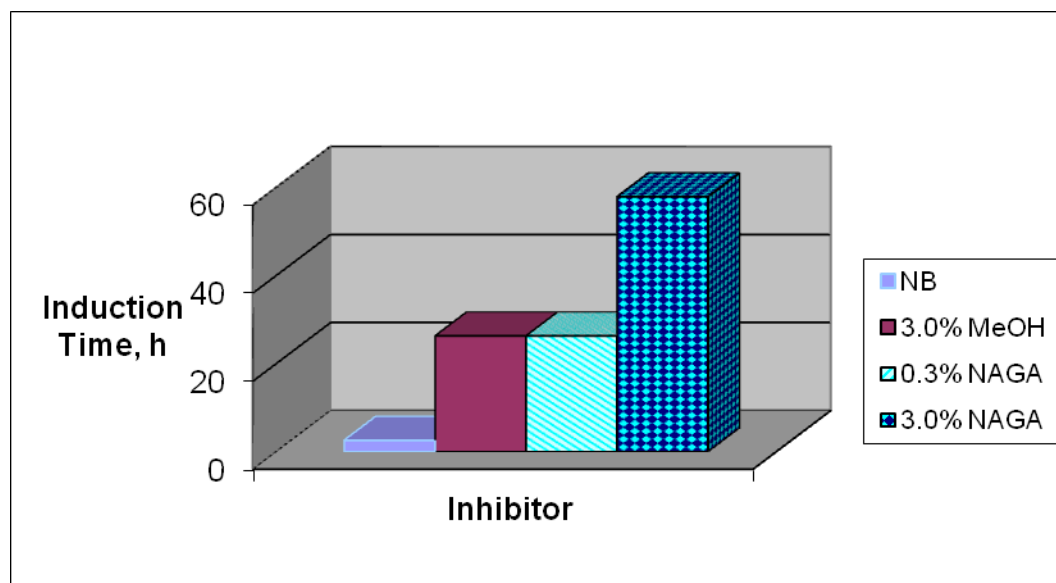


Figure 11. Gas-hydrate inhibition by N-acetylglucosamine.

Note that longer induction times mean greater hydrate inhibition. In Figure 11 it is seen that 0.3% NAGA retarded hydrate formation to the same extent as the order-of-magnitude larger concentration of methanol; 3% NAGA had 2 to 3 times lengthier induction times for hydrates to form compared to a like concentration of methanol.

CONCLUSION

Not only is hydrate inhibition of a new compound demonstrated, but the primary importance is that compound occurs naturally in the environment and could be readily produced en masse at low cost.

PUBLICATIONS

An article is in preparation pertaining to the work, and a provisional patent is under advisement.

REFERENCES

Barrett, J., 2001. Thermal hysteresis proteins. *The International Journal of Biochemistry & Cell Biology* 33, 105-117.

Beveridge, T.J., and Murray, R.G.E., 1980. Sites of metal deposition in the cell wall of *Bacillus subtilis*. *Journal of Bacteriology* 141 (2), 876-887.

Chao, H.M., Houston, M.E., Hodges, R.S., Kay, C.M., Sykes, B.D., Loewen, M.C., Davies, P.L., Sonnichsen, F.D., 1997. A diminished role for hydrogen bonds in antifreeze protein binding to ice. *Biochemistry* 36, 14652-14660.

Gilbert, J.Z., Davies, P.L., Laybourn-Parry, J., 2005. A hyperactive, Ca^{2+} -dependent antifreeze protein in an Antarctic bacterium. *FEMS Microbiology Letters* 245, 67-72.

Gordienko, R., Ohno, H., Singh, V.K., Jia, Z., Ripmeester, J.A., Walker, V.K., 2010. Towards a green hydrate inhibitor: Imaging antifreeze proteins on clathrates, *PLoS One*, 5 (2), www.plosone.org.

Gordon, M.S., Ambdur, B.H., Scholander, P.F., 1962. Freezing resistance in some northern fishes. *Biology Bulletin* 122, 52-62.

Hammerschmidt, E.G., 1934. Formation of gas hydrates in natural gas transmission lines. *Industrial & Engineering Chemistry* 26, 851-855.

Kelland, M.A., Svartaas, T.M., Ovstus, J., Tomita, T., Chosa, J., 2006. Studies on some Zwitterionic surfactant gas hydrate anti-agglomerants. *Chemical Engineering Science* 61, 4048-4049.

Konno, Y., Masuda, Y., Hariguchi, Y., Kurihara, M., Ouchi, H., 2010. Key factors for depressurization-induced gas production from oceanic methane hydrates. *Energy & Fuels* 24, 1736-1744.

Lederhos, J.P., Long, J.P., Sum, A., Christiansen, R.L., and Sloan, E.D., Jr., 1996. Effective kinetic inhibitors for natural gas hydrates. *Chemical Engineering Science* 51 (8), 1221-1229.

Moridis, G.J., Reagan, M.T., 2007. Gas production from oceanic Class 2 hydrate accumulations. *Proceedings of Offshore Technology Conference 2007*, #18866.

Ohtake, M., Yamamoto, Y., Kawamura, T., Wakisaka, A., de Souza, W.F., de Freitas, M.V., 2005. Clustering structure of aqueous solution of kinetic inhibitor of gas hydrates. *Journal of Physical Chemistry B*, 109, 16879-16885.

Ramsey, J.A., 1964. The rectal complex of the mealworm *Tenebrio molitor*, L. (Coleoptera, Tenebrionidae). *Philosophical Transactions of the Royal Society of London B* 248, 279-314.

Rutqvist, J., Moridis, G.J., Grover, T., Collett, T., 2009. Geomechanical response of permafrost-associated hydrate deposits to depressurization-induced gas production.

Journal of Petroleum Science and Engineering 67, 1-12.

Tyshenko, M.G., Doucet, D., Davies, P.L., and Walker, V.K., 1997. The antifreeze potential of the spruce budworm thermal hysteresis protein. *Nature Biotechnology* 15, 887-890.

Vollmer, W., Blanot, D., de Pedro, M.A., 2008. Peptidoglycan structure and architecture. *FEMS Microbiology Reviews* 32 (2), 149-167.

Xiao, C., and Adidharma, H., Dual, 2009. Dual function inhibitors for methane hydrate. *Chemical Engineering Science* 64, 1522-1527.

Zhang, D.Zo., Liu, B., Feng, D.R., He, Y.M., Wang, S.Q., Wang, H.H. and Wang, J.F., 2004. Significance of conservative asparagines residues in the thermal hysteresis activity of carrot antifreeze protein. *Biochemical Journal* 377, 589-595.

Ziegenhain, W.T., 1931. Every precaution taken to eliminate clogging of new Chicago gas line. *Oil & Gas Journal* 30 (19), 34.

TASK 7: Scoping study using Spatio-Temporal Measurement of Seep Emissions by Multibeam Sonar at MC118.

The multibeam scanning sonar project is continued under Phase 4 and progress is reported in that area of this report.

TASK 8: Validate high-frequency scatter on SSDR data by acquisition of targeted cores and velocity profiles at MC118 Hydrate Mound.

Development of a Shallow Sediment Velocity Probe (SSVP) for use in the Gas Hydrates Research Consortium Sea Floor Observatory Program at MC118

Introduction

A need for improved knowledge of sediment characteristics as part of the studies of the Gas Hydrates at the MC118 site prompted a desire to measure the velocity of these sediments. The successful installation of the Pore Fluid Array and Temperature Array with sensors installed to depths below the bottom of nearly 10 meters at MC118 opened the possibility of installing acoustic sensors on a similar probe as a method of measuring sediment velocity.

Background

The concept includes developing a series of acoustic sensors that can be attached to this type of a probe, survive the installation trauma and operate at sufficient depths to allow this concept to work. This also requires developing a data acquisition package that can survive these conditions, is capable of driving and communicating with acoustic sensors, and can achieve a measurement accuracy sufficient to meet the needs of the studies at MC118. SDI has offered to include this development as part of an ongoing

electronics package development aimed to provide rapid acoustic shallow water sediment measurement capability.

Activities during this period

During the previous period the activities on this project were delayed while efforts to deploy the Horizontal Line Arrays took priority. That effort continued through the end of September, 2010 cruises. With the HLA deployment now awaiting better weather, the activities on the sediment probe have resumed. Up to this point, the software and instrumentation development systems had been purchased and used in the development of the software. On the hardware side, the hydrophones and acoustic radiator have been purchased, the hydrophone preamps designed and the circuit cards produced.

The bottom detection switch, battery power supply, electronics housing and probe design have been the subject of the effort in this design phase.

Design Overview and Progress

The sediment probe will consist of a 10 meter long probe with imbedded hydrophones and a control head. The control head will include the controller/data logger, a bottom proximity sensor, the battery power supply and the acoustic source. Mounted above the control head will be an ultra-short baseline (USBL) transponder to provide positioning information to the ship.

The operational plan includes lowering the sediment probe to a depth of 30 to 50 meters above the sea floor, using the USBL system to navigate the sensor to the desired location, free falling the sediment probe into the seafloor, having the bottom insertion detected by the bottom proximity sensor, leaving the probe in place for a suitable time to measure sediment velocity distribution along the probe length and having the ship winch pull the probe free of the sea floor. The sediment probe can then be navigated to a new position and the process repeated without retrieving the probe to the surface.

We are in the process of replacing the original planned bottom proximity sensor with an accelerometer. We originally considered acoustic bottom detection and mechanical bottom detection. The accelerometer bottom detection uses the probe impact with the sea floor as a method of turning on the sampling. A programmable sampling duration can be used to stop the sampling prior to pulling the probe from the sediment. A programmable minimum time before the start of the next sampling will eliminate false a restart due to accelerations during removal.

The system power source has been narrowed to a trade-off between a pressure compensated AGM battery pack and an alkaline pack inside the electronics housing. The pressure compensated rechargeable battery pack eliminated the need to open the electronics housing each time battery replacement is necessary but this pressure compensated battery is bulky, Lithium-Ion and Nickel metal-hydride battery packs offer lighter weight but this is not a factor for this design.

Schedule

The present development should allow the sediment probe to be used on the fall cruises this year.

TASK 9: Recipient shall model carbonate/hydrate mound in Mississippi Canyon 118 using modified version of (THROBS).

This preliminary examination of the hydrate phase at MC118 implies that it will be necessary to develop a multi-component simulator in order to model the observed gas and hydrate phase compositions at the Hydrate Mound. The computer program (CSMHYD.exe) developed by Dendy Sloan (Colorado School of Mines) was used to establish the appropriate stability curve, i.e., hydrate dissociation pressure as a function of temperature and salinity.

Since the vent gas at the Hydrate Mound is mostly methane, it was decided to use the methane PVT properties for the “equivalent” gas phase. Other required hydrate properties (e.g. density, compressibility, thermal expansion coefficient, specific heat, heat of formation) were estimated based on published data.

THROBS was modified (January to April 2009) to include the stability curve for Structure II hydrate as deduced from the computer Program (CSMHYD.exe).

SAIC has performed parametric calculations to examine the following aspects of hydrate formation/decomposition at Hydrate Mound:

1. Gas influx rates required for hydrate formation.
2. Effect of salinity on hydrate distribution.
3. Effect of temperature gradient
4. Conditions required the co-existence of 3-phases (hydrate, gas, liquid) and for gas venting at the sea-floor.

This project continues into Phase 4.

TASK 10. Administrative oversight of the Monitoring Station/Sea-floor Observatory Project.

Administration of the Consortium is the responsibility of the University of Mississippi and includes formal Project Proposals to federal funding agencies, Technical Progress Reports, Final Project Reports, informal monthly updates, reports of Consortium meetings, cruise reports, participation in national meetings, organizing meetings between researchers, organizing and participating in program reviews, organizing and participating in research activities, including research cruises. This responsibility was completed for FY08 with the completion and acceptance of the year-end report to DOE, 42877R12. Further administrative duties and responsibilities are addressed in Phase 4.

PHASE 3 Tasks for FY 2009:

TASK 1: Project Management Plan

This task is complete.

TASK 2: Geological and Geophysical Baseline Characterization of Gas Hydrates at MC118, Gulf of Mexico

Abstract:

The University of South Carolina (Earth and Ocean Sciences) continued to participate in geophysical activities as part of the Gulf of Mexico-Hydrates Research Consortium. During the reporting period July through December 2010, we finalized the purchase, and received, the 3D seismic volume of the MC118 research site from WesternGeco, and we obtained a new copy of the Surface Source / Deep Receiver (SSDR) data set corrected for time discrepancies. We summarize our technical activities in three areas:

- Preliminary Interpretation, Integration, and Analysis of SSDR, Seismic, and Chirp Datasets
- Revision of Rock Physics Models
- Planning Activities for Jumbo Piston Cores

Introduction:

Acquisition of the WesternGeco 3D seismic volume and the corrected SSDR data set, to supplement the TGS data set, has resulted in a more detailed preliminary interpretation. At 2 ms sampling, the WesternGeco seismic dataset is inherently higher resolution than the TGS data set a 4 ms sampling, and evident from review of the data. Highlights are documented in three areas

- Preliminary Interpretation of the Updated SSDR Dataset
- Preliminary Interpretation of the WesternGeco 3D Seismic Volume
- Preliminary Integration of the Datasets

During the second half of 2010 we refined the rock physics models that were developed during the first half of 2010. Based on frictional interaction between sediment grains, the updates provide an additional degree of freedom to calibrate the model against measured field data. A presentation and poster of the rock physics model development were made, respectively to the Annual Meeting of the GoM-HRC and to the Annual Fall Meeting of the American Geophysical Union.

We participated in Consortium planning activities for acquiring up to five jumbo piston cores at the MC118. Based on preliminary results of integrating the SSDR, seismic, and CHIRP data sets with the high resolution bathymetry, we were able to refine locations and rational for ranking the proposed sites. We also proposed post cruise activities.

Results and Discussion

A. Preliminary Interpretation, Integration, and Analysis of SSSR, WesternGeco Seismic, and CHIRP Datasets

I. Preliminary Analysis of the Updated SSSR Dataset

- Activities and results of preliminary analysis are listed here:
- Recent pre-processing of SSSR hi-resolution acoustic data and correction of the timing problem.
- Interpretation and integration of the TGS 3D data with the SSSR 2D hi-resolution acoustic data and the AUV 2D chirp data.
- Pseudo 4D seismic analysis to gain insights about the gas hydrate stability zone from MC118.
- Seafloor pockmarks and craters are located above the crestal faults, which are likely the main conduits for thermogenic gases.
- Shallow gas hydrate formation and accumulation appear to be concentrated near faults and fractures.
- Gas hydrate stability zone shows transients on the scale of five to six years based on pseudo 4D seismic analysis. Apparent gas hydrate dissociation is present based on biochemical and geochemical evidence. Mechanisms unclear.
- Gas hydrate stability zone exhibits heterogeneity in the subsurface beneath Woolsey Mound.

II. Preliminary Analysis of the WesternGeco 3D Seismic Volume

At the beginning of the reporting period, we finalized purchase of the WesternGeco 3D seismic volume over the MC118 area, and took delivery in mid August. This is an industry quality, high resolution seismic 3D data volume carved out of a data set acquired in 2002. The data were acquired using In-Line and Cross-Line spacings of 12.5 m in each direction.

Earth and Ocean Sciences at the University of South Carolina took delivery of the 3D seismic data from WesternGeco in August 2010. Since then, the stacked 3D data cube has been loaded into the Kingdom Suite and Hampson-Russell post-processing codes for display, interpretation, and analysis.

The data delivered include two types: 1) a CMP processed 3D seismic volume in time (10 s with 2 ms sampling) and 2) pre-stack time migrated gathers, also in time. The 3D seismic volume extends 1 mile beyond the boundaries of the MC118 area as shown in Figure 12. In Figure 12a, the red plus signs show the locations of the 253 CMPs marking the locations for which we have stacking velocities; this chart also outlines the surface area covered by the 3D seismic volume. The blue dashed lined box outlines the boundaries of MC118. As revealed in the figure, the survey was shot with In-Line survey lines running at a 45 degree angle from Northwest to Southeast. Locations for twenty-two (out of 911) In-Lines are plotted in Figure 12b; four of the In-Line slices (or time sections) are shown in Figure 13; four time slices through the data are shown in Figure 14. The 3D seismic volume has a total of approximately 414,916 CMP locations from the 911 In-Lines and 911 Cross-Lines.

The pre-stack time migrated gathers, encompassing more than 22 million traces, are awaiting completion of upgrades to the Linux server.

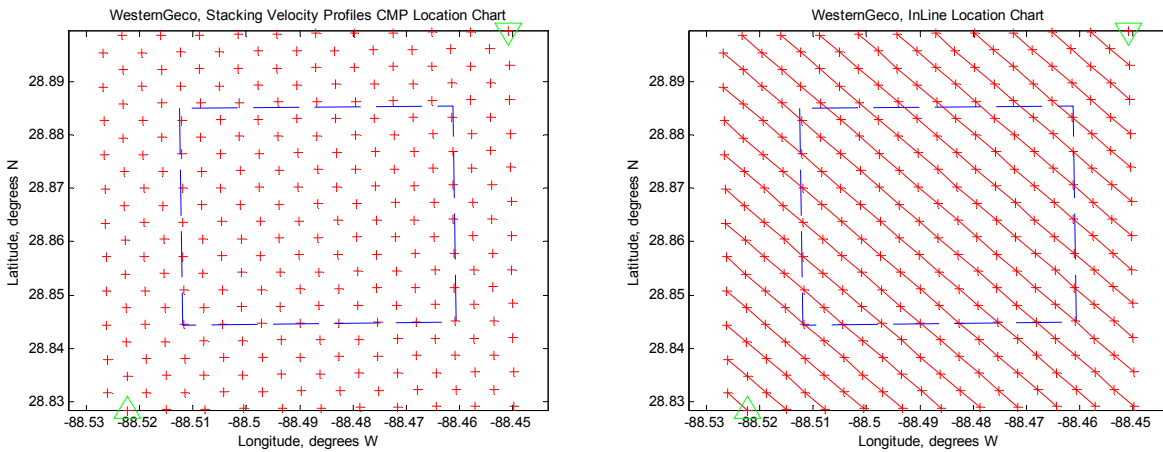


Figure 12. CMP (red plus symbol) location map for WesternGeco 3D seismic volume stacking velocities with MC118 boundaries (blue dashed box): a) CMP locations of 3D seismic volume with stacking velocity profiles, b) the 22 InLine locations that coincide with the stacking velocity locations.

III. Preliminary Integration of the Datasets

- Woolsey Mound at MC118 presents a very complex, and possibly dynamic, scenario for gas hydrate, where salt, thermogenic hydrocarbons, faults, and fractures play a significant role in the mound's evolution.
- Gas hydrate formation, accumulation and dissociation are closely related to deep-seated faults which provide hydrocarbons from below the sea floor and into the water column.
- Pseudo 4D seismic analysis reveals a subsurface dynamic system that appears to change in as short time frame as 5 to 6 years. Therefore, regular detailed seismic observations of MC118 over time would be beneficial to capturing these changes quantitatively.
- Quantitative estimation of gas hydrate saturation cannot be precisely assessed without well-log constraints. Geophysical borehole logging (i.e. resistivity, density, and sonic) would provide calibration information for seismic interpretation, building geological models, and refining calculations of the gas hydrate stability zone (GHSZ).

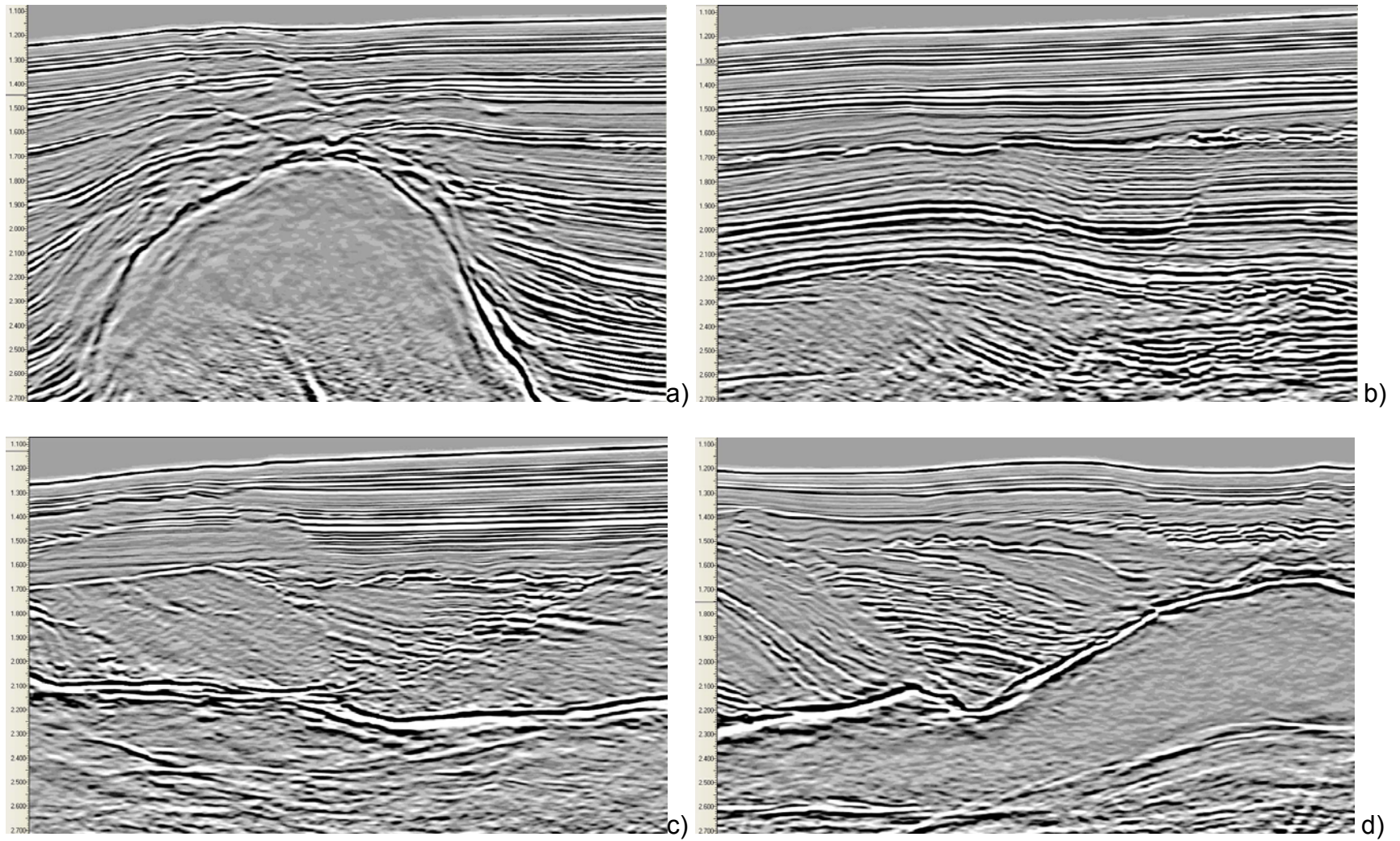


Figure 13. WesternGeco 3D seismic stacked data vertical sections: a) In-Line: Rel-397; b) In-Line: Rel-497; c) In-Line: Rel-597; d) In-Line: Rel-597.

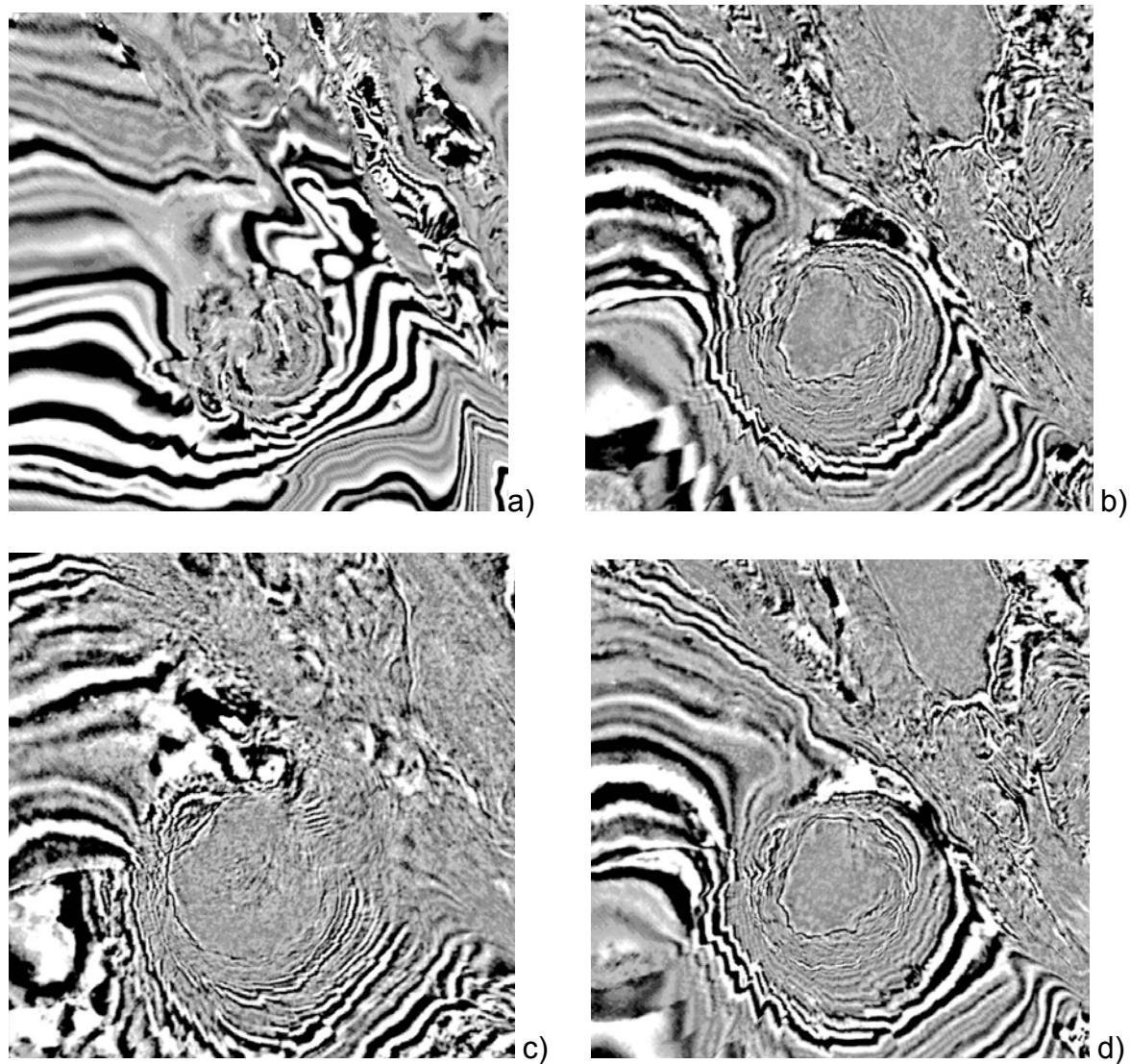


Figure 14. WesternGeco 3D seismic stacked data, time slices: a) 1500 ms ; b) 2000 ms; c) 2500 ms; d) 3000 ms.

B. Revision of Rock Physics Models

We continued development of the effective-medium rock physics models for unconsolidated sediments. Specifically, we modified the equations of the model to incorporate a parameter to specify the amount of slip between grain particles. The model developed during the first half of 2010 relied on the effective-medium model of Dvorkin and Nur (1996) and the unconsolidated sediments framework of Helgerud (2001). This parameter provides an additional degree of freedom to help match measurements from well logs when comparing velocities versus porosity. The motivation for this change came from recent results published in Jenkins et al. (2005).

I. Well Known Effective-Medium Models

In this section we reproduce the equations of the two most widely used effective-medium models for unconsolidated sediments (Walton, 1987; Dvorkin and Nur, 1996).

A. Walton Models

Two models are presented in Walton (1987, eqns. 4.10 and 4.16). For infinitely rough spheres (Walton, 1987, eqn. 4.10) under hydrostatic strain, the effective moduli are

$$\lambda^* = \frac{\phi n C (-\epsilon)^{\frac{1}{2}}}{10\pi^2 B (2B + C)} = \frac{C}{10(2B + C)} \left(\frac{3\phi^2 n^2 p}{\pi^4 B^2} \right)^{\frac{1}{2}}$$

$$\mu^* = \frac{\phi n (5B + C) (-\epsilon)^{\frac{1}{2}}}{10\pi^2 B (2B + C)} = \frac{(5B + C)}{10(2B + C)} \left(\frac{3\phi^2 n^2 p}{\pi^4 B^2} \right)^{\frac{1}{2}}$$

where

$$B = \frac{1}{4\pi} \left(\frac{1}{\mu} + \frac{1}{\lambda + \mu} \right)$$

$$C = \frac{1}{4\pi} \left(\frac{1}{\mu} - \frac{1}{\lambda + \mu} \right)$$

For perfectly smooth spheres (Walton, 1987, eqn. 4.16) under hydrostatic strain, the effective moduli are

$$\lambda^* = \mu^* = \frac{\phi n (-\epsilon)^{\frac{1}{2}}}{10\pi^2 B} = \frac{1}{10} \left(\frac{3\phi^2 n^2 p}{\pi^4 B^2} \right)^{\frac{1}{2}}$$

Alternatively, the effective bulk modulus, $K^* = \lambda^* + \frac{2}{3}\mu^*$ is given in the form (Walton, 1987, eqn. 4.18)

$$K^* = \frac{1}{6} \left(\frac{3\phi^2 n^2 p}{\pi^4 B^2} \right)^{\frac{1}{2}}$$

B. Dvorkin and Nur Model

Dvorkin and Nur (1996, eqn. 4), under slightly different assumptions, presented their Hertz-Mindlin model for unconsolidated sediments for infinitely rough spheres, and write the effective moduli in the form

$$K_{HM} = \left[\frac{n^2 (1 - \phi_0)^2 G^2}{18\pi^2 (1 - \nu)^2 P} \right]^{\frac{1}{3}}$$

$$G_{HM} = \frac{5 - 4\nu}{5(2 - \nu)} \left[\frac{3\pi^2(1 - \phi_c)^2 G^2}{2\pi^2(1 - \nu)^2} P \right]^{\frac{1}{3}}$$

C. Jenkins Update (Extended Walton Model)

Jenkins et al (2005, eqns. 2 and 1) provide an update to the Walton (1987) models, consolidating the mathematical presentation of the infinitely rough and perfectly smooth sphere models into a single expression, as

$$\lambda^E = \frac{k\nu}{9\pi(1 - \nu)} \frac{\mu}{\left[\frac{8\pi(1 - \nu)p}{2} \frac{\nu k}{\mu} \right]^{\frac{1}{3}}} \frac{[2 - \nu - 2\alpha(1 - \nu)]}{(2 - \nu)}$$

$$\mu^E = \frac{k\nu}{5\pi(1 - \nu)} \frac{\mu}{\left[\frac{8\pi(1 - \nu)p}{2} \frac{\nu k}{\mu} \right]^{\frac{1}{3}}} \frac{[2 - \nu + 3\alpha(1 - \nu)]}{(2 - \nu)}$$

In this so-called extended Walton model Jenkins et al. (2005) introduced the friction parameter alpha, α . In this update, $\alpha = 0$ and $\alpha = 1$, respectively, are the end states of a perfectly smooth sphere (frictionless interaction) and an infinitely rough sphere (fully frictional, or no-slip).

II. Revised Formulation of Model

Though the Dvorkin and Nur (1996) model is likely more frequently referenced than Walton (1987), it has occasionally been noted that the Dvorkin and Nur (1996) model over predicts the compressional velocity and significantly over predicts the shear velocity (Dai et al, 2004; Sava and Hardage, 2006).

A. Effective-Medium Model

Here we adopt the extended Walton model to use as our effective-medium model, but use the nomenclature from Dvorkin and Nur (1996). Similar to Dvorkin and Nur (1996), we use an expression for bulk modulus in place of the Lamé coefficient. Therefore, our Hertz-Mindlin effective-medium model is written

$$K_{HM} = \left[\frac{k^2(1 - \phi_c)^2 G^2}{18\pi^2(1 - \nu)^2} P \right]^{\frac{1}{3}}$$

$$G_{HM} = \frac{1}{5} \left[\frac{3k^2(1 - \phi_c)^2 G^2}{2\pi^2(1 - \nu)^2} P \right]^{\frac{1}{3}} \frac{[2 - \nu + 3\alpha(1 - \nu)]}{(2 - \nu)}$$

The parameter k is the average number of contacts per particle (or coordination number), ϕ_c is the critical porosity, G is the shear modulus of the sediment grain material, and ν is Poisson's ratio for the grain material. The two equations above replace the Hertz-Mindlin effective-medium models used in the discussion in the previous semi-annual report,

B. Baseline Model for Unconsolidated Sediments

To implement the selected effective-medium model we adopt the framework for unconsolidated sediments (Dvorkin and Nur, 1996; Helgerud, 2001). The equations for

the effective dry-rock moduli are as follows:

Porosity $\phi < \phi_c$

$$K_{Dry} = \left[\frac{\phi/\phi_c}{K_{HM} + \frac{4}{3}G_{HM}} + \frac{1 - \phi/\phi_c}{K + \frac{4}{3}G_{HM}} \right]^{-1} - \frac{4}{3}G_{HM}$$

$$G_{Dry} = \left[\frac{\phi/\phi_c}{G_{HM} + \frac{G_{HM}}{6} \left(\frac{9K_{HM} + 8G_{HM}}{K_{HM} + 2G_{HM}} \right)} + \frac{1 - \phi/\phi_c}{G + \frac{G_{HM}}{6} \left(\frac{9K_{HM} + 8G_{HM}}{K_{HM} + 2G_{HM}} \right)} \right]^{-1} - \frac{G_{HM}}{6} \left(\frac{9K_{HM} + 8G_{HM}}{K_{HM} + 2G_{HM}} \right)$$

Porosity $\phi > \phi_c$

$$K_{Dry} = \left[\frac{(1 - \phi)/(1 - \phi_c)}{K_{HM} + \frac{4}{3}G_{HM}} + \frac{(\phi - \phi_c)/(1 - \phi_c)}{K + \frac{4}{3}G_{HM}} \right]^{-1} - \frac{4}{3}G_{HM}$$

$$G_{Dry} = \left[\frac{(1 - \phi)/(1 - \phi_c)}{G_{HM} + \frac{G_{HM}}{6} \left(\frac{9K_{HM} + 8G_{HM}}{K_{HM} + 2G_{HM}} \right)} + \frac{(\phi - \phi_c)/(1 - \phi_c)}{\frac{G_{HM}}{6} \left(\frac{9K_{HM} + 8G_{HM}}{K_{HM} + 2G_{HM}} \right)} \right]^{-1} - \frac{G_{HM}}{6} \left(\frac{9K_{HM} + 8G_{HM}}{K_{HM} + 2G_{HM}} \right)$$

Gassmann' equations

$$K_{Sat} = K \frac{\phi K_{Dry} - (1 + \phi) \frac{K_f K_{Dry}}{K} + K_f}{(1 - \phi) K_f + \phi K \frac{K_f K_{Dry}}{K}}$$

$$G_{Sat} = G_{Dry}$$

Velocity equations

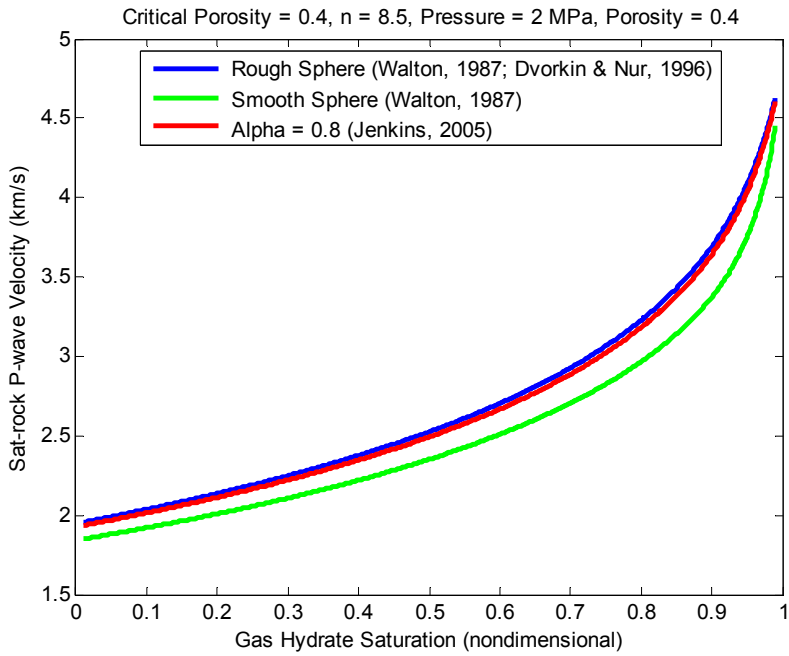
$$V_p = \sqrt{\frac{K_{Sat} + \frac{4}{3}G_{Sat}}{\rho_B}}$$

$$V_s = \sqrt{\frac{G_{Sat}}{\rho_B}}$$

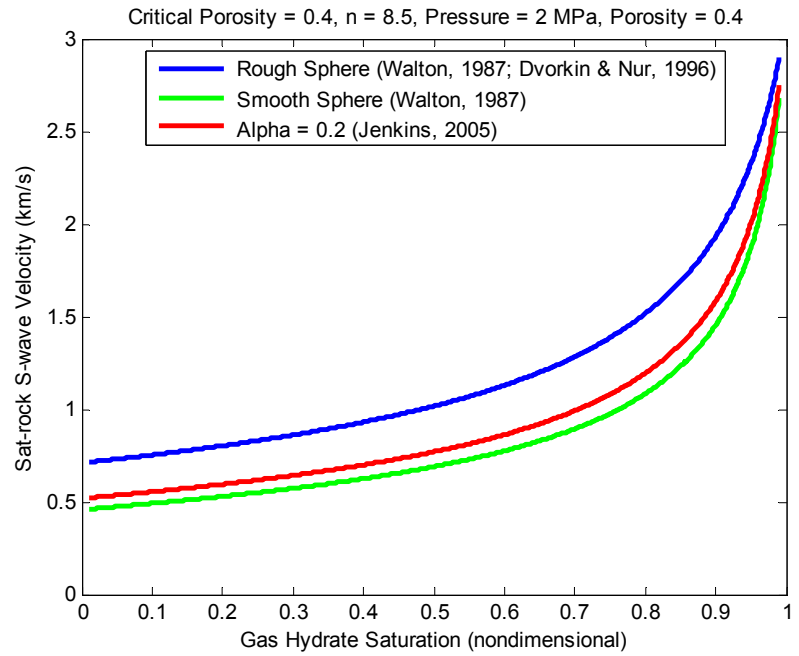
Bulk density

$$\rho_B = \phi \rho_w + (1 - \phi) \rho_{solid}$$

With this baseline model for unconsolidated sediments we compare calculated compressional and shear velocities for the infinitely rough sphere and perfectly smooth sphere models with the extended Walton model as rewritten above. Graphical results are shown (see Figure 15).



a)



b)

Figure 15. Model runs, (a) compressional velocity with alpha equal to 0.8, (b) shear velocity with alpha equal to 0.2.

III. Model Configurations for Gas Hydrates in Unconsolidated Sediments

For our model, configurations for gas hydrates in unconsolidated sediments, we adopt the pore-fluid and rock matrix models from Helgerud et al (1999) and Helgerud (2001). See Figure 16, and the equations below.

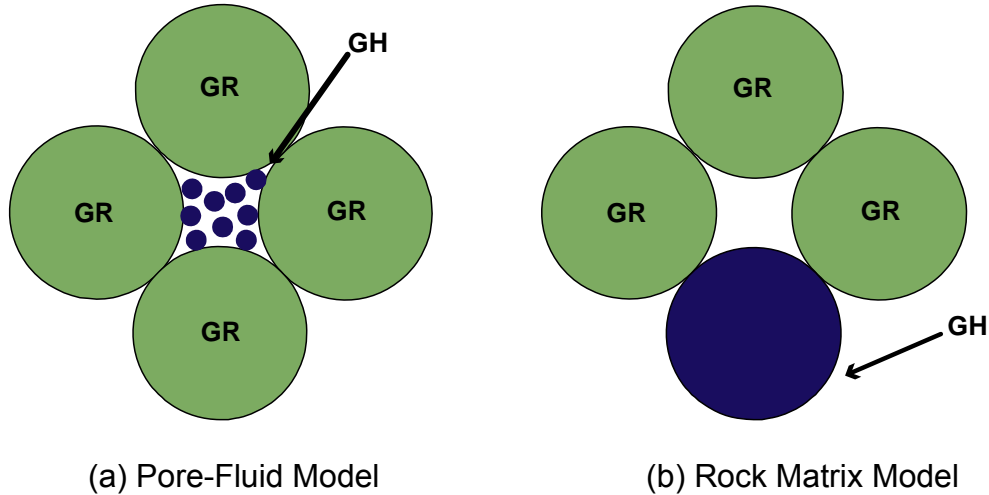


Figure 16. Model configurations for gas hydrates in unconsolidated sediment, (a) pore-fluid model - gas hydrate homogeneously distributed throughout the pore space, (b) rock matrix model - gas hydrate is part of the rock matrix and contributes to its stiffness.

A. Pore-Fluid Configuration

The pore-fluid model requires replacing the fluid bulk modulus with

$$K_f = \left[\frac{S_w}{K_w} + \frac{(1-S_w)}{K_h} \right]^{-1}$$

and updating the calculation of the bulk density as follows,

$$\rho_B = \phi[(1-S_h)\rho_f + S_h\rho_h] + (1-\phi)\rho_{solid}$$

B. Rock Matrix Configuration

Modifications to the baseline model are more extensive for the rock matrix model. First a reduced porosity is defined:

$$\phi_r = \phi S_w = \phi(1-S_h)$$

Then the grain moduli are recalculated with

$$K = \frac{1}{2} \left(f_h K_h + [1-f_h] K_s + \left[\frac{f_h}{K_h} + \frac{(1-f_h)}{K_s} \right]^{-1} \right)$$

$$G = \frac{1}{2} \left(f_h G_h + [1-f_h] G_s + \left[\frac{f_h}{G_h} + \frac{(1-f_h)}{G_s} \right]^{-1} \right)$$

where

$$f_h = \frac{\phi(1 - S_w)}{1 - \phi S_w}$$

Then the calculation for bulk density is updated:

$$\rho_B = \phi_r \rho_f + (1 - \phi_r) \rho_{r-solid}$$

C. Planning Activities for Jumbo Piston Cores

The Consortium has planned a field cruise to the Observatory site, MC118, in order to collect up to five Jumbo Piston Cores in early 2011. In the absence of drilling, coring, and logging a 500 m well, Jumbo Piston Cores, with a barrel length of 20 m, will provide valuable information and data to further the ongoing geophysical and seismic interpretation efforts of the site by USC. Planning activities included I) outlining principal geophysical objectives; II) proposed coring sites (Figure 17) with coordinate locations, and rationale for suggested rankings of the sites, and III) proposed post-cruise activities.

I. Principal Objectives

Nine principal geophysical objectives are established here:

1. Sample upper 20 m of stratigraphic section;
2. Calibrate seismic datasets (CHIRP, SSSR, TGS-Nopec, WesternGeco) for lithology and log response [resistivity, gamma-ray, sonic];
3. Characterize sediments (and pore fluids) in vicinity of an active fault;
4. Compare with sediments (and pore fluids) removed from fault;
5. Evaluate shallow resistivity anomalies;
6. Constrain initial interpretations from 4-D seismic analysis (TGS and SSSR);
7. Ground-truth high frequency scattering signal in SSSR;
8. Provide age control for recent movement on deep-seated faults (Blue, Pink, and Yellow);
9. Establish baseline for future heat flow transect across active fault segment.

II. Proposed Sites (with Refined Coordinate Locations) and Rationale for Rankings

Table 1. Refined Coordinate Locations for Jumbo Piston Core targets.

Core Designation	UTM		Latitude and Longitude	
	X (m)	Y (m)	Lat (N)	Lon (W)
PC-1	354582	3192814	28° 51' 17.329"	88° 29' 26.988"
PC-2	354262	3192149	28° 50' 55.597"	88° 29' 38.486"
PC-3	354581	3193155	28° 51' 28.406"	88° 29' 27.182"
PC-4	354160	3192942	28° 51' 21.315"	88° 29' 42.618"
PC-6	354982	3192331	28° 51' 1.803"	88° 29' 12.006"
PC-7	355050	3193452	28° 51' 38.245"	88° 29' 10.014"
PC-8	354827	3191660	28° 50' 39.944"	88° 29' 17.414"

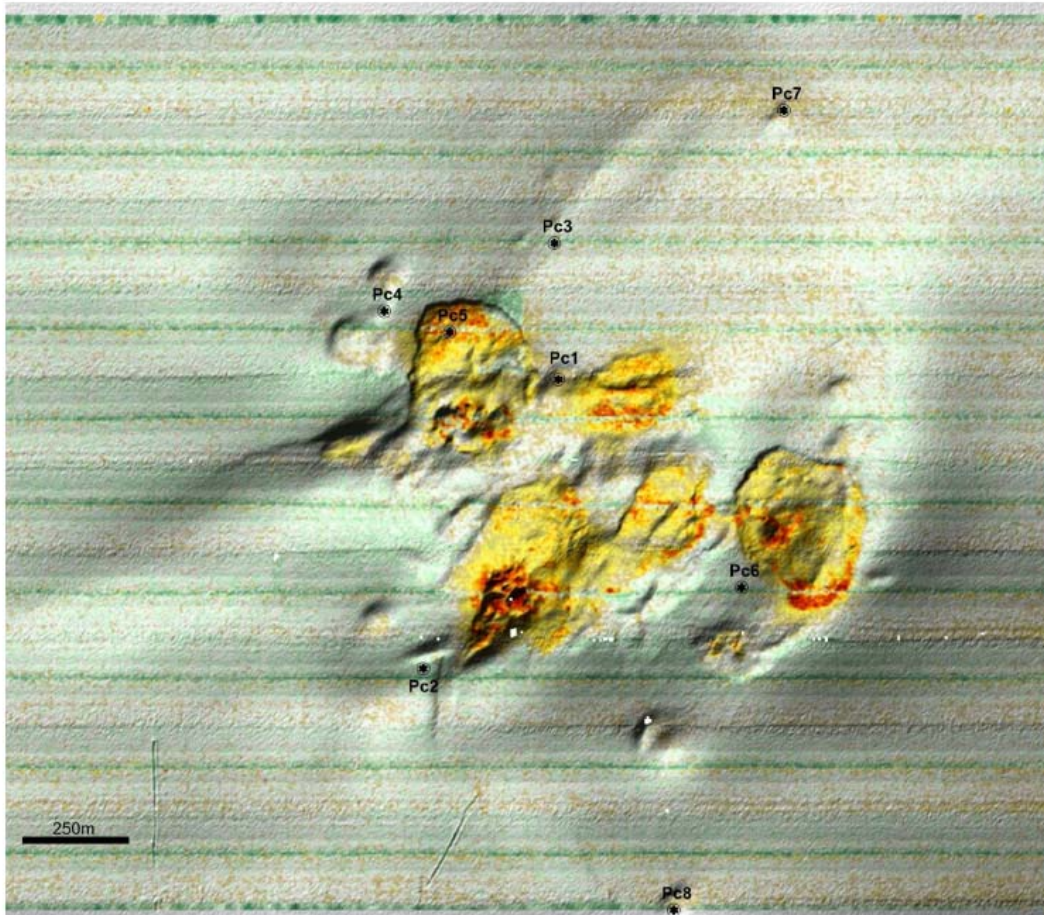


Figure 17. Proposed jumbo piston core locations on shaded bathymetry of Woolsey Mound and surrounding area.

B. Rationale for Rankings (illustrated in Figures 18, 19, 20).

JPC5 was eliminated since maximum benefit can be attained with CMRET's 10m probe. Our suggestions for ranking the coring sites are as follows:

- **JPC1** - penetrates the blue fault, currently delivering fluids to the seafloor; should calibrate high-frequency scattering on SDR data (?hydrate saturation);
- **JPC3** (it provides age constraint for recent movement of the blue fault);
- **JPC6** - penetrates the pink fault, currently delivering fluids to the seafloor; penetrates seismic blanking on CHIRP data; fills gap in isopach mapping effort;
- **JPC8** penetrates another deep-seated fault; should calibrate the high frequency scattering on SDR data (?hydrate saturation); the fault is likely to be an active fluids pathway based on preliminary 4D seismic analysis;
- **JPC4** - close to where hydrates were found in 2008; near the blue fault;
- **JPC7** - potential site of venting from 2000/2006 across the yellow fault based on preliminary 4D seismic analysis; should calibrate high-frequency scattering on SDR data (?hydrate saturation);
- **JPC2** - penetrates an upthrown block with a compressed stratigraphic section.

Proposal for Jumbo Piston Cores site locations

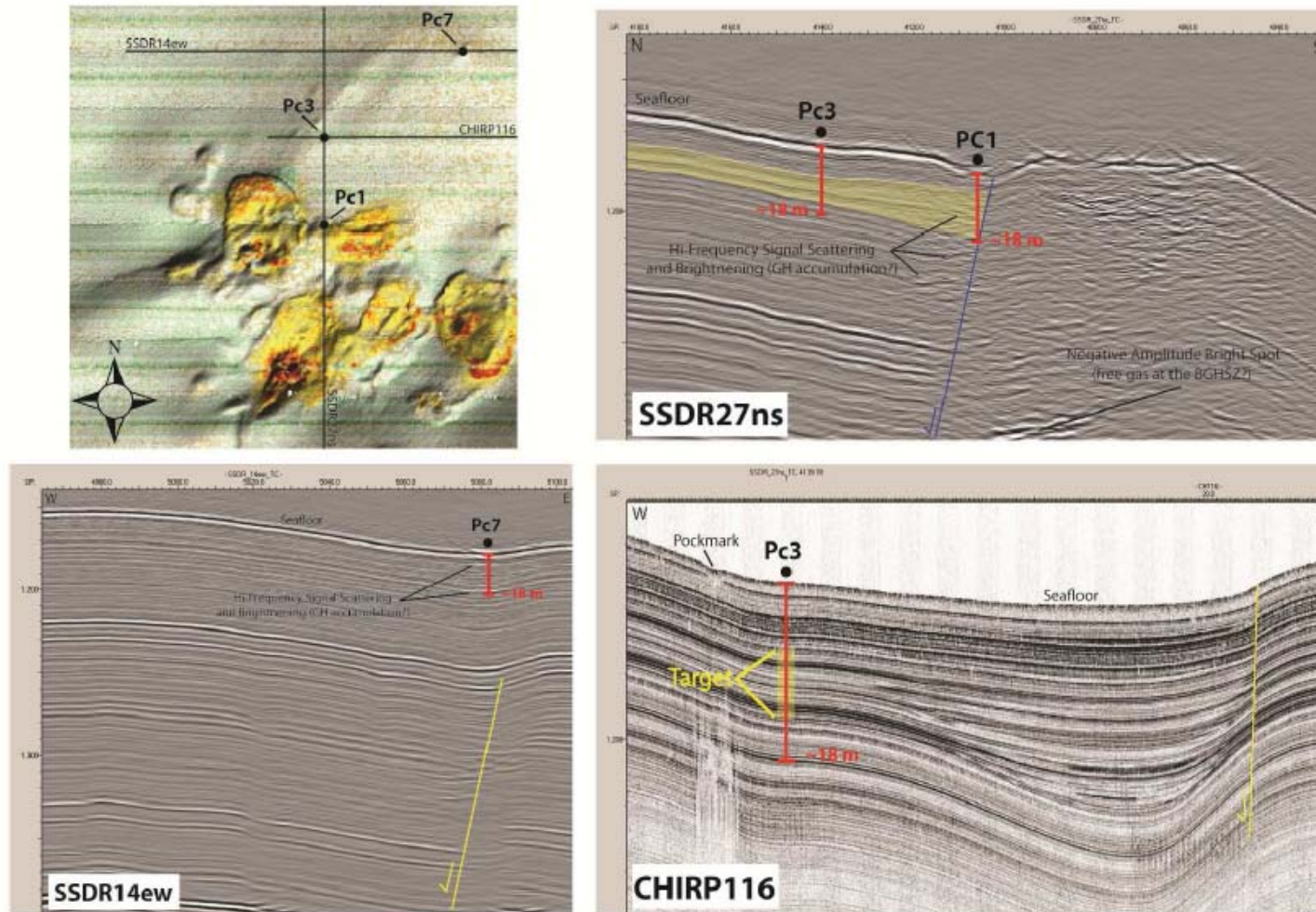


Figure 18. Sites PC-1, PC-3, and PC-7: Left to right and top to bottom; a) bathymetry and transect location, b) SSDR north-south transect, c) SSDR east-west transect, d) close-up CHIRP transect.

Proposal for Jumbo Piston Cores site locations

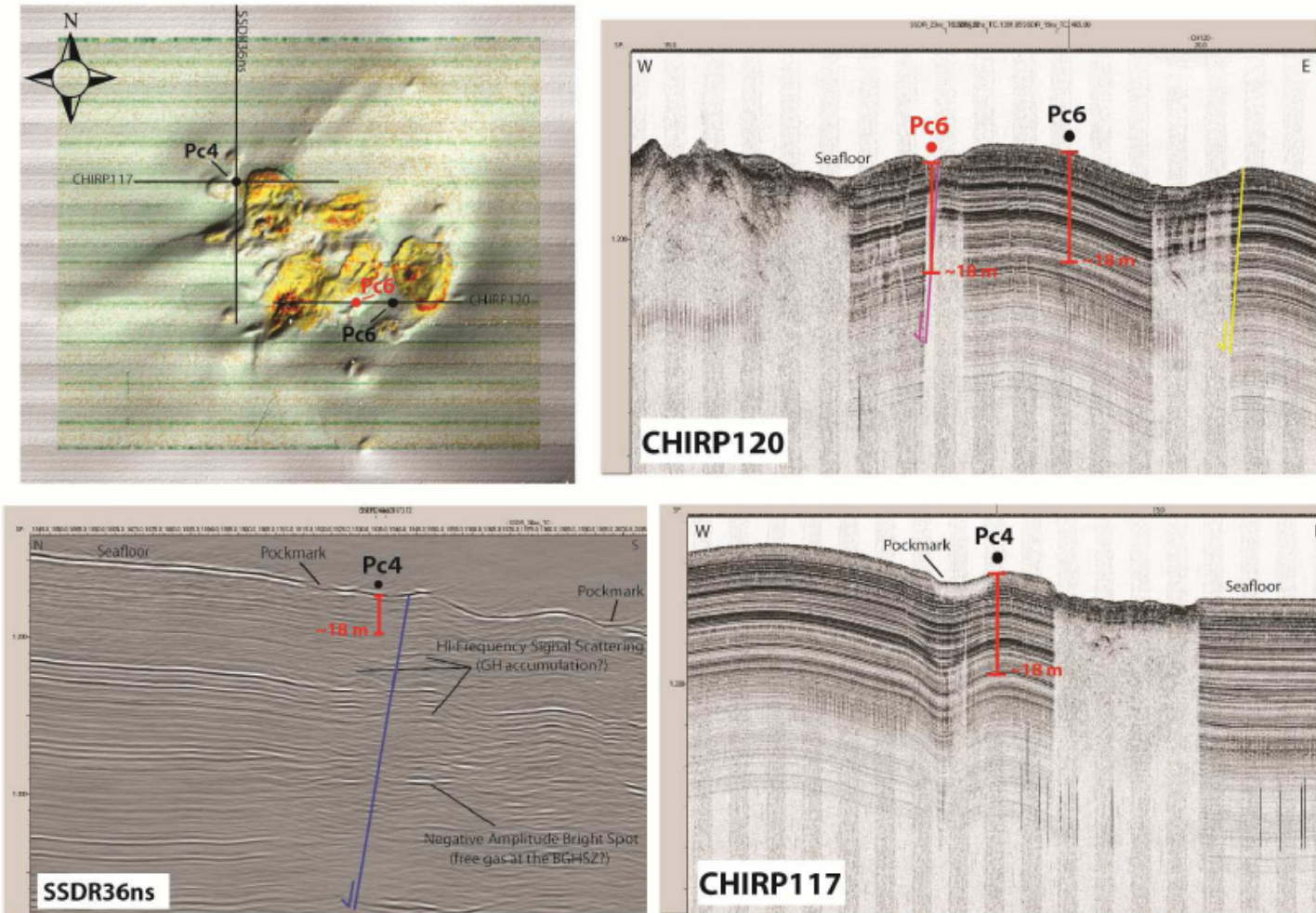


Figure 19. Sites PC-4 and PC-6: Left to right and top to bottom; a) bathymetry and transect location, b) SSSR east-west transect, c) SSSR north-south transect, d) close-up of CHIRP transect.

Proposal for Jumbo Piston Cores site locations

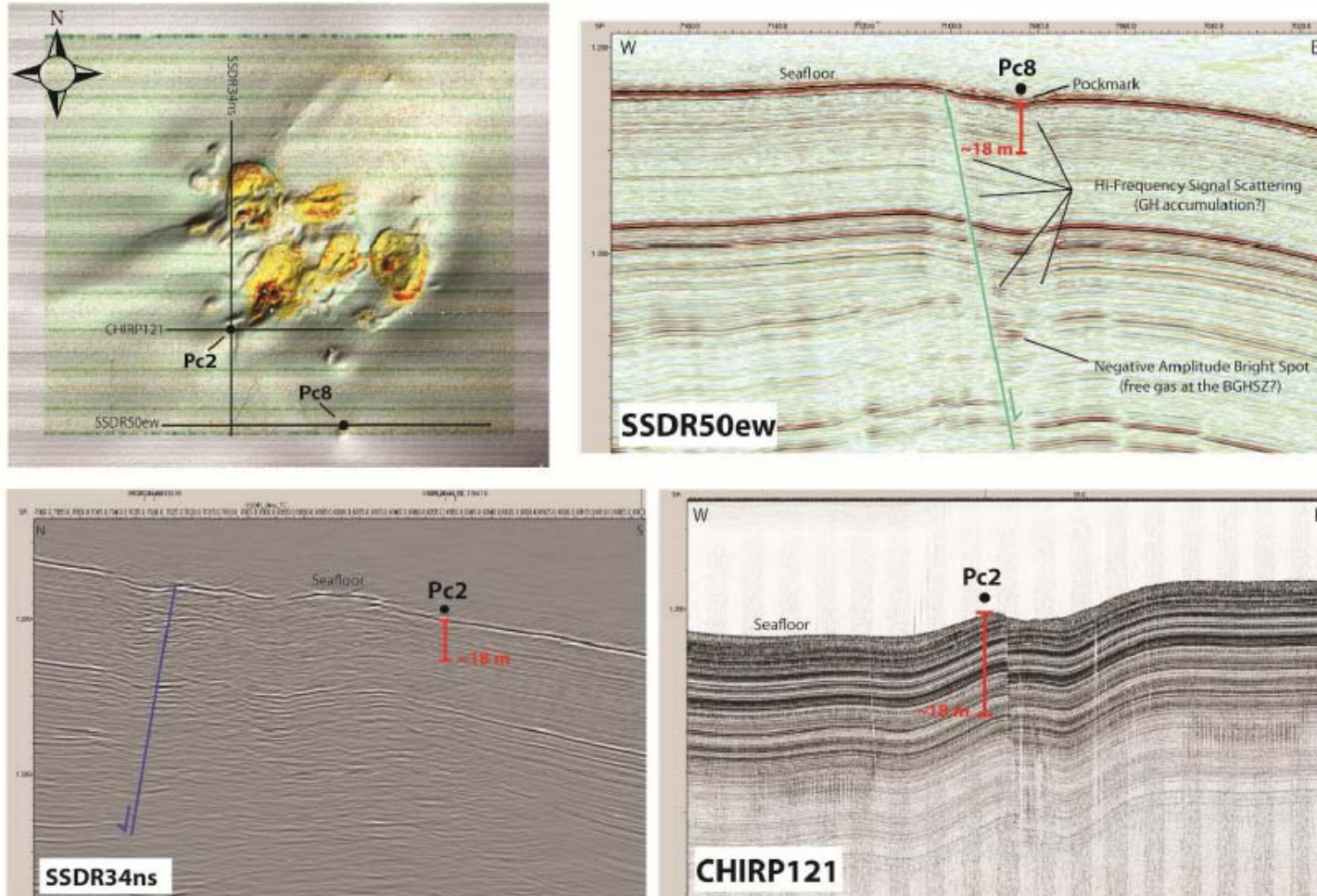


Figure 20. Sites PC-2 and PC-8: Left to right and top to bottom; a) bathymetry and transect location, b) SS DR east-west transect, c) SS DR north-south transect, d) close-up of CHIRP transect.

III. Proposed Post-Cruise Activities

1. Assist with core description (J. Salazar)
2. Integration with high-resolution seismic datasets (J. Salazar)
3. Evaluate rock properties from acoustic logs (D. Terry)
4. Integrate age constraints with 3-D seismic interpretation (A. Simonetti)

Papers, Posters, Presentations

Presentations, Annual Meeting of the Gulf of Mexico Hydrates Research Consortium, Oxford, Mississippi.

Simonetti, A.; Knapp, J. H.; Knapp, C. A.; 2010. Developments in Seismic Imaging of the MC118 from 2D, 3D and 4D Data. Presentation to the Annual Meeting of the Gulf of Mexico Hydrates Research Consortium, Oxford, MS, 26-27 November 2010.

Terry, D. A.; Knapp, C. C.; Knapp, J. H.; 2010. Rock Physics Models for Marine Gas Hydrates. Presentation to the Annual Meeting of the Gulf of Mexico Hydrates Research Consortium, Oxford, MS, 26-27 November 2010.

Presentations, American Geophysical Union Annual Convention, San Francisco, CA, 13-17 December 2010.

Terry, D. A.; Knapp, C. C.; Knapp, J. H.; 2010. Comparison of Effective-Medium Models for Marine Gas Hydrate Templates. Poster Presentation at the 2010 American Geophysical Union Fall Meeting, 13-17 December 2010 (Poster OS53A-1361).

Wood, W. T.; Knapp, C. A.; Knapp, J. H.; 2010. Constraints on Methane and Methane Hydrate Distribution at a Gulf of Mexico Seep Using Waveform Inversion of Seismic Data. Oral Presentation at the 2010 American Geophysical Union Fall Meeting, 13-17 December 2010 (Paper OS44A-04).

References

Dai, J.; Xu, H.; Snyder, F.; Dutta, N.; 2004. Detection and estimation of gas hydrates using rock physics seismic inversion: Examples from the northern deepwater Gulf of Mexico. *The Leading Edge*, January 2004, p. 60-66.

Dvorkin, J.; Nur, A.; 1996. Elasticity of high-porosity sandstones: Theory for two North Sea data sets. *Geophysics*, v. 61, n. 5, pp. 1363-1370.

Helgerud, M. B.; 2001. Wave Speeds in Gas Hydrate and Sediments Containing Gas Hydrate: A Laboratory and Modeling Study. Ph.D. Dissertation, Stanford University, 249 pp.

Helgerud, M. B.; Dvorkin, J.; Nur, A.; Sakai, A.; Collett, T. S.; 1999. Elastic-wave velocity in marine sediments with gas hydrates: Effective medium modeling. *Geophys. Res. Lett.*, v. 26, p. 2021-2024.

Jenkins, J.; Johnson, D.; La Ragione, L.; Makse, H.; 2005. Fluctuations and the effective moduli of an isotropic, random aggregate of identical, frictionless spheres. *J. Mech. Phys. Solids*, v. 53, pp. 197-225.

Sava, D.; Hardage, B.; 2006. Rock physics models of gas hydrates from deepwater, unconsolidated sediments. Annual Meeting of the SEG/New Orleans 2006, p. 1913-1917.

Walton, K.; 1987. The effective elastic moduli of a random packing of spheres. *J. Mech. Phys. Solids*, v. 35, pp. 213-226.

TASK 3: Near seafloor geology at MC118 using converted shear-waves from 4C seafloor sensor data.

Since no 4C data have been collected from the MC118 site, this task has not progressed visibly. However, a contract has been tendered by WHOI to do the data collection in March-April of 2011 using their nodes and personnel aboard a CMRET chartered vessel. CMRET will provide the source guns and the compressor to effect the survey. Data will be delivered to UT-Austin in SEG Y and SEED formats. This task is being rewritten for submission to DOE and all funds previously directed toward collecting the 4C data will be redirected to this effort.

TASK 4: Geochemical investigations at MC 118: Pore fluid time series and gas hydrate stability.

This task is continued into Phase 4 where the complete update of activities is reported.

TASK 5: Automated Biological/Chemical Monitoring System (ABCMS) for Offshore Oceanographic Carbon Dynamic Studies. Development of a Marine Lander Survey Vehicle for Gas Hydrate Research

This task is continued into Phase 4 where the complete update of activities is reported.

TASK 6: Quantification of Seep Emissions by Multibeam Sonar at MC118.

This task is continued into Phase 4 where the complete update of activities is reported.

TASK 7: Modeling a carbonate/hydrate mound in Mississippi Canyon 118 using modified version of (THROBS).

The hydrate mound in Mississippi Canyon Block 118 (MC 118), as described by McGee et al. (McGee, T. et al., 2008. Structure of a carbonate/hydrate mound in the northern Gulf of Mexico, paper to be presented at the International Conference on gas Hydrates, Vancouver, Canada, July 6-10, 2008), contains mostly Structure II thermogenic hydrates formed by gases upflowing along a nearly vertical fault system extending from a salt diapir that underlies several hundred meters beneath the hydrate mound. The surface of the hydrate mound is characterized by several crater clusters; these crater clusters have been grouped into three major complexes based on topographic relief and gas venting (McGee et al., 1998). At present, the SE complex exhibits no venting activity; the NW complex has moderate activity, and the SW complex shows moderate to high venting activity. The venting activity has most likely changed over time. In addition to variable venting activity over time, the following observations are relevant to the modeling of hydrates at this site:

1. Salinities as high as 5 times that of sea-water have been recorded around the vents in the NW complex. High salinity and gas venting suggests the presence of 3-phase conditions (gas + hydrate + liquid).
2. Chemical composition of vent gas is different from that of the hydrate. It has been suggested that the difference is due to molecular fractionation (Roger Sassen, quoted by McGee et al., 2008). Treatment of this aspect will require a “compositional” simulator.
3. Presence of multiple BSRs. It is possible that this is due to the existence of gas hydrates that are stable to greater depths (higher temperatures?) than that encountered above the “shallowest” BSR. Clearly, a compositional simulator is needed for modeling this phenomenon.
4. Acoustic wipeout zones, observed in seismic profiles, have been interpreted to indicate the possible presence of free gas (“chimney” flow) and/or other inhomogeneities (e.g. carbonate/hydrate blocks in the sediments). Modeling of chimney flow and/or other inhomogeneities can only be done by a multi-dimensional hydrate simulator.

Prior to the start of Year 1 (2008-2009) of SAIC effort, our hydrate simulator (THROBS) was restricted to one-dimension and Structure I methane hydrate. It was recognized that THROBS will have to be generalized in several respects in order to treat the phenomena of interest. Required changes include:

1. Incorporation of the stability curve and other hydrate properties (heat of melting, hydration number, and thermomechanical properties) for structure II hydrates.
2. Replacement of methane gas equation-of-state (EOS) and gas solubility relationship by an EOS and solubility curve that reflects the gas composition.
3. Development of a multi-dimensional version of THROBS.

Given the fiscal constraints, SAIC undertook a limited research effort during the first year (2008-2009). Specifically, we incorporated structure II hydrate stability curve and relevant properties (item 1 above) into THROBS simulator. The gas mixture forming the hydrate was represented as a single gas. The modified THROBS simulator has been used to model (1) the hydrate distribution above the shallowest BSR, (2) presence of high salinity fluids within the hydrate stability zone, and (3) gas venting at the sea-floor. The work performed during Year 1 is described in a report by Garg and Pritchett (S. K. Garg and J. W. Pritchett, Modeling Studies of Hydrate Mound, Mississippi Canyon 118, Gulf of Mexico, Report submitted to the University of Mississippi, September 2009).

As previously mentioned, a “compositional” (i.e. multi-gas) simulator is needed to account for the various gas components present in MC 118 hydrates; such a treatment for the gas composition is necessary for modeling phenomena such as molecular

fractionation and multiple BSRs. During Year 2 (2009-2010), we initiated the development of a multi-component (methane, ethane, and propane) simulator. Because of funding limitations, this effort was spread over a couple of years. The work has been divided into two parts, i.e. (1) development of a computationally efficient multi-component equation-of-state (i.e. PVT behavior of 3-gas components, water, and salt; phases will include hydrate and precipitated salt as solid phases, water with dissolved gases and salt as a liquid phase, and a gas phase), and (2) modification of the simulator to accommodate the new equation –of-state.

This task is continued into Phase 4 where the complete update of activities is reported.

Task 8: Administrative oversight of the Monitoring Station/Sea-floor Observatory Project.

Administration of the Consortium is the responsibility of the University of Mississippi and includes formal Project Proposals to federal funding agencies, Technical Progress Reports, Final Project Reports, informal monthly updates, reports of Consortium meetings, cruise reports, participation in national meetings, organizing meetings between researchers, organizing and participating in program reviews, organizing and participating in research activities, including research cruises. This responsibility is completed for FY09 with the completion and acceptance of this year-end report to DOE, 42877R18. A compilation of administrative duties and responsibilities is presented in Phase 4, Task 7.

Task 9. Project Summary Updates:

These appear as Task 8 in Phase 4.

PHASE 4 Tasks FOR FY2010

TASK 1: Program Management Plan

This task is nearing completion.

TASK 2: Integration of Multiple Methods of Geological and Geophysical investigations to advance Shallow Subsurface Characterization at MC118, site of the Gulf of Mexico Hydrates Research Consortium's Seafloor Observatory

This task includes several subtasks that are quite diverse:

Subtask 2.1: Contract heat-flow data collection surveys across the hydrate mound area at MC118. As with the jumbo piston coring (JPC) effort, TDI-Brooks will notify us when they have a heat-flow cruise going to or near MC118 so that we can incur minimum mobilization expenses. We are in regular communication with TDI-Brooks on this

subject. Analyses of the JPCs will help identify specific targets for this effort but we have already identified several faults from which we hope to collect heat-flow and accompanying chemical data. Heat-flow data from 15-20 probe location targets selected by the Consortium should help establish temperature conditions across faults, pockmarks and other surface features believed to be associated with fluid migration at MC118. They may establish constraints of the hydrates stability zone (HSZ) including its likely vertical extent at Woolsey Mound.

Subtask 2.2. Contract to have giant piston cores collected from areas of interest at the Observatory site. TDI Brooks contacted MMRI/CMRET with a potential date for this cruise in November. Although the cruise was ultimately cancelled due to unfavorable weather conditions, the MMRI sent out calls to geologists, geophysicists and geochemists for input into sites to be cored for this task. Each participant was asked to nominate as many as 5 sites and provide justification for coring at each. On short notice, the response to this request was excellent and we received nominations for 14 sites. In follow-up discussions, we were able to pare that number down to 8 with justifications from industry seismic data, high resolution chirp and surface-source-deep-receiver data, resistivity data (from our June 2009 resistivity survey), previous core data and previous findings of the geochemical and microbial biology groups. Prioritization of coring locations are based on the importance of maximum core penetration (64ft, or ~20m), likelihood of penetrating the high frequency scatter zone suspected of being indicative of hydrates in the shallow subsurface, the potential to ground-truth shallow seismic data already collected at MC118, and the potential to constrain lithologic, paleontologic and stratigraphic parameters at the observatory site. This cruise is expected to happen in January.

Subtask 2.3. Process and interpret polarity-preserving chirp data collected with the NIUST AUV-borne system, to define the shallow geometry of the fluids/gas pipe system and integrate these results with the geological (core analyses) and geophysical data. The chirp system is being installed on the STRC AUV. A shake-down cruise to test the system is tentatively scheduled for May, with potential survey dates in July.

Subtask 2.4. Perform sedimentological, lithological, paleontological and geophysical analyses of newly recovered cores (Phase 4, subtask 2.2) and integrate the results with previous core studies. Negotiations are underway to have the electric logging of the JPCs (and later the 10m gravity cores) performed at the Naval Research Laboratory (NRL) facilities at John C. Stennis Space Center, MS. Following this logging, the cores will be split, photographed, logged manually and subsampled for grain-size analyses, mineralogical analyses, microfossil analyses and lithologic analyses. The infrared camera that will be tested for hydrates identification in unopened cores has been purchased in hopes that it can be used on the JPC cruise, anticipated in January.

Subtask 2.5. Collect solid outcropping gas hydrates and/or authigenic carbonate/hydrates samples at the MC118 Observatory site using the existing pressure-chamber sampler in conjunction with the STRC ROV. The station Service Device ROV is being adapted to attempt this task during a June cruise following the April cruise

during which we hope to recover gravity cores from areas of known hydrate outcroppings. Additional pressure chambers are being built for this purpose.

Subtask 2.6. Refurbish 4C nodes, donated by CGG Veritas for deployment and use in shear experiments as defined in Phase 2 task 3, and Phase 3 task 3. The nodes that were to have been made available for this part of Task 2 have become too cumbersome and potentially expensive to pursue. A within scope change is being sought to cancel this part of this task so that we can subcontract Wood Hole Oceanographic Institution to provide Ocean Bottom Seismometers to the Consortium to effect this work. Funds allocated to refurbishment of the nodes will be redirected to this effort.

TASK 3: Modeling a carbonate/hydrate mound in Mississippi Canyon 118 using modified version of (THROBS).

Introduction

The hydrate mound in Mississippi Canyon Block 118 (MC 118), as described by *McGee et al.* (2008), contains mostly Structure II thermogenic hydrates formed by gases upflowing along a nearly vertical fault system extending from a salt diapir lies several hundred meters beneath the hydrate mound. The surface of the hydrate mound is characterized by several crater clusters; these crater clusters have been grouped into three major complexes based on topographic relief and gas venting (*McGee et al.*, 2008). At present, the SE complex exhibits no venting activity; the NW complex has moderate activity, and the SW complex shows moderate to high venting activity. The venting activity has most likely changed over time. In addition to variable venting activity over time, the following observations are relevant to the modeling of hydrates at this site:

1. Salinities as high as 5 times that of sea-water have been recorded around the vents in the NW complex. High salinity and gas venting suggests the presence of 3-phase conditions (gas + hydrate + liquid).
2. Chemical composition of vent gas is different from that of the hydrate. It has been suggested that the difference is due to molecular fractionation (*Sassen*, 2006). Treatment of this aspect will require a “compositional” simulator.
3. Presence of multiple BSRs. It is possible that this is due to the existence of gas hydrates that are stable to greater depths (higher temperatures?) than that encountered above the “shallowest” BSR. Clearly, a compositional simulator is needed for modeling this phenomenon.
4. Acoustic wipeout zones, observed in seismic profiles, have been interpreted to indicate the possible presence of free gas (“chimney” flow) and/or other inhomogeneities (e.g. carbonate/hydrate blocks in the sediments). Modeling of chimney flow and/or other inhomogeneities can only be done by a multi-dimensional hydrate simulator.

Prior to the start of Year 1 (2008-2009) of SAIC effort, our hydrate simulator (THROBS) was restricted to one-dimension and Structure I methane hydrate. It was recognized that THROBS will have to be generalized in several respects in order to treat the phenomena of interest. Required changes include:

1. Incorporation of the stability curve and other hydrate properties (heat of melting, hydration number, and thermomechanical properties) for structure II hydrates.
2. Replacement of methane gas equation-of-state (EOS) and gas solubility relationship by an EOS and solubility curve that reflects the gas composition.
3. Development of a multi-dimensional version of THROBS.

Given the fiscal constraints, SAIC undertook a limited research effort during the first year (2008-2009). Specifically, we incorporated structure II hydrate stability curve and relevant properties (item 1 above) into THROBS simulator. The gas mixture forming the hydrate was represented as a single gas. The modified THROBS simulator was used to model (1) the hydrate distribution above the shallowest BSR, (2) presence of high salinity fluids within the hydrate stability zone, and (3) gas venting at the sea-floor. The work performed during Year 1 is described in a report by Garg and Pritchett (S. K. Garg and J. W. Pritchett, Modeling Studies of Hydrate Mound, Mississippi Canyon 118, Gulf of Mexico, Report submitted to the University of Mississippi, September 2009).

As previously mentioned, a “compositional” (i.e. multi-gas) simulator is needed to account for the various gas components present in MC 118 hydrates; such a treatment for the gas composition is necessary for modeling phenomena such as molecular fractionation and multiple BSRs. During Year 2 (2009-2010), we initiated the development of a multi-component (methane, ethane, and propane) simulator. Because of funding limitations, this effort will need to be spread over a couple of years. The work has been divided into two parts, i.e. (1) development of a computationally efficient multi-component equation-of-state (i.e. PVT behavior of 3-gas components, water, and salt; phases will include hydrate and precipitated salt as solid phases, water with dissolved gases and salt as a liquid phase, and a gas phase), and (2) modification of the simulator to accommodate the new equation –of-state.

In preparation for the extension of the approach to treat multidimensional problems, SAIC completed the adoption of the existing (single gas) THROBS equation-of-state for use in the multidimensional STAR simulator. Test calculations have verified that, with the new STAR/HYDCH4 constitutive description, the two codes (THROBS and STAR) produce identical results when used to solve 1-D problems. Since the MC 118 site analysis will eventually require a multidimensional treatment, this is a necessary step in the development. With the existing THROBS constitutive description incorporated into STAR, it is now possible to carry out preliminary multidimensional studies and we are in a better position to proceed toward the final goal of a multidimensional, multi-component modeling capability. A description of STAR/HYDCH4 was provided in a previous letter report (July 2010).

Work performed during the report period

Contract Matters

SAIC subcontract for Year 2 with the University of Mississippi was finalized towards the end of October 2009. Because of late start, we had requested a no-cost extension to the end of October 2010. The requested extension and the SAIC subcontract for Year 3 with the University of Mississippi were finalized at the end of September 2010.

Technical Progress

During the current report period (July 1, 2010 to December 31, 2010), work was continued on the development of a multi-component equation-of-state.

We seek to describe a system consisting of up to three hydrocarbon gases (principally methane, with smaller amounts of ethane and propane) together with a saline brine in the pressure/temperature range at which hydrates may form (generally between 0°C and 35°C temperature and between 1 MPa and 100 MPa pressure). In the previous reporting period, we focused on the PVT properties for the hydrocarbon gases, and developed a module for computing the relevant properties for a gaseous mixture consisting of methane, ethane, and propane. In the following, we describe the development of a module for computing hydrate/liquid/gas equilibrium conditions.

Two methods for calculating hydrate/liquid/gas equilibrium conditions for aqueous/hydrocarbon systems are available in the literature. The first is a general-purpose first-principles statistical thermodynamic approach described by *Sloan* (1998); see in particular Chapter 5. This procedure has been embodied in a stand-alone computer program called CSMHYD, also available with *Sloan* (1998). The second approach is the much simpler and more heuristic “distribution coefficient” or “K-value” method, which permits equilibrium conditions to be estimated using algebraic formulae. This approach is described at considerable length by *Sloan* (1998).

It had been the original intent of the present authors to employ the “K-value” approach in the development of the new STAR/THROBS compositional constitutive description for the three-component hydrocarbon case. To this end, we first undertook to use the formulation of *Mann et al.* (1989) (see *Sloan* (1998) for a discussion of various K-value formulations) to try to estimate equilibrium conditions as a function of temperature for a non-saline aqueous system (techniques for taking dissolved-salt effects into account are discussed below) in equilibrium with a gaseous phase consisting of 96% methane (CH₄), 3% ethane (C₂H₆) and 1% propane (C₃H₈) by volume. This composition is representative of the vent gases emanating from the Mississippi Canyon 118 hydrate site (*Sassen et al.*, 2006). Structure II hydrate was assumed. These “K-value” results were then compared to those from similar calculations using the more general-purpose CSMHYD program of *Sloan* (1998).

Unfortunately these comparisons suggested that the “K-value” approach, while useful for preliminary estimation purposes, is insufficiently robust for use in a general-purpose simulator. Figure 21 illustrates the results of this comparison for P_{eq} , the “equilibrium pressure” at which all three phases may coexist, as a function of temperature. The two methods produce comparable results over a pressure range extending from approximately 2 MPa to 20 MPa, but outside that range the “K-value” method diverges markedly from the CSMHYD representation. For pressures less than

about 1.7 MPa the “K-value” P/T relationship has a negative derivative, and the equilibrium temperature appears to diverge completely for pressures exceeding 50 MPa or so.

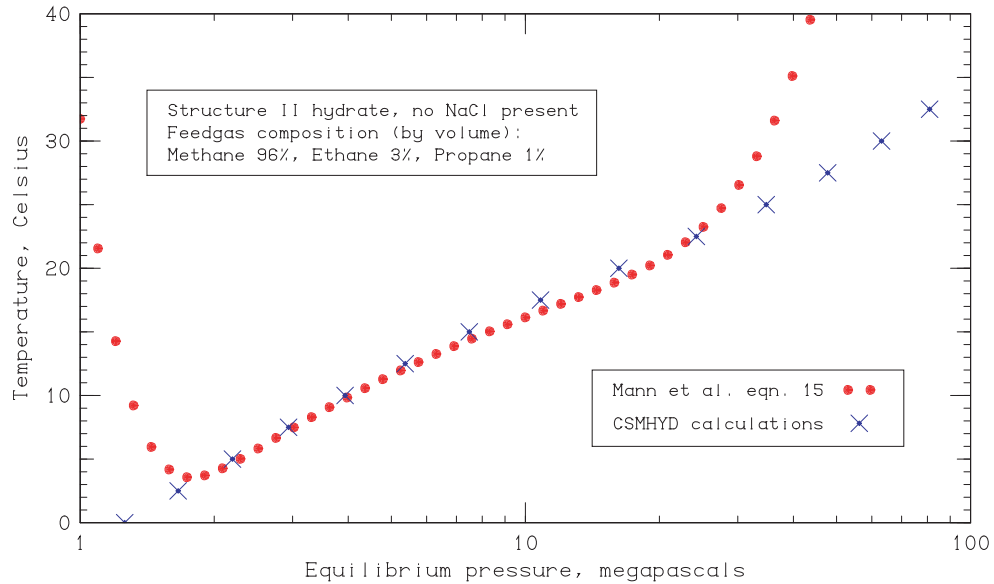


Figure 21. Comparison of (equilibrium pressure / temperature) relationship for a salt-free system with Structure II hydrate and with a feedgas composition of 96% CH₄, 3% C₂H₆ and 1% C₃H₈ (mole fractions), according to algebraic fits (red symbols) of *Mann et al.* (1989), and to the CSMHYD program (blue symbols) of *Sloan* (1998).

The clear superiority of the CSMHYD results mandated that this more general-purpose approach would be required for the development of our new constitutive model. But direct use of CSMHYD within the STAR or THROBS context would have been impractical, for several reasons. First is the fact that the CSMHYD source-code was not available to the present authors. Second, CSMHYD is a far more general-purpose description than is needed for the present purposes, and thus even if the source-code had been available, its direct use would have been much too computationally inefficient for practical calculations using the reservoir simulator.

Accordingly, we adopted an intermediate approach. The CSMHYD program was exercised extensively to characterize three-phase equilibrium conditions for a three-component hydrocarbon gas (CH₄, C₂H₆ and C₃H₈) in equilibrium with H₂O as a function of temperature. The composition of the gaseous phase is specified by the values of two dimensionless parameters *H* and *G*:

$$H = (\text{Ethane} + \text{Propane}) / (\text{Methane} + \text{Ethane} + \text{Propane})$$

$$G = \text{Propane} / (\text{Ethane} + \text{Propane})$$

where:

<Methane> = number of moles of CH₄ in the gaseous phase,

<Ethane> = number of moles of C₂H₆ in the gaseous phase, and

<Propane> = number of moles of C₃H₈ in the gaseous phase.

CSMHYD calculations were carried out for temperature *T* = 0°C, 5°C, 10°C, ..., 35°C, for *H* = 0.00, 0.02, 0.04, ..., 0.10 and for *G* = 0, 0.125, 0.25, 0.375, 0.5 and 1.0. The

calculated results for each of the 248 cases considered (equilibrium pressure P_{eq} and the equilibrium composition of the hydrocarbon mixture in the solid hydrate phase) were recorded, and are listed in the Appendix.

The CSMHYD calculations described above were carried out for four-component systems (H_2O , CH_4 , C_2H_6 and C_3H_8) without dissolved salt ($NaCl$). Of course, in reality the “equilibrium pressure” (the pressure at which all three phases – hydrocarbon gas, solid hydrate, and aqueous brine with dissolved hydrocarbons – can coexist) may be regarded as depending upon temperature, brine-phase salinity, and the composition of the gaseous phase. Defining brine salinity as:

$$S = \text{dissolved NaCl mass} / (\text{dissolved NaCl mass} + \text{liquid } H_2O \text{ mass})$$

it is useful to define an “adjusted temperature” T_{adj} by:

$$T_{adj} = T + 60 \times S$$

where both T_{adj} and T (the actual measured temperature of the system) are expressed in degrees Celsius. The effect of non-zero salinity upon the equilibrium relations is to raise the equilibrium pressure (see e.g., Sloan, 1998; Garg *et al.*, 2008), so that the equilibrium pressure at (T, S) is essentially the same as that for pure water at $(T_{adj}, S = 0)$. So, the equilibrium conditions (equilibrium pressure, and the composition of the solid hydrate phase) may be regarded as a function of T_{adj} and the composition of the gaseous phase or “feedgas” (as specified by the H and G parameters – see above). Using the above relation for T_{adj} , mathematical fits were formulated to the computed CSMHYD results listed in the Appendix which yield equilibrium pressure and the hydrate hydrocarbon composition (molar ratios of $CH_4:C_2H_6:C_3H_8$) as functions of T_{adj} ($= T + 60 S$) and the values of H and G describing the composition of the feedgas. These fits employ smooth interpolations (with continuous partial derivatives) among the values obtained from CSMHYD listed in the Appendix.

Figure 22 shows the behavior of the resulting smooth fit to the CSMHYD data for the equilibrium pressure P_{eq} as a function of the adjusted temperature T_{adj} ($= T + 60 S$) for various representative values of the feedgas composition parameters H and G . The “equilibrium pressure” is the pressure value at which both a gaseous hydrocarbon phase and a solid hydrate phase may coexist. Solid hydrate will be unstable and will decompose into free gas and liquid water at pressures less than P_{eq} . At any fixed value of T_{adj} , the equilibrium pressure tends to increase as the feedgas methane (CH_4) content increases relative to the other hydrocarbons (decreasing values of H), and also increases with decreasing propane (C_3H_8) content (decreasing values of G). Thus, as the mean molecular weight of the feedgas mixture increases, the equilibrium pressure tends to decline and the region in which solid hydrate is stable becomes larger (*i.e.* extends down to lower pressures).

At equilibrium, the relative abundances of the heavier components (ethane and propane) are significantly higher in the solid hydrate phase than in the gaseous phase (the “feedgas”), and the hydrate-phase methane abundance is correspondingly reduced relative to that of the gaseous phase. For the solid hydrate phase, we define a quantity corresponding to H as follows:

$$H^* = (\langle \text{Ethane} \rangle + \langle \text{Propane} \rangle) / (\langle \text{Methane} \rangle + \langle \text{Ethane} \rangle + \langle \text{Propane} \rangle)$$

where in this case the mole fractions refer to the solid hydrate phase:

<Methane> represents the number of moles of CH₄ in the solid hydrate,

<Ethane> represents the number of moles of C₂H₆ in the solid hydrate, and

<Propane> represents the number of moles of C₃H₈ in the solid hydrate.

Representative results for $H^*(T_{adj}, G, H)$ are displayed in Figure 23. There is a general tendency for H^* to decrease somewhat with increasing temperature, at least up to 25°C - 30°C or so, but note that in all cases $H^* \gg H$, that is, the population of the heavier components is significantly larger in the hydrate phase than in the gas phase with which it is in equilibrium. Furthermore, for a particular value of H , the value of H^* tends to increase if the propane fraction increases relative to the ethane fraction (that is, for increasing values of gas-phase G). H^* also increases as H itself increases, but note that the ratio of the two (H^*/H) declines somewhat with increasing values of H (i.e., declining gas-phase methane concentration).

Figure 24 displays the composition of the non-methane portion of the hydrocarbons present at equilibrium in the solid hydrate phase, and illustrates how the propane (C₃H₈) content of the solid hydrate is substantially amplified relative to that of the feedgas. This is described by the dimensionless quantity G^* , defined as:

$$G^* = \text{<Propane>} / (\text{<Ethane>} + \text{<Propane>})$$

where in this case again,

<Ethane> represents the number of moles of C₂H₆ in the solid hydrate, and.

<Propane> represents the number of moles of C₃H₈ in the solid hydrate.

The tendency for propane to be preferentially concentrated in the hydrate phase decreases slightly with increasing temperature up to $T_{adj} = 25^\circ\text{C} - 30^\circ\text{C}$ or so, and then increases slightly again with further increases in temperature. As these curves show, the value of G^* depends significantly upon the value of G itself (the ratio of propane volume to [ethane plus propane] volume in the gas phase), and is relatively insensitive to H (the ratio of the heavier hydrocarbon volumes to the total hydrocarbon volume in the gas phase). For small values for G , the hydrate-phase propane fractionation effect is quite pronounced. If the gas-phase G value is 0.1, the corresponding hydrate-phase G^* value will be at least 0.47, and even for relatively large gas-phase G values, for example, $G = 0.4 - 0.5$, the hydrate-phase G^* value is nearly twice as large.

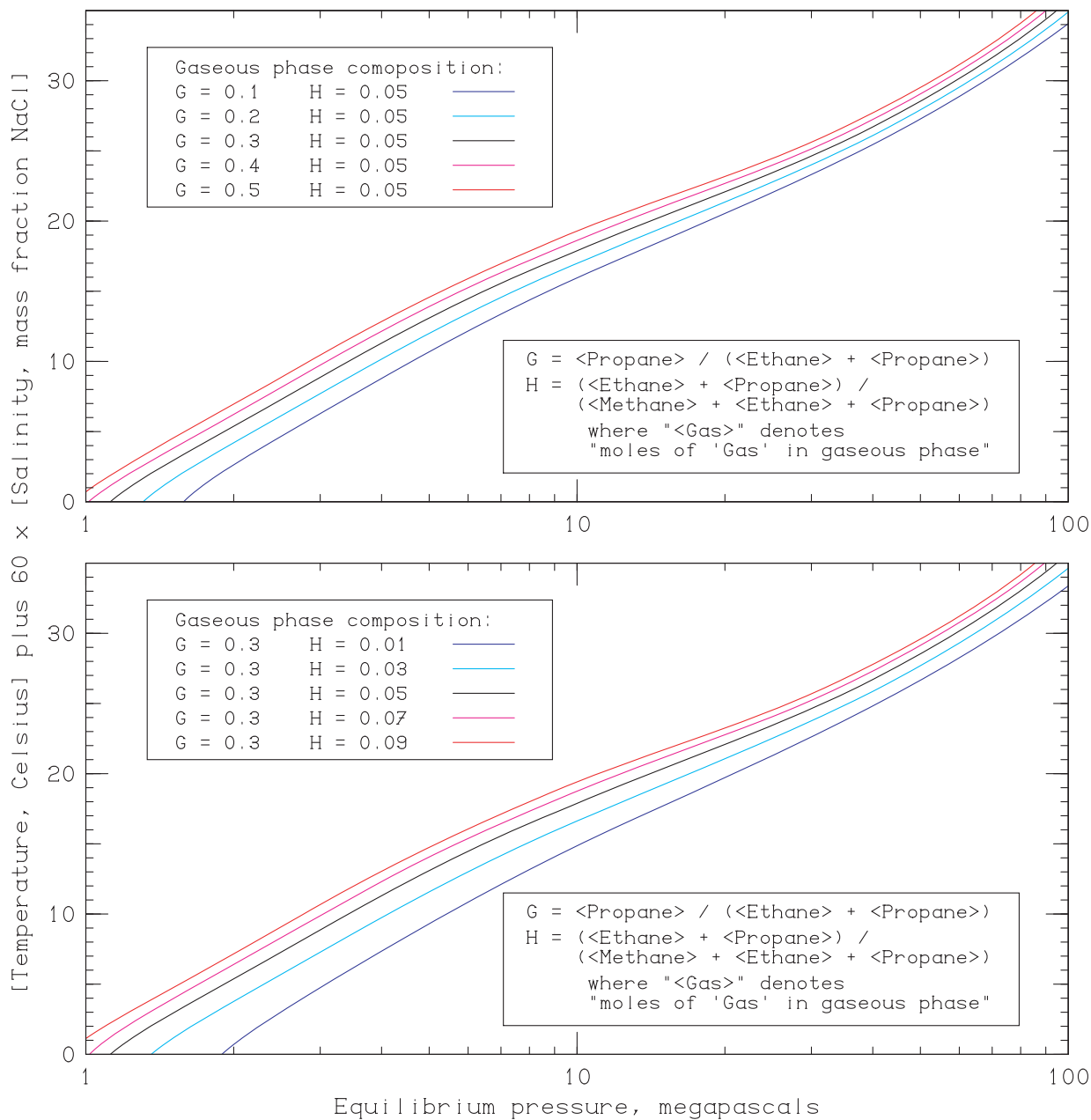


Figure 22. Influence of feed-gas composition, brine salinity and temperature upon equilibrium pressure where three hydrocarbon-containing phases (gaseous, aqueous and solid hydrate) may coexist.

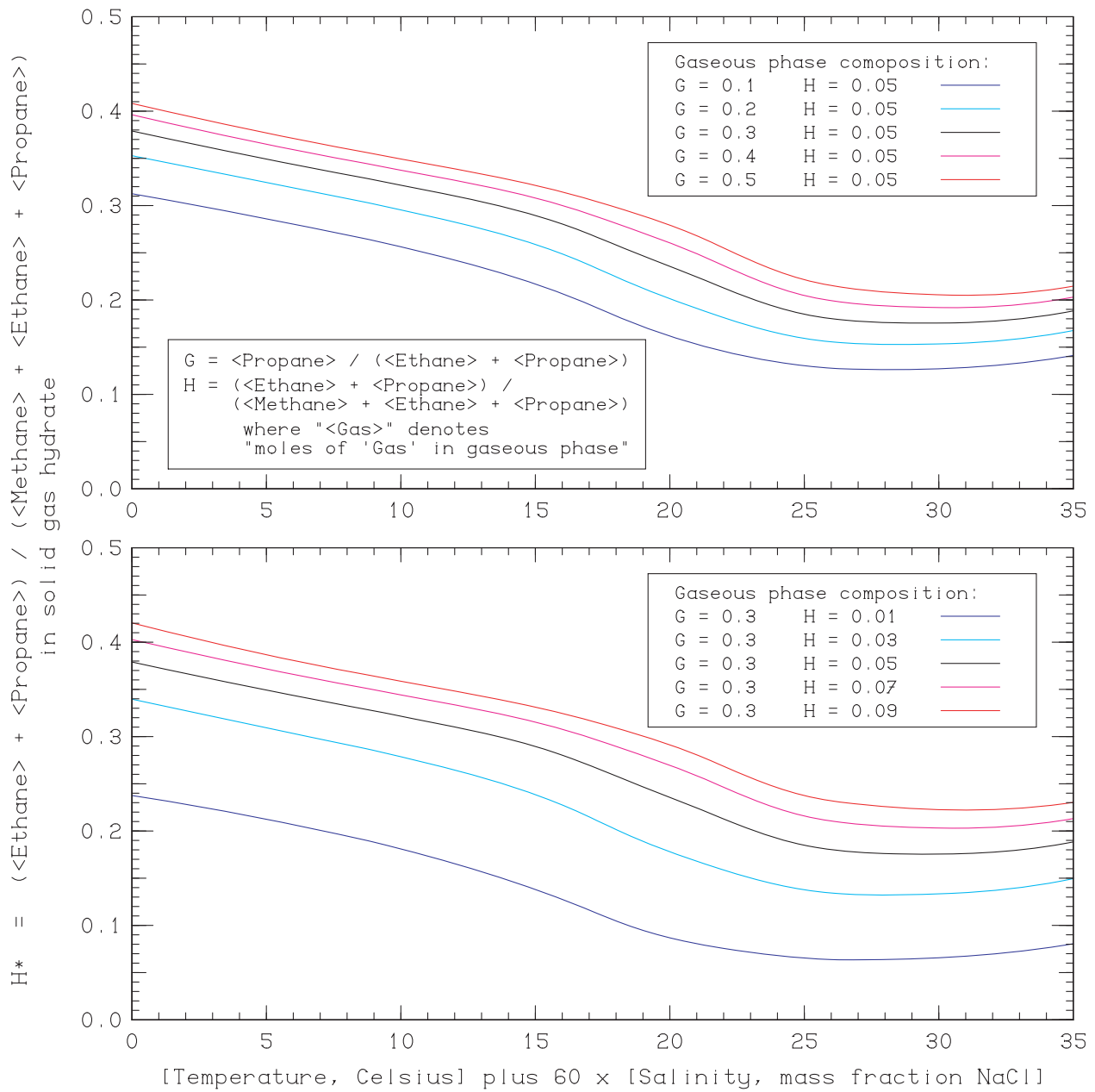


Figure 23. Influence of feed-gas composition, brine salinity and temperature upon solid hydrate CH_4 content relative to other hydrocarbons.

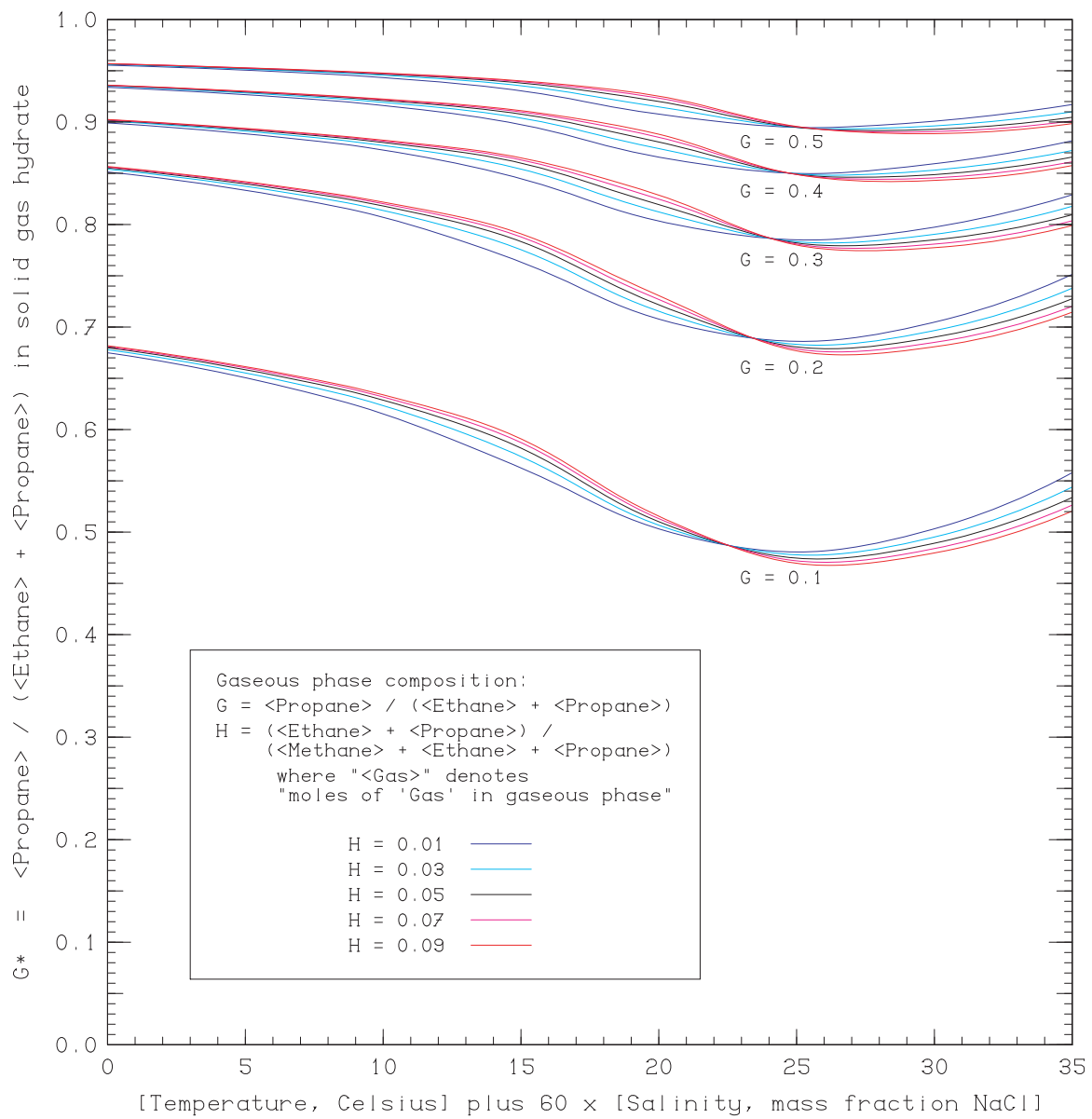


Figure 24. Influence of feed-gas composition, brine salinity and temperature upon solid hydrate C_3H_8 content relative to C_2H_6 .

Future Work

Because of the significant additional effort required to formulate the correlations for the hydrate-liquid-gas equilibrium conditions, the code development is somewhat behind schedule. During the next few months, we will continue to work on incorporating the new constitutive description into the THROBS and/or STAR simulator(s).

References

Garg, S.K., Pritchett, J.W., Katoh, A., Baba, K., Fuji, T. (2008), A mathematical model for the formation and dissociation of methane hydrates in the marine environment, *Journal of Geophysical Research*, Vol. 113, B01201, doi:10.1029/2006JB004768.

Mann, S.L., McClure, L.M., Poettmann, F.H., Sloan, E.D. (1989), Vapor-Solid Equilibrium Ratios for Structure I and II Natural Gas Hydrates, *Proceedings 68th Gas Processors Association Annual Convention*, San Antonio, Texas, March 13-14, pp. 60-74.

McGee, T., Woolsey, J.R., Lapham, L., Kleinberg, R., Macelloni, L., Battista, B., Knapp, C., Caruso, S., Goebel, V., Chapman, R., Gerstoft, P. (2008), Structure of a Carbonate/Hydrate Mound in the Northern Gulf of Mexico, *Proceedings of the 6th International Conference on Gas Hydrates (ICGH 2008)*, Vancouver, British Columbia, Canada, July 6-10, 10 pp.

Sassen, R., Roberts, H.H., Jung, W., Lutken, C.B., DeFreitas, D.A., Sweet, S.T., Guinasso, N.L. (2006), The Mississippi Canyon 118 Gas Hydrate Site: A Complex Natural System, *Offshore Technology Conference*, Houston, Paper No. 18132.

Sloan, E.D. Jr. (1998), *Clathrate Hydrates of Natural Gases*, Marcel Dekker Inc., New York, 703 pp.

Appendix: Results of CSMHYD Calculations

CSMHYD results listed in Tables 2.1 – 2.8.

Input specifications to CSMHYD:

- Structure II hydrate assumed.
- H₂O present, NaCl absent.
- Three hydrocarbon species present (CH₄, C₂H₆, C₃H₈).
- Feedgas mole fraction of CH₄ = (1 – H)
- Feedgas mole fraction of C₂H₆ = H × (1 – G)
- Feedgas mole fraction of C₃H₈ = H × G
- Values of T_{adj} considered: 0°C, 5°C, 10°C, 15°C, 20°C, 25°C, 30°C, and 35°C.
- Values of H considered: 0.00, 0.02, 0.04, 0.06, 0.08, and 0.10.
- Values of G considered: 0.000, 0.125, 0.250, 0.375, 0.500, and 1.000.
- Output quantities: P_{eq} , H^* and G^* where:
$$H^* = (\langle C_2H_6 \rangle + \langle C_3H_8 \rangle) / (\langle CH_4 \rangle + \langle C_2H_6 \rangle + \langle C_3H_8 \rangle) \text{ in hydrate,}$$
$$G^* = \langle C_3H_8 \rangle / (\langle C_2H_6 \rangle + \langle C_3H_8 \rangle) \text{ in hydrate, and}$$

“< >” means “moles”.

TABLE 2. CSMHYD results

Table 2.1: CSMHYD results for $T_{adj} = 0^{\circ}\text{C}$:

H	G	P_{eq} (MPa)	H^*	G^*
0.00	0.000	2.56	0.0000	0.0000
0.02	0.000	2.27	0.1142	0.0000
0.02	0.125	1.89	0.2348	0.7509
0.02	0.250	1.60	0.2888	0.8768
0.02	0.375	1.42	0.3204	0.9282
0.02	0.500	1.29	0.3418	0.9558
0.02	1.000	0.96	0.3913	1.0000
0.04	0.000	2.13	0.1795	0.0000
0.04	0.125	1.55	0.3042	0.7535
0.04	0.250	1.22	0.3518	0.8786
0.04	0.375	1.07	0.3776	0.9293
0.04	0.500	0.99	0.3929	0.9565
0.04	1.000	0.74	0.4356	1.0000
0.06	0.000	2.04	0.2220	0.0000
0.06	0.125	1.36	0.3400	0.7547
0.06	0.250	1.11	0.3794	0.8790
0.06	0.375	0.94	0.4040	0.9295
0.06	0.500	0.84	0.4209	0.9568
0.06	1.000	0.61	0.4638	1.0000
0.08	0.000	1.92	0.2531	0.0000
0.08	0.125	1.24	0.3633	0.7556
0.08	0.250	0.98	0.4033	0.8797
0.08	0.375	0.84	0.4239	0.9297
0.08	0.500	0.74	0.4408	0.9569
0.08	1.000	0.54	0.4853	1.0000
0.10	0.000	1.83	0.2767	0.0000
0.10	0.125	1.11	0.3828	0.7566
0.10	0.250	0.90	0.4168	0.8798
0.10	0.375	0.77	0.4396	0.9299
0.10	0.500	0.68	0.4568	0.9569
0.10	1.000	0.48	0.5035	1.0000

Table 2.2: CSMHYD results for $T_{adj} = 5^{\circ}\text{C}$:

H	G	P_{eq} (MPa)	H^*	G^*
0.00	0.000	4.40	0.0000	0.0000
0.02	0.000	3.93	0.0996	0.0000
0.02	0.125	3.19	0.2070	0.7275
0.02	0.250	2.75	0.2600	0.8638
0.02	0.375	2.46	0.2917	0.9205
0.02	0.500	2.24	0.3131	0.9511
0.02	1.000	1.74	0.3591	1.0000
0.04	0.000	3.61	0.1611	0.0000
0.04	0.125	2.66	0.2767	0.7316
0.04	0.250	2.20	0.3214	0.8665
0.04	0.375	1.93	0.3463	0.9220
0.04	0.500	1.74	0.3630	0.9521
0.04	1.000	1.32	0.4005	1.0000
0.06	0.000	3.38	0.2028	0.0000
0.06	0.125	2.35	0.3127	0.7339
0.06	0.250	1.91	0.3513	0.8676
0.06	0.375	1.66	0.3730	0.9228
0.06	0.500	1.48	0.3880	0.9526
0.06	1.000	1.11	0.4237	1.0000
0.08	0.000	3.20	0.2331	0.0000
0.08	0.125	2.15	0.3355	0.7353
0.08	0.250	1.73	0.3704	0.8685
0.08	0.375	1.49	0.3906	0.9232
0.08	0.500	1.33	0.4049	0.9528
0.08	1.000	0.98	0.4407	1.0000
0.10	0.000	3.06	0.2563	0.0000
0.10	0.125	2.00	0.3518	0.7362
0.10	0.250	1.60	0.3845	0.8689
0.10	0.375	1.37	0.4039	0.9235
0.10	0.500	1.22	0.4181	0.9529
0.10	1.000	0.89	0.4548	1.0000

Table 2.3: CSMHYD results for $T_{adj} = 10^\circ\text{C}$:

H	G	P_{eq} (MPa)	H^*	G^*
0.00	0.000	7.40	0.0000	0.0000
0.02	0.000	6.71	0.0841	0.0000
0.02	0.125	5.62	0.1743	0.6944
0.02	0.250	4.90	0.2267	0.8452
0.02	0.375	4.39	0.2600	0.9096
0.02	0.500	4.01	0.2829	0.9445
0.02	1.000	3.12	0.3314	1.0000
0.04	0.000	6.21	0.1404	0.0000
0.04	0.125	4.73	0.2459	0.7014
0.04	0.250	3.94	0.2923	0.8499
0.04	0.375	3.45	0.3184	0.9124
0.04	0.500	3.11	0.3355	0.9463
0.04	1.000	2.36	0.3715	1.0000
0.06	0.000	5.84	0.1803	0.0000
0.06	0.125	4.19	0.2839	0.7053
0.06	0.250	3.43	0.3237	0.8523
0.06	0.375	2.97	0.3455	0.9137
0.06	0.500	2.66	0.3598	0.9469
0.06	1.000	2.00	0.3917	1.0000
0.08	0.000	5.55	0.2101	0.0000
0.08	0.125	3.83	0.3079	0.7077
0.08	0.250	3.10	0.3429	0.8536
0.08	0.375	2.67	0.3622	0.9144
0.08	0.500	2.38	0.3753	0.9475
0.08	1.000	1.78	0.4058	1.0000
0.10	0.000	5.32	0.2332	0.0000
0.10	0.125	3.57	0.3246	0.7095
0.10	0.250	2.86	0.3565	0.8547
0.10	0.375	2.46	0.3744	0.9151
0.10	0.500	2.19	0.3868	0.9478
0.10	1.000	1.63	0.4170	1.0000

Table 2.4: CSMHYD results for $T_{adj} = 15^\circ\text{C}$:

H	G	P_{eq} (MPa)	H^*	G^*
0.00	0.000	13.04	0.0000	0.0000
0.02	0.000	12.04	0.0658	0.0000
0.02	0.125	10.51	0.1327	0.6428
0.02	0.250	9.31	0.1817	0.8135
0.02	0.375	8.37	0.2173	0.8909
0.02	0.500	7.63	0.2435	0.9331
0.02	1.000	5.83	0.3009	1.0000
0.04	0.000	11.27	0.1143	0.0000
0.04	0.125	8.95	0.2045	0.6533
0.04	0.250	7.48	0.2553	0.8230
0.04	0.375	6.50	0.2857	0.8967
0.04	0.500	5.81	0.3055	0.9372
0.04	1.000	4.33	0.3452	1.0000
0.06	0.000	10.67	0.1510	0.0000
0.06	0.125	7.95	0.2468	0.6600
0.06	0.250	6.45	0.2919	0.8277
0.06	0.375	5.54	0.3168	0.8996
0.06	0.500	4.93	0.3327	0.9387
0.06	1.000	3.64	0.3650	1.0000
0.08	0.000	10.19	0.1797	0.0000
0.08	0.125	7.25	0.2741	0.6645
0.08	0.250	5.80	0.3138	0.8308
0.08	0.375	4.96	0.3351	0.9015
0.08	0.500	4.40	0.3487	0.9398
0.08	1.000	3.24	0.3777	1.0000
0.10	0.000	9.81	0.2025	0.0000
0.10	0.125	6.75	0.2932	0.6675
0.10	0.250	5.35	0.3286	0.8326
0.10	0.375	4.56	0.3475	0.9025
0.10	0.500	4.03	0.3599	0.9403
0.10	1.000	2.97	0.3872	1.0000

Table 2.5: CSMHYD results for $T_{adj} = 20^\circ\text{C}$:

H	G	P_{eq} (MPa)	H^*	G^*
0.00	0.000	24.44	0.0000	0.0000
0.02	0.000	23.11	0.0486	0.0000
0.02	0.125	21.15	0.0900	0.5767
0.02	0.250	19.43	0.1250	0.7648
0.02	0.375	17.90	0.1549	0.8573
0.02	0.500	16.55	0.1806	0.9114
0.02	1.000	12.54	0.2513	1.0000
0.04	0.000	22.04	0.0869	0.0000
0.04	0.125	18.81	0.1492	0.5811
0.04	0.250	16.22	0.1958	0.7727
0.04	0.375	14.16	0.2310	0.8650
0.04	0.500	12.53	0.2574	0.9177
0.04	1.000	8.78	0.3131	1.0000
0.06	0.000	21.18	0.1176	0.0000
0.06	0.125	17.08	0.1903	0.5852
0.06	0.250	14.07	0.2393	0.7789
0.06	0.375	11.90	0.2725	0.8708
0.06	0.500	10.34	0.2948	0.9220
0.06	1.000	7.18	0.3375	1.0000
0.08	0.000	20.49	0.1427	0.0000
0.08	0.125	15.78	0.2199	0.5884
0.08	0.250	12.58	0.2677	0.7837
0.08	0.375	10.46	0.2972	0.8748
0.08	0.500	9.04	0.3160	0.9244
0.08	1.000	6.28	0.3512	1.0000
0.10	0.000	19.93	0.1634	0.0000
0.10	0.125	14.79	0.2419	0.5906
0.10	0.250	11.52	0.2872	0.7873
0.10	0.375	9.50	0.3134	0.8772
0.10	0.500	8.19	0.3297	0.9260
0.10	1.000	5.70	0.3605	1.0000

Table 2.6: CSMHYD results for $T_{adj} = 25^\circ\text{C}$:

H	G	P_{eq} (MPa)	H^*	G^*
0.00	0.000	45.76	0.0000	0.0000
0.02	0.000	44.00	0.0405	0.0000
0.02	0.125	41.34	0.0713	0.5492
0.02	0.250	39.04	0.0967	0.7394
0.02	0.375	37.00	0.1182	0.8360
0.02	0.500	35.19	0.1368	0.8947
0.02	1.000	29.40	0.1918	1.0000
0.04	0.000	42.60	0.0731	0.0000
0.04	0.125	38.21	0.1190	0.5462
0.04	0.250	34.72	0.1529	0.7371
0.04	0.375	31.83	0.1793	0.8355
0.04	0.500	29.37	0.2006	0.8948
0.04	1.000	22.20	0.2576	1.0000
0.06	0.000	41.48	0.0999	0.0000
0.06	0.125	35.88	0.1534	0.5430
0.06	0.250	31.69	0.1899	0.7357
0.06	0.375	28.36	0.2169	0.8349
0.06	0.500	25.62	0.2380	0.8950
0.06	1.000	18.08	0.2911	1.0000
0.08	0.000	40.59	0.1223	0.0000
0.08	0.125	34.10	0.1793	0.5407
0.08	0.250	29.48	0.2159	0.7341
0.08	0.375	25.90	0.2422	0.8344
0.08	0.500	23.01	0.2623	0.8955
0.08	1.000	15.51	0.3108	1.0000
0.10	0.000	39.88	0.1413	0.0000
0.10	0.125	32.73	0.1994	0.5381
0.10	0.250	27.81	0.2351	0.7329
0.10	0.375	24.08	0.2604	0.8341
0.10	0.500	21.13	0.2792	0.8957
0.10	1.000	13.81	0.3235	1.0000

Table 2.7: CSMHYD results for $T_{adj} = 30^{\circ}\text{C}$:

H	G	P_{eq} (MPa)	H^*	G^*
0.00	0.000	80.02	0.0000	0.0000
0.02	0.000	77.36	0.0396	0.0000
0.02	0.125	73.00	0.0713	0.5694
0.02	0.250	69.43	0.0958	0.7516
0.02	0.375	66.39	0.1156	0.8433
0.02	0.500	63.76	0.1320	0.8985
0.02	1.000	55.72	0.1780	1.0000
0.04	0.000	75.29	0.0712	0.0000
0.04	0.125	68.32	0.1166	0.5617
0.04	0.250	63.16	0.1472	0.7447
0.04	0.375	59.07	0.1699	0.8376
0.04	0.500	55.67	0.1875	0.8944
0.04	1.000	46.05	0.2325	1.0000
0.06	0.000	73.65	0.0971	0.0000
0.06	0.125	64.94	0.1487	0.5562
0.06	0.250	58.90	0.1805	0.7396
0.06	0.375	54.28	0.2028	0.8338
0.06	0.500	50.56	0.2197	0.8917
0.06	1.000	40.39	0.2608	1.0000
0.08	0.000	72.37	0.1188	0.0000
0.08	0.125	62.40	0.1728	0.5509
0.08	0.250	55.81	0.2041	0.7354
0.08	0.375	50.90	0.2254	0.8305
0.08	0.500	47.00	0.2411	0.8897
0.08	1.000	36.64	0.2783	1.0000
0.10	0.000	71.36	0.1374	0.0000
0.10	0.125	60.45	0.1917	0.5472
0.10	0.250	53.58	0.2218	0.7319
0.10	0.375	48.39	0.2418	0.8280
0.10	0.500	44.39	0.2564	0.8877
0.10	1.000	33.99	0.2903	1.0000

Table 2.8: CSMHYD results for $T_{adj} = 35^\circ\text{C}$:

H	G	P_{eq} (MPa)	H^*	G^*
0.00	0.000	129.54	0.0000	0.0000
0.02	0.000	124.89	0.0438	0.0000
0.02	0.125	116.61	0.0846	0.6222
0.02	0.250	110.52	0.1122	0.7870
0.02	0.375	105.68	0.1327	0.8659
0.02	0.500	101.65	0.1488	0.9133
0.02	1.000	90.09	0.1906	1.0000
0.04	0.000	121.37	0.0774	0.0000
0.04	0.125	108.99	0.1313	0.6093
0.04	0.250	100.91	0.1623	0.7762
0.04	0.375	94.89	0.1834	0.8571
0.04	0.500	90.08	0.1990	0.9070
0.04	1.000	77.05	0.2368	1.0000
0.06	0.000	118.66	0.1043	0.0000
0.06	0.125	103.78	0.1624	0.6004
0.06	0.250	94.72	0.1928	0.7683
0.06	0.375	88.18	0.2126	0.8518
0.06	0.500	83.07	0.2270	0.9026
0.06	1.000	69.58	0.2603	1.0000
0.08	0.000	116.53	0.1264	0.0000
0.08	0.125	99.97	0.1851	0.5934
0.08	0.250	90.34	0.2140	0.7626
0.08	0.375	83.52	0.2324	0.8472
0.08	0.500	78.26	0.2454	0.8998
0.08	1.000	64.61	0.2751	1.0000
0.10	0.000	114.88	0.1450	0.0000
0.10	0.125	97.09	0.2027	0.5881
0.10	0.250	87.08	0.2298	0.7581
0.10	0.375	80.09	0.2467	0.8439
0.10	0.500	74.75	0.2587	0.8972
0.10	1.000	61.06	0.2854	1.0000

TASK 4: Geochemical investigations at MC 118: Pore fluid time series and gas hydrate stability.

Introduction.

Monitoring geochemical constituents over time is an essential task to determine gas hydrate stability and to quantify the flux of methane from the hydrate reservoirs. Hydrate stability is controlled by high pressure, low temperature, moderate salinity, and saturated gas content. When these conditions are not ideal, hydrates are destabilized via dissolution and dissociation, shown in Figure 25. **Dissociation** occurs when the pressure/temperature regime is outside of the hydrate stability zone and results in the release of gaseous methane. **Dissolution** occurs when the methane concentration in the surrounding seawater is below saturation and results in the release of dissolved methane from the hydrate. By understanding how these mechanisms work, we can truly evaluate the stability of worldwide hydrate deposits.

Hydrate dissociation has been widely studied and pressure, temperature, and salinity variables are often well defined in studies of natural hydrate deposits. However, *in situ* CH₄ concentrations are difficult to measure and have not been sufficiently analyzed. Yet we know that ocean water is devoid of methane and pore-fluids surrounding gas hydrates are greatly under-saturated with respect to CH₄ (Lapham et al., 2010). This means that shallow forming hydrates are meta-stable and should be dissolving. Because we found under-saturated conditions where hydrates were present, we hypothesized that kinetic factors, such as oil coatings, biofilms, or the hydrate structure, also control hydrate stability.

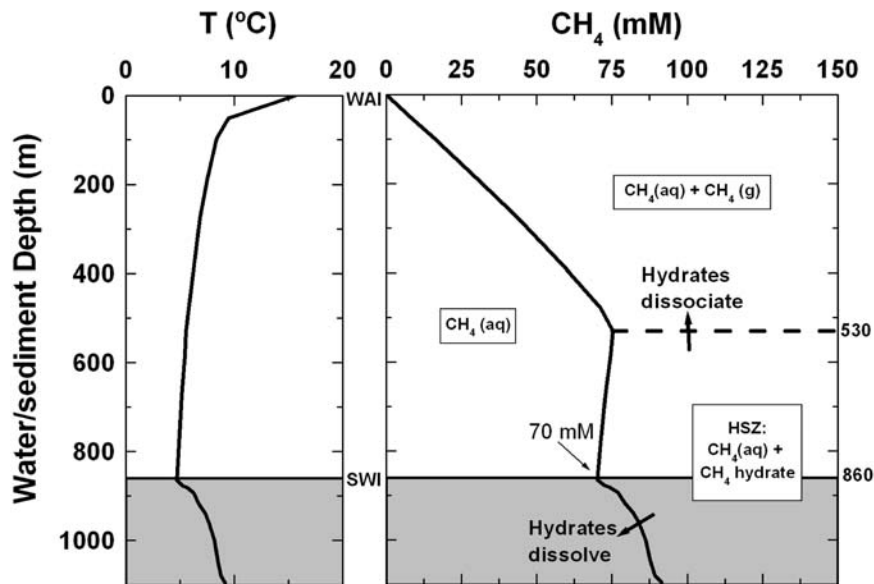


Figure 25. Our group has clarified the distinction between hydrate dissociation and dissolution.

Project goal

It is the goal of our work in the consortium to gather information on in situ methane concentrations over space and time both at the MC 118 monitoring station site and in the lab. By monitoring chemistries at the seafloor, and working with consortium geophysical partners, we hope to assess geochemical variability to define and give meaning to observed acoustic anomalies. We have preliminary evidence that geophysical temporal variability is reflected in geochemical variability (Lapham et al., 2008). Such information is critical to truly evaluating the stability of worldwide hydrate deposits.

Hypotheses posed

Hypothesis 1: Geophysical temporal variability will result in geochemical variability. By monitoring geochemical variability over time we can determine what is causing geophysical variability.

Hypothesis 2: While within the appropriate temperature and pressure field hydrate deposits are “meta-stable” when exposed to in situ CH₄ concentrations which are well below saturation. Under these conditions they dissolve at rates significantly below those predicted by thermodynamic equilibrium.

Approach

Several seafloor instruments have been designed and deployed to measure in situ methane gradients in both space and time. The Pore-Fluid Array (PFA) was developed to work in conjunction with geophysical techniques (Lapham et al., 2008) and is continuously being modified. Two PFA'S are currently deployed at the MC-118 site.

Main tasks completed

- Data from the first (2006) PFA deployment show that dissolved methane concentrations vary over time and are sensitive to tectonic activity. Prior to this deployment, such information was speculative.
- We have also built smaller, SSD-deployable pore-water instruments called peepers. These also show under-saturated pore-fluids at MC 118.
- Mini-PFA samplers have been constructed, deployed at a secondary site and analyzed. Results show porewaters at equilibrium methane concentrations, the first time such concentrations have been measured, to our knowledge.
- Lab experiments to measure hydrate dissolution have been conducted in pressure chambers. Dissolution rates calculated from the *in situ* CH₄ data are significantly below those predicted by assuming thermodynamic equilibrium.

Details of each hypothesis

Hypothesis 1: Geophysical temporal variability will result in geochemical variability. By monitoring geochemical variability over time we can determine what is causing geophysical variability.

Progress to date: We have been unable to retrieve the PFA samplers at MC 118 due to issues with the SSD. However we have developed two new mini-PFAs and deployed and recovered them at a secondary site. We are also working with consortium members to deploy these mini-PFAs on a retrievable ROVARD system. This system is completely autonomous of the SSD and may also enable us to retrieve samplers.

mini-PFA

We constructed two newly designed mini-PFAs that contain osmosamplers (Figure 26). Towards that end we participated in a R/V Tully Cruise in the Pacific Northwest and deployed and recovered these newly designed osmo-samplers at Barkley Canyon and Bubbly Gulch (Figure 27).

The mini-PFAs are essentially the same as the larger PFAs deployed at MC 118. There are four OsmoSampler pumps within the gray box in Figure 26. Each pump is attached to a port along a probe tip. The difference with this probe tip, compared to the larger PFA, is that it is short and can sample different sediment depth ranges from 2cm to 60cm. This allows for a more quantitative assessment of the methane flux from the sediments. The samplers are capable of storing up to ten months of water samples in ~300 meters of small-diameter copper tubing. Since the pumping rate of the samplers is known (~0.5mL/day), by cutting the copper coils in 4 meter sections, we can obtain a sample every ~6 days. Then, each sample can be analyzed for a variety of chemistries (CH₄ concentrations and stable isotopes, sulfate, and chloride) to provide a time-series over ~ a ten month period.

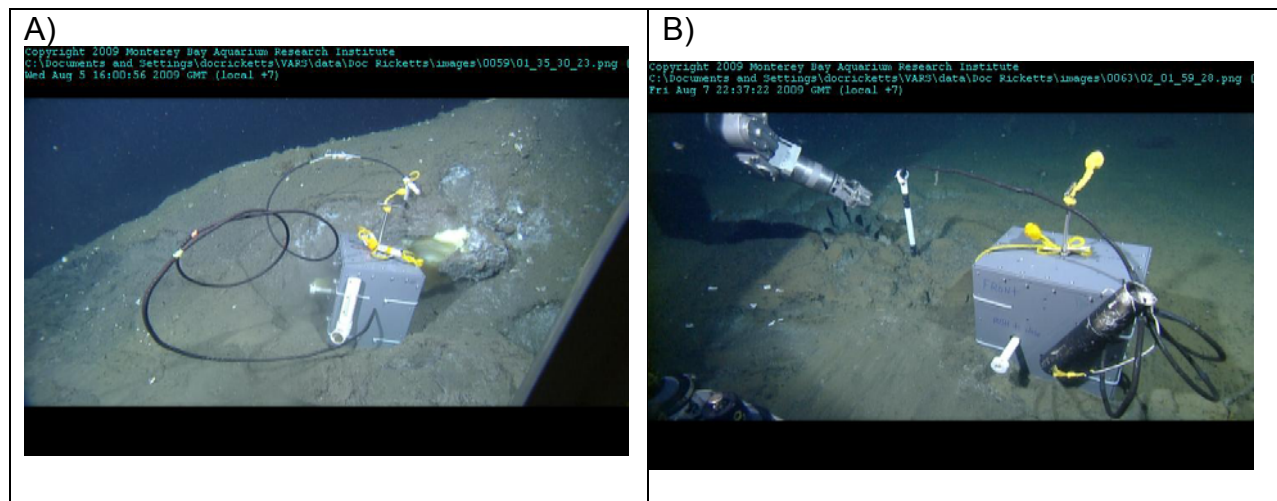


Figure 26. Seafloor pictures of mini-PFAs. Both were deployed with ROV Doc Ricketts (MBARI) and retrieved with ROV ROPOS. A) Barkley Canyon and B) Bubbly Gulch.

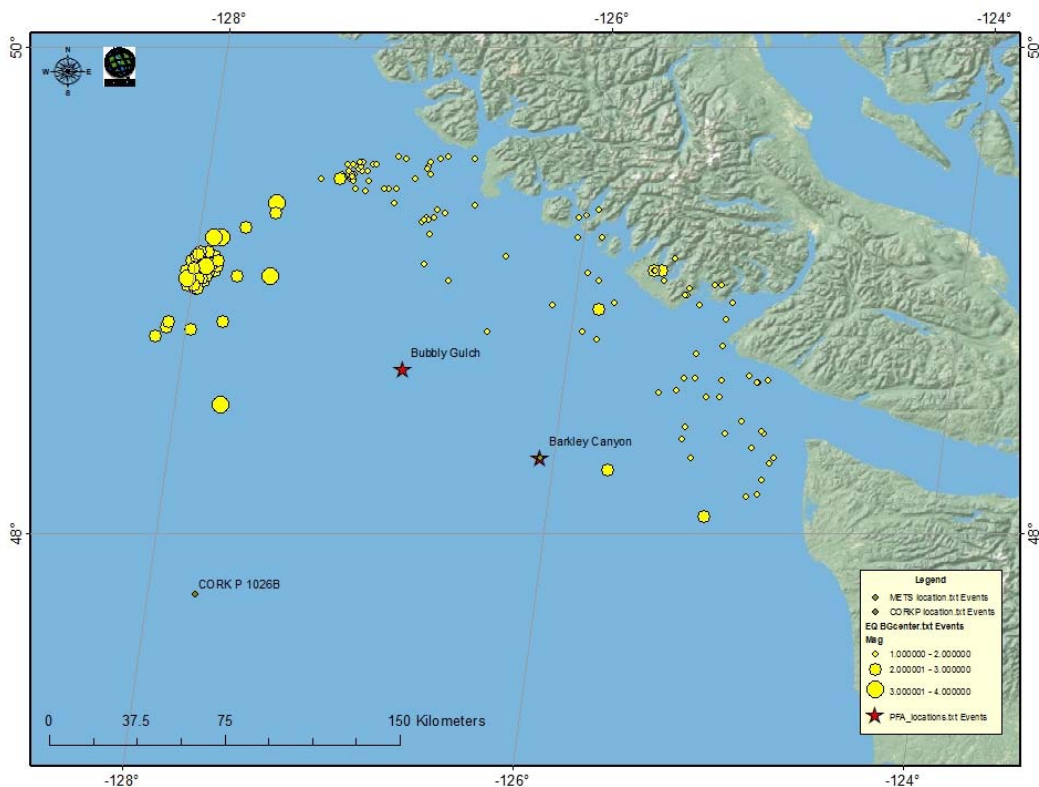


Figure 27. Location of mini-PFAs offshore Vancouver Island. The stars indicate the two sites, Barkley Canyon and Bubbly Gulch.

Design of the mini-PFAs.

Test deployment. Two of these newly designed mini-PFAs were deployed off Vancouver Island in a gas hydrate site in August 2009 (Figure 27). In May 2010, using the ROV ROPOS, we retrieved them and are currently processing the pore-fluids contained within the copper coils. Along with the OsmoSamplers, the mini-PFAs are equipped with bottom water temperature probes; temperature data from both instruments (data not shown) We have analyzed for methane concentrations, methane $\delta^{13}\text{C}$, sulfate and chloride (Figure 28). We have also analyzed for ethane and propane concentrations (data not shown). Complete interpretation of these data is pending. However, the preliminary results demonstrate that these instruments are capable of capturing geochemical variability at these sites with a resolution of approximately 6 days. Such geochemical variability has been shown to be related to geophysical variability giving an indication of geophysical changes that may be occurring at this site (Lapham et al. 2008). The methane concentrations measured in these samples approach and exceed expected methane saturation values (58 to 70mM) for these sites. To our knowledge this is the first time such high concentrations of dissolved methane have been measured from natural environments. The methane $\delta^{13}\text{C}$ values that we measure at the sites are indicative of biogenic methane at Bubbly Gulch and thermogenic methane at Barclay Canyon. This data-set gives an example of the sort of data we hope to obtain from MC 118.

Highlights of mini-PFA accomplishments

- 2 mini-PFAs were deployed off Cascadia Margin in Aug 2009 and recovered in April 2010. Each had 4 OsmoSamplers with ~300 meters of copper tubing per sampler.
- One mini-PFA was placed at Barkley Canyon (850m water depth) to determine saturation state of methane within 4 cm of the hydrate surface
- One was placed at a new site, “Bubbly Gulch” (1250m water depth) where the seafloor was bulging, creating cracks in the sediments from which bubbles escaped.
- Based on the measured concentration gradient from Barkley Canyon, the methane flux is calculated to give a dissolution rate of 0.3cm/year.
- We are currently working to develop a PFA to deploy at MC 118 without the SSD.

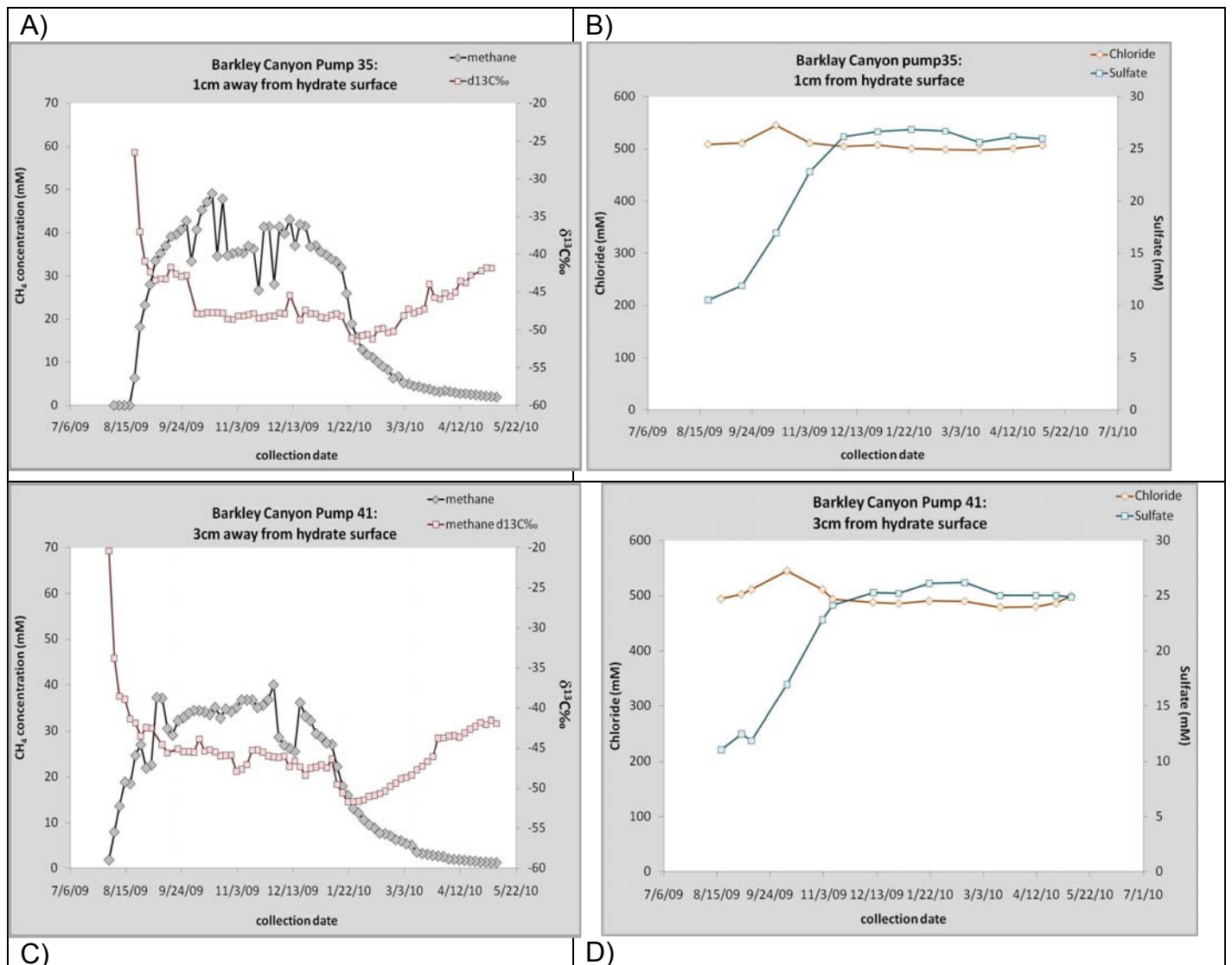


Figure 28: Time-series data for two samplers within the mini-PFA deployed at Barkley Canyon. A) methane concentrations and stable isotopes 1cm from hydrate surface. B) sulfate and chloride concentrations 1cm from hydrate surface. C) methane concentrations and stable isotopes 3cm from hydrate surface. D) Sulfate and chloride concentrations 3cm from hydrate surface. Complete interpretation of data is pending.

Hypothesis 2: While within the appropriate temperature and pressure field hydrate deposits are “meta-stable” when exposed to in situ CH₄ concentrations which are well below saturation. Under these conditions they dissolve at rates significantly below those predicted by thermodynamic equilibrium.

The distinction between Disassociation and Dissolution.

There are three primary factors that control the stability of gas hydrates: pressure, temperature, and the concentration of the guest molecules in the surrounding environment. Pressure and temperature govern the stability of hydrate structure. When pressure regimes are too low or temperatures are raised too high hydrate becomes unstable and decomposes by **dissociation**. Dissociation is a relatively fast, often violent form of decomposition that results in the release of methane gas bubbles (CH_{4(g)}) to the surrounding water. If the pressure and temperature regime are within the range of hydrate stability, but the concentration of the guest molecule in the surrounding water is below saturation, the hydrate will become unstable and decompose by **dissolving** into the surrounding water. In this case, decomposition is typically at a slower rate and in a less spectacular manner than that observed during dissociation. It is the mechanisms that control dissolution in natural environments that are of most interest in the current proposal. Please see Figure 25.

Rehder et al. (2004) and Hester et al. (2009) used artificially produced hydrate in natural conditions to measure the dissolution rate of hydrates in regimes where temperature and pressure conditions would not result in dissociation of the hydrate. Using synthetic hydrate in under-saturated seawater conditions resulted in dissolution rates for both experiments exceeding 100 cm/yr. However, observations of natural hydrate formations do not support such high rates of dissolution in under-saturated water conditions. Bush Hill is a large gas hydrate pingo located on the seafloor in the Gulf of Mexico in 570 m of seawater. The pressure at this site is ~840psi and temperature averages 7.9°C (MacDonald et al. 2005). These values are within the hydrate stability field, thus we would not expect hydrate dissociation to be occurring at this site. However, the surrounding seawater is under-saturated with respect to methane concentrations, thus we would expect that the hydrate outcrop should be dissolving into the surrounding seawater. Video equipment installed by MacDonald et al. (2005) monitored the Bush Hill hydrate formation over the period of a year. Despite changes in microbial mat cover and inhabitation by marine life, over the observation period, the shape and size of the hydrate formation remained relatively little changed, and certainly was not dissolving at a rate of 100 cm/yr. Similarly, a hydrate outcrop observed at Barkley Canyon (Cascadia Margin) was observed first in 2004 and again revisited in 2006, photographs of the hydrate formation indicate little change in the size over the two year period indicating that dissolution rates at this site are also less than 100 cm/yr. Lapham et al. (2010) provide further evidence of slow dissolution rates at a Barkley Canyon site. In their study, Lapham et al. (2010) estimated hydrate dissolution rates of outcropping hydrate to be ~3.5 cm/yr based on observations of an opening fissure in the hydrate formation. This value is approximately an order of magnitude lower than the calculated dissolution rate given the concentration of methane in the surrounding seawater assuming diffusion controlled dissolution (30cm/yr). They also provided dissolution rates for buried hydrates based on flux calculations from measured

concentration gradients in water surrounding buried hydrates and found dissolution rates two orders of magnitude lower than those estimated from outcrops (Lapham et al., 2010).

Two mechanisms have been proposed to account for observed stability of hydrate in conditions where under-saturated methane concentrations should result in rapid dissolution of hydrate formations. The first proposed mechanism is the so-called “push-pop” model in which the dissolution of hydrate from the top of the formation is being approximately balanced by resupply of hydrate formation from the bottom as gas migrating upward through the sediment enters the hydrate stability zone (HSZ) and begins to form hydrate from the bottom of the formation. However, Lapham et al. (2010) measured methane concentrations in the porewater of the sediment drape overlying the hydrate formation at the Barkley Canyon and Mississippi sites. They found uniformly low methane concentrations (~0-5 mM). Thus it does not seem that the hydrate formations are rapidly shedding methane to the overlying seawater, indicating that the “apparent” natural hydrate stability at these sites is not the result of resupply of hydrate from below approximately balancing dissolution of hydrate to the overlying seawater. Using sulfate concentrations and $\delta^{13}\text{C}$ values to constrain anaerobic methane oxidation rates, Lapham et al. (2010) found that although microbial methanotrophy was likely occurring at these sites, even accounting for this consumption of methane the porewaters surrounding the hydrate are still highly under-saturated with respect to methane. The second hypothesis to explain the apparent stability of natural hydrate in under-saturated water is that conditions in or components of natural hydrate are acting to slow the dissolution rate below what would be expected by pure diffusion controlled dissolution. Figure 29, showing pictures of the so-called sleeping dragon outcrop from 2006 and 2010 show the similarities (and some differences) in the feature. While analysis continues, the basic shape and morphology of the outcrop have persisted over 4 years, consistent with stability of these outcrops.

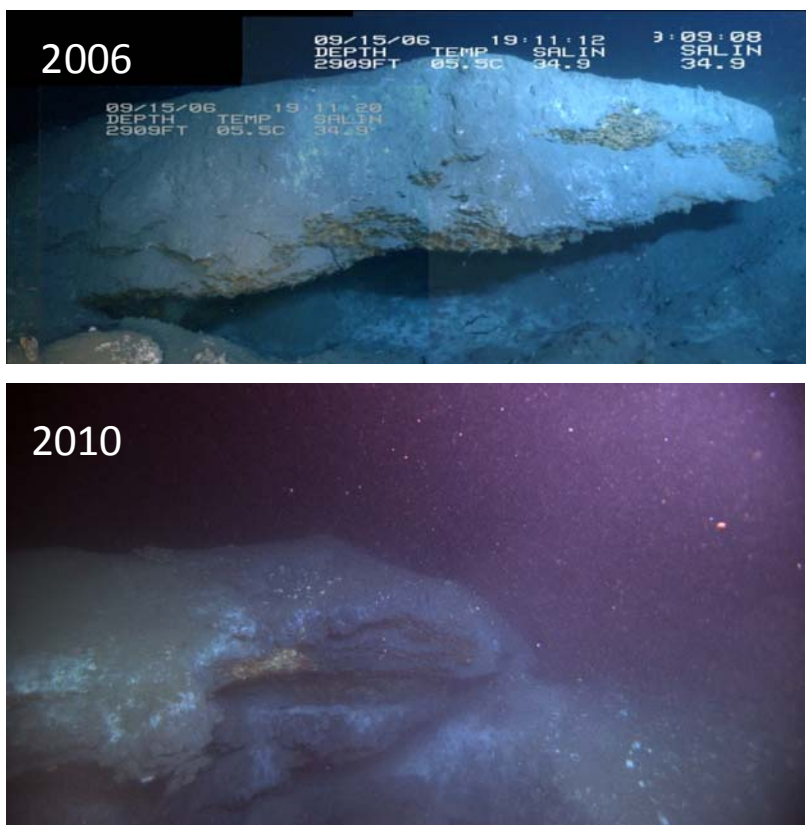


Figure 29. Photo-comparison of “sleeping dragon” at MC 118 between 2006 (photo courtesy of GOMHRC and the Johnson SeaLink and 2010 (photo courtesy of Chuck Fisher and the Lophelia II cruise).

Laboratory Component

In summary, studies examining dissolution of artificial hydrates have found rates in excess of 100cm/yr (Hester et al. 2004, Bigalke et al. 2009, Rehder et al. 2009); however observations of natural hydrate formations have given rise to estimates of dissolution rates an order of magnitude lower (MacDonald et al. 2005; Lapham et al. 2010). We wish to examine factors that could be acting to inhibit dissolution of gas hydrates to understand the controls on dissolution in the natural environment.

We initially hypothesized that the gas composition of natural hydrates could be acting to slow dissolution rates. We know that incorporation of ethane and propane into the hydrate structure (strII) act to stabilize the hydrate; we were interested in discovering if this enhanced stability also contributes to slow dissolution of the hydrate. In order to test this possibility we measured the dissolution rate of pure methane (strI hydrate) in the lab. We calculated a flux of 0.14mM/hour as the average of two experiments (Figure 30a) which gives us a dissolution rate of 30cm/yr. We then measured the dissolution rate of a mixed-gas (C₁-C₃; str II) hydrate to measure whether the increased stability of strII hydrates would also result in slower dissolution rates. However, we calculated a similar dissolution rate of 27 cm/yr (Figure 30b)

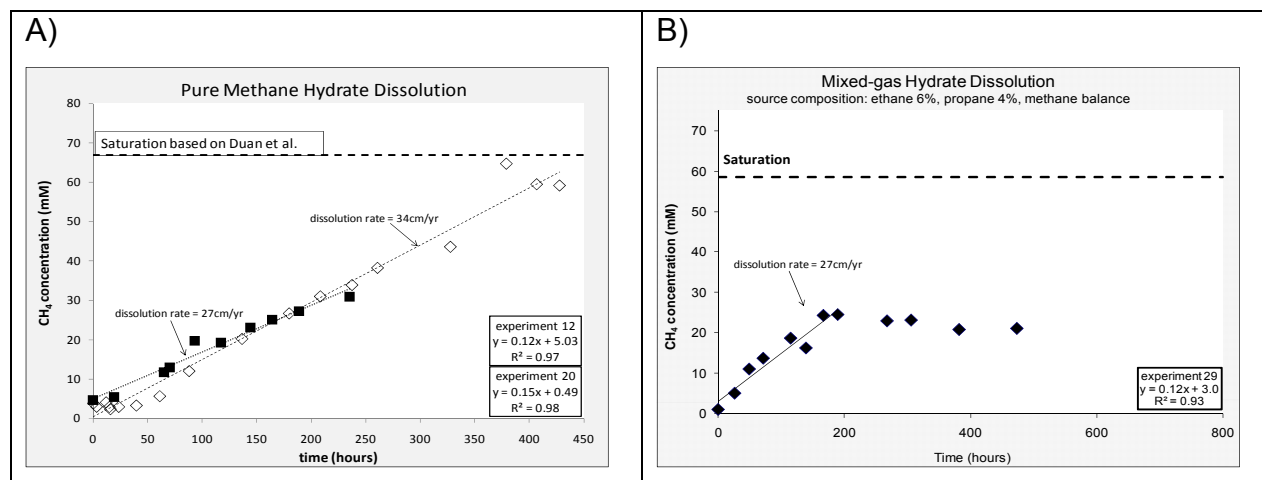


Figure 30. Results of Dissolution Experiments Comparing Dissolution Rates of StrI and StrII hydrates. In panel A are the results of two (replicated) experiments measuring the dissolution rate of methane (strI) hydrate in the lab. Panel B gives the results for strII (mixed-gas) hydrate. Dissolution of strI and strII hydrates over time are similar.

Thus, we failed to find any difference in dissolution rates of mixed-gas and pure methane hydrates formed in the lab demonstrating that the presence of C₂ and C₃ hydrocarbons does not slow the dissolution rate of hydrate.

Another potential factor that could be inhibiting hydrate dissolution is the presence of oils. Such oils on the surface of hydrate could act as “armoring agents” to slow dissolution rates. However, instead of slowing dissolution, the addition of oil sped up hydrate dissolution (Figure 31)!

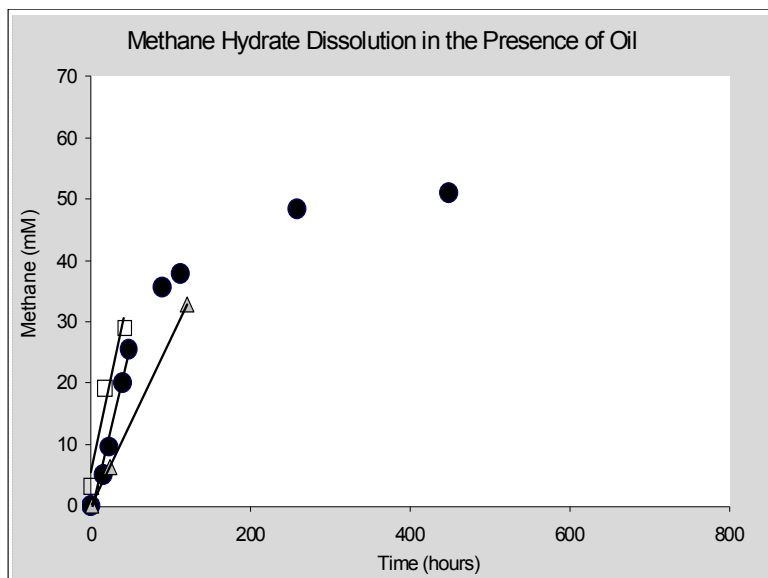


Figure 31. Effect of Oil on hydrate dissolution.

TABLE 3. Dissolution rates of natural and artificial hydrate are summarized below. It appears from this summary that rates on the order of 100 cm per year are the result of stirring or currents in the water column. Diffusion controlled dissolution is on the order of 30 cm per year. Rates in nature are on the order of 0.3 to 3 cm/year.

Hydrate Type	Dissolution rate	Study
synthetic hydrate in water column	167 cm/yr	Rehder et al. (2009)
synthetic hydrate in water column	110 cm/yr	Hester et al. (2004)
synthetic hydrate stirred lab study	~100 cm/yr	Bigalke et al. (2009)
<i>In situ</i> natural hydrate in water column at Barkley Canyon site	3.5 cm/yr	Lapham et al. (2010)
Synthetic methane hydrate lab experiment, no stirring	30 cm/yr	Our lab experiments
Synthetic mixed-gas hydrate lab experiment, no stirring	27 cm/yr	Our lab experiments
Synthetic methane hydrate lab experiment, no stirring, with oil	~100 cm/yr	Our lab experiments
<i>In situ</i> measurements of Barkley Canyon hydrate dissolution	Max = 0.3 cm/yr	Our field measurements With osmo sampler, figure 4.

1. Publications

- a. Lapham, L.L., J.P. Chanton, R. Chapman, and C.S. Martens. 2010. Methane under-saturated fluids in deep-sea sediments: Implications for gas hydrate stability. Accepted for publication Earth and Planetary Science Letters. 298 275-285.
- b. Luzinova, Y, G. T. Dobbs, L. Lapham, J. Chanton, B. Mizaikoff. Detection of cold seep derived authigenic carbonates with infrared spectroscopy. Marine Chemistry, in press.
- c. Lapham, LL., R. Y, Wilson, B. Anderson, Samantha Joye, Ian MacDonald, J. P. Chanton, Towards understanding processes controlling naturally forming gas hydrate through both in situ and laboratory experiments. Geochim. Cosmochim Acta, in preparation.

2. Cruise participation

- a. September 2010. Jeff Chanton to MC 118 to retrieve and replace PFA sampler box. Water column work successful.

3. Presentations

- a. Fall AGU Lapham, L. R. Wilson, C. Paull, J. Chanton and M. Riedel. Measuring in situ dissolved methane concentrations in gas hydrate-rich systems Part 1: Investigating the correlation between tectonics and methane release from sediments. , presented at 2010 Fall Meeting, AGU, San Francisco, Calif., 13-17 Dec.
- b. Fall AGU. Wilson, R M., L. L. Lapham, M. Riedel, and J. P. Chanton. Measuring In situ Dissolved Methane Concentrations in Gas Hydrate-Rich Systems. Part 2: Investigating Mechanisms Controlling Hydrate Dissolution. presented at 2010 Fall Meeting, AGU, San Francisco, Calif., 13-17 Dec.
- c. Fall AGU. Sleeper, K., Bell, R., Short, T., Chanton, J., Wilson, R. D'Emidio, M., Macelloni, L. (2010), The Detection of Elevated Methane Concentration Indicate The Presence of Deep-Water Plumes Northwest of the DWH Site, Abstract OS21G-05 presented at 2010 Fall Meeting, AGU, San Francisco, Calif., 13-17 Dec.

TASK 5: Automated Biological/Chemical Monitoring System (ABCMS) for Offshore Oceanographic Carbon Dynamic Studies: Development of the Marine Lander Survey Vehicle for Gas Hydrate Research

The University of Georgia has assigned the University of Mississippi/DOE grant number 037757-02. In addition, a contract has been established between the University of Georgia (UGA) and SRI International (SRI) to support the SRI effort in the integration of in situ mass spectrometry with microbe sampling for gas hydrates research. The beginning and end dates of the project period are November 2010 through August 2011, respectively. General schematics have been drawn for the Lander components

which include the underwater mass spectrometer and multi filtration system. The Lander and surface vessel will be linked by the same fiber optic cable used for the SSD ROV. The electronics interfacing the fiber optic cable and Lander instrumentation have been installed in a pressure housing and have undergone extensive laboratory testing.

Individual filter assemblies, or packs have been constructed (Figure 32) and will be installed in the Lander in groups of 30. Over 60 filter packs have been constructed to allow two complete filter groups to be deployed (one at a time) prior to disassembly, cleaning and reloading. The filter packs will be prefilled with distilled water to prevent contamination from surrounding water during deployment. Once deployed and upon pump activation, the distilled water will be displaced with seawater at the desired depth and location. The pump will continue to move seawater through the filter until the desired volume has been reached or the filter has been clogged. After collecting a sample, the pump injector can move from one filter pack to another so that multiple filters can be collected with varying pore sizes per sampling location. Upon recovery, the filter packs have pressure relief valves that will aid in equalizing the internal pressure that could potentially build as a result of deep water sampling.



Figure 32. Filter assembly mounted on distilled water pumping station.

The Lander frame has been constructed of stainless steel and is configured to house the filter rack (containing up to 30 individual filter packs); membrane introduction mass spectrometer (MIMS) and lithium battery pack; and Lander battery packs (Figure 33). The Lander has also been equipped with a color video camera that can send live video through the fiber optic interface to the surface vessel. The camera (with LED light ring) is positioned downward to view the seafloor and the additional lighting is angled to avoid backscatter from suspended solids. The camera and lights can be turned on/off as needed to avoid unnecessary drain on the Lander's batteries. The MIMS is mounted with multiple hinge clamps that can readily fasten the MIMS housing and battery pack in position. The MIMS interfaces with the Lander's electronics package where the RS-232 communication is converted to the fiber optic cable mounted on the R/V *Pelican*.

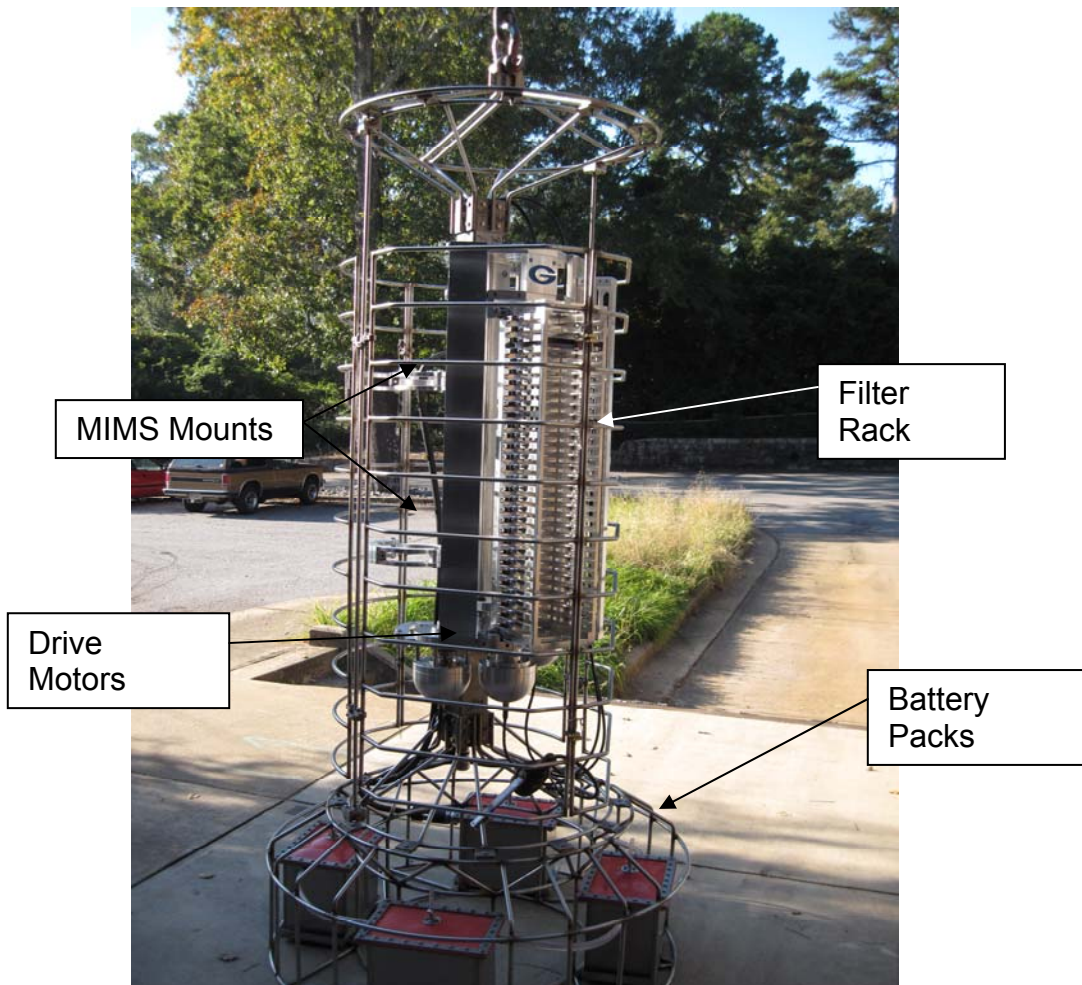


Figure 33. Marine Lander assembly.

Tim Short (SRI) transported the MIMS to UGA in Athens, GA in late August 2010 to test communication through the Lander electronics, a test optical fiber and the shipboard de-multiplexer electronics to a laptop computer. An IP address conflict prevented using the MIMS Ethernet communication link, so instead the MIMS serial (RS-232) output was converted to Ethernet for transmission over the optical fiber and converted back to a serial link using the shipboard electronics for communication with the laptop computer. Communication with the MIMS was established successfully. MIMS data were viewed in real time and control commands sent to the MIMS while also communicating with, and controlling the filtration system on the Lander.

SRI has also continued efforts to investigate methods to improve detection limits for methane using the MIMS by implementing a cold trap system between the membrane inlet and the ion source of the mass spectrometer. The major component of the cold trap will be a Model K508 cooler assembly from RICOR Cryogenic & Vacuum Systems. The chiller and two types of cold fingers were ordered through RMA Global, LLC and have all been received.

The conceptual design for a new smaller and lower power MIMS instrument has been established and nearly all of the major internal components (e.g., mass analyzer, high vacuum pump, roughing pump, and water sampling pump) have been ordered. An Inficon E3000 200 atomic mass unit (amu) sensor will serve as the mass analyzer. This analyzer has a more rugged construction than the CPM200 sensor used in previous SRI underwater MIMS systems. It also has two filaments in the ion source that are designed for high water vapor environments. The two filaments provide redundancy in case one filament fails during deployment. The high vacuum pump for the new system will be a Pfeiffer HiPace10 turbo pump, which is smaller and lower power than the Varian pumps used in prior instruments, and also allows use of a smaller lower power KNF diaphragm pump as the backing pump.

A simulated deployment test has been scheduled for the Lander at the Southwest Research Institute facility in San Antonio, Texas. The Lander will be outfitted with the existing MIMS for this test. By completing the simulated deployment to 1000 m, it is anticipated that any potential problems with the system can be identified prior to actual deployment at the MC118 Gulf of Mexico site.

TASK 6: Quantification of Seep Emissions by Multibeam Sonar at MC118.

EFFORT SUMMARY:

A Benthic Lander (Figure 34) has been constructed with a sonar/rotator/compass mounted with an axle. The sonar/compass unit is connected to the rotator by an axle. The compass/sonar head can be tilted along two axes such that the beam fans at an angle to perpendicular to minimize sonar returns from the seabed and surface. The compass housing has interior nickel magnetic shielding, with additional nickel shielding above the rotator.

A rotatable camera is mounted on a central (protection) pole to ensure rotator functioning, warn of seabed approach during deployment, and determine if bridle cable becomes entangled with the rotator. Also a CTD is mounted on a stabilization fin. All

sensors (Compass, CTD+O₂, camera, and sonar) are connected to an electronics bottle where serial signals are converted to Ethernet and connected to an Ethernet switch. Also connected to the switch is an embedded computer that controls the sensors and logs data. Data from the electronics bottle is converted to serial and transmitted through a 100-m cable to a shipboard computer.

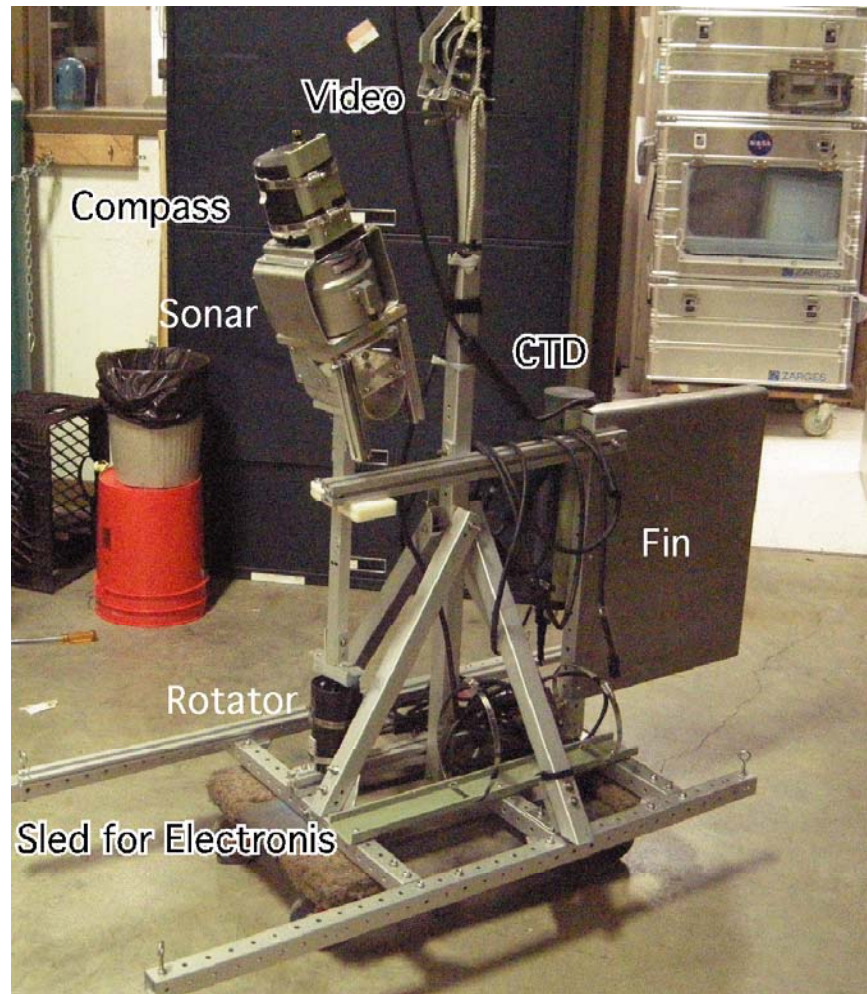


Figure 34. Photo of benthic lander.

Molex connectors in the bottle have all been potted to prevent them from being pushed into non-contact when connected. The electronics bottle uses separate regulators for each electronics item and sensor, with fan cooling. Electronics in the bottle are mounted on a sled and secured in place with Velcro. The sled also can be mounted in a smaller, 1000-m depth bottle.

We have developed a capability of making deepsea cable splices, by using vacuum-degassed potting compounds, and test the cables by winch-lowering to 300 m at sea, and have made cables and spare cables for connecting all sensors to the electronics bottles.

The lander was shipped to Russia on Friday, Feb 4, and construction of a second lander is almost finished, allowing for a planned field deployment in the Coal Oil Point seep field on Friday Feb. 11. A collaborative cruise/deployment is planned for the first week of March with Vernon Asper (USM), allowing a dual sonar application. Dr. Leifer leaves for Vladivostok, Russia (hand transporting electronics) March 21 for a month long expedition and deployment of the system in the East Siberian Sea. We also are acquiring a housing from Vernon to use for our Ocean Optics spectrometer for integration into the system, and are experimenting with potting USB cameras for inexpensive deepsea monitoring.

Task 7: Administrative oversight of the Monitoring Station/Sea-floor Observatory Project.

Administration of the Consortium is the responsibility of the University of Mississippi and includes formal Project Proposals to federal funding agencies, Technical Progress Reports, Final Project Reports, informal monthly updates, reports of Consortium meetings, cruise reports, participation in national meetings, organizing meetings between researchers, organizing and participating in program reviews, organizing and participating in research activities, including research cruises. For this reporting period, these include:

- Technical semiannual progress report 42877R16 was completed and submitted to DOE during this reporting period as were regular monthly reports documenting progress of subcontractors and the Consortium in general.
- The Gulf of Mexico Hydrates Research Consortium has held several web-conferences regarding the OBS experiment, the possibility of cabling the observatory to land via a platform in the Gulf, and future funding directions and procedures.
- We have continued evaluations of the effects of the DeepWater Horizon disaster. Many Consortium members have been involved in various ways – Rapid Response work, NRDA proposals and work, Northern Gulf Institute proposals and funding, NASA funding and doubtless many more. This work continues into the foreseeable future at our site 10 miles from the Macondo wellhead. We are prepared with additional chemical sensors, historical data and a research reserve.
- Geophysicist Simona Caruso, former MMRI visiting scholar from the University of Rome, la Sapienza, now part of the seismic data collection, processing and interpretation team at Fugro, Aberdeen, presented Fugro's Monthly Technical Meeting via WebConference, August 25, *Innovative approaches to the treatment of data from a hydrate / carbonate mound in the Northern Gulf of Mexico (Mississippi Canyon Block 118)*, to Fugro and selected guest audiences worldwide. Simona is actively engaged in innovative processing and while maintaining her ties with the Consortium has served a very substantial role in interpreting what is happening, physically, at MC118.
- Leonardo Macelloni and Martina Pierdominico traveled to Lafayette, LA to meet with C&C Technology, September 13-17, 2010. The purpose of the meeting was to discuss multi-beam processing methods in general and to attempt to correct navigation inconsistencies in data collected by the Eagle Ray AUV. The

mapping capabilities of the MMRI/CMRET/STRC team continue to improve and to attract the attention of geoscientists worldwide.

- STRC hosted Peer Fietzek, Director of R&D for Contros GmbH of Kiel, Germany, September 22, 2010. Dr Fietzek made a power point presentation to STRC staff on near-IR methane detectors and then spent ample time (extending into the evening hours) facilitating the analysis and interpretation of several seacasts worth of data collected in June, 2010 at MC118.
- UM Consortium members Carol Lutken and Leonardo Macelloni attended the Annual Meeting of the Gulf Coast Association of Geological Societies in San Antonio Texas October 10-12 where they presented the poster, *Spatial distribution of seafloor bio-geological and geochemical processes as proxy to evaluate fluid-flux regime and time evolution of a complex carbonate/hydrates mound, northern Gulf of Mexico* the summary of their GCAGS paper, co-authored with Consortium members Simona Caruso, Charlotte Brunner, Laura Lapham and Allen Lowrie, that was chosen to receive the Second Place GCSSEPM / GCAGS Grover E. Murray Best Published Paper Award as one of the most outstanding papers published in this year's *GCAGS Transactions*.
- The STRC shop has successfully designed and constructed a new deployment and recovery device referred to as the ROVARD (ROV Assisted Recovery Device). The device was designed to make the deployment of the Chimney Sampler Array possible. It debuted during a research cruise on the R/V *Pelican* to MC118, September 9-14. We have received no less than 4 additional requests for application of this method to seafloor deployments.
- An extensive (ten-hour) reconnaissance mission with the Station Service Device ROV was conducted to investigate the 2nd Pour Fluid Array (PFA-2), which was located for *the first time* and evaluated for recovery of the sampler package. Push cores were also recovered from the site, via the SSD.
- The SSD was used to survey possible deployment sites for the CSA and collected additional push-cores from several possible locations.
- The SSD was used to investigate the habitats along an active fault scarp, and to collect push cores and oil/water slurpers of sediment and oil samples for microbial and chemical analysis.
- The CSA, a geochemical component of the Seafloor Observatory, was deployed for the first time at MC118, in September, 2010.
- A series of seacasts was made with the Pelican's rosette on which the CTD was enhanced with the Gandhi sensor package (Gandhi is an enhanced CTD package intended for real-time chemical surveys on the ROV and includes several additional sensors - most notably a METS methane sensor).
- The Mola Mola photo-AUV was taken to further its engineering tests and improve its navigation.
- The new launch and recovery technique for the SSD – replacing the midwater weight (anchor) with weights attached to the cable – worked famously, though in calm seas.
- A second September cruise to MC118, aboard the R/V *Pelican*, was accomplished September 26 – October 1, 2010. The Benthic Boundary Layer Array was successfully deployed for its second multi-month deployment. A

Contros sensor was added to the array for direct methane measurements to augment the Aquatrack, CDOM, and Chyl-a fluorometers and the CTD, O2 and ORP/pH sensors.

- The SSD vehicle dove on the ROVARD to verify its location on the seafloor as well as its position and orientation. The SSD was then used to remove one of the chimneys from the lander for greater spatial separation between the two chimneys. The Peepers, which were also deployed on the ROVARD, were observed to have been properly installed to the correct depth below the surface.
- The SSD was transferred to the MMRI shop in full operational.
- The MMRI hosted the fall meeting of the Consortium at the Conference Center facilities at the Inn at Ole Miss, October 26-27, 2010. The 55 attendees presented/viewed research accomplishments on Tuesday and spent Wednesday morning discussing directions for the future. Wednesday afternoon was devoted to Oil Spill response work. The meeting was recorded and webinar provided for participants who could not attend, physically.
- Subsamples of 6 push-cores recovered from Woolsey Mound in September have been analyzed, in part. All were found to be “oily” and in particular, contain anomalously high concentrations of the highly toxic PAHs (poly-aromatic hydrocarbons). Additional chemical analyses continue in an effort to identify source information for these toxins.
- Visiting scholar, Michela Ingrassia was able to participate in the BOEMRE and NOAA-sponsored *Lophelia* II cruise in the northern Gulf in October-November. Thanks to Michela’s efforts, Woolsey Mound was added to the cruise’s list of dive sites. PI Chuck Fisher reported the highest diversity of benthic fauna of all sites they visited and installed permanent markers for use in future documentation of change at the site.
- The opportunity to participate in a TDI Brooks’ November Jumbo Piston Coring cruise came up in mid-November. We contacted the geology-geophysics groups for suggested targets and justifications and they fired back their JPC wish-lists with lightning speed. Justifications from industry seismic data, high resolution chirp and surface-source-deep-receiver data, resistivity data (from our June 2009 resistivity survey), previous core data and previous findings of the geochemical and microbial biology groups were all used in selecting targets. Prioritization of coring locations are based on the importance of maximum core penetration (64ft, or ~20m), likelihood of penetrating the high frequency scatter zone suspected of being indicative of hydrates in the shallow subsurface, the potential to ground-truth shallow seismic data already collected at MC118, and the potential to constrain lithologic, paleontologic and stratigraphic parameters at the observatory site. Although the cruise was postponed until January, we are prepared with target sites for this coring effort and are also prepared to send geologists and geochemists to assist in and advise on the sample-collecting efforts.
- A new 12 second seismic dataset has been acquired from Western Geco and, following analyses will provide a time dimension to the subsurface analyses of the block. Integration of these industry data sets with the high resolution SSDR and chirp is providing amazing insights into the shallow subsurface geology and structure as well as the seafloor at MC118. This information is critically important

to the site-selection processes for the Jumbo Piston and heat-flow cruises, to be conducted in 2011.

- As is evident on the updated publications list, many Consortium members made presentations at the Annual meeting of the American Geophysical Union in San Francisco, December 13-17. A special session on the oil spill was led by Consortium members Ray Highsmith and Mandy Joye. Talks by many other members were part of this session.
- A contract has been tendered by WHOI to do the 4C data collection in March-April of 2011 using their nodes and personnel aboard a CMRET chartered vessel. CMRET will provide the source guns and the compressor to effect the survey. Data will be delivered to UT-Austin in SEGY and SEED formats. This task is being rewritten for submission to DOE and all funds previously directed toward collecting the 4C data will be redirected to this effort.
- Additional geochemical instruments have been acquired or constructed and are enabling Consortium researchers to add to the ever-growing store of chemical data relating to Woolsey Mound.
- Work on the model of hydrate stability at MC118 has progressed to the point that the equation of state has been used in simulated runs. The Equation of State has been developed to include the multigas hydrates present as well as their phase behaviors under conditions prevailing at MC118. This includes developing constitutive relations for the gaseous phase for ethane and propane, with profoundly different saturation pressures from methane, indirectly.
- Work by Consortium member, Rudy Rogers at Mississippi State University is the first to report **hydrate inhibition by bacterial cell wall material**. Data were gathered showing this water-insoluble peptidoglycan polymeric compound, to be increasingly effective as an inhibitor by increasing its surface area through cell lysing. A smaller, water-soluble, molecular component of the peptidoglycan polymer was tested and shown to retain hydrate-inhibiting properties. In tests comparing with a methanol standard, this water-soluble, glycan strand performed better in delaying gas hydrate formation (i.e., longer induction times) than similar amounts of methanol, the chemical currently used to inhibit hydrate formation in pipelines.

Task 8. Project Summary Updates:

The website updates are the responsibility of the CMRET. Publications are added to the Consortium list as they appear and a revised list of recent publications accompanies this report.

The Consortium has long expressed a desire/need for a website dedicated to the Consortium work and accomplishments associated with the development of the Seafloor Observatory. Marco D'Emidio, whose expertise is GIS (Geoinformatics Systems) as well as geology, has developed the geological and geophysical pages for the website, including core locations and descriptions, cruise reports, online geophysical data collected by the CMRET, reports of meetings and many maps derived from Consortium effort. Marco is working with MMRI's University of Mississippi's Geoinformatics Systems to get the Consortium's website live and user-friendly.

CONCLUSIONS

This report covers the accomplishments of the ninth six-month period (fifth for the FY08 awards; third for the FY09 awards) of funding of Cooperative agreement Project #DE-FC26-06NT42877, between the Department of Energy and the Center for Marine Resources and Environmental Technology, University of Mississippi. The efforts of the Hydrates Research Consortium are reviewed: cruises to test, deploy and recover instruments have been made, an new industry seismic dataset has been acquired, innovative data processing techniques employed to evaluate seismic datasets, both standard and Consortium-developed, and an improved image of the subsurface structure of the carbonate-hydrate mound at MC118 is emerging. HLA configuration and deployment challenges have been evaluated and a new technique and schedule for HLA deployment has been developed for 2011. June and August cruises have been scheduled to complete this task. New constraints on hydrate formation have been established, multibeam technology used effectively to measure both volume and frequency of bubble plumes at vents, a probe that will measure sound speed in situ at MC118 begun to be built, and a preliminary hydrate 3-gas model completed. Reports have been completed and web and paper updates to various components of the project completed. Manuscripts have been submitted to peer-reviewed journals and additional papers and presentations have resulted from Consortium research efforts. Progress in AUV tasks and in deployment methods has been made. Additional devices and sensors have been acquired and others fabricated. A busy cruise schedule has been established for 2011 that includes AUV surveys, major deployments, additional test deployments and retrieval of instrumentation that remains on the sea-floor. Every effort has been – and will continue to be – made to maximize Consortium members' access to and benefit from the cruises scheduled for 2011. Additional efforts to monitor developments resulting from the vast amounts of hydrocarbons spilled into the seawater at MC252 are ongoing, with Consortium researchers making significant findings/contributions to unraveling that developing predicament.

ACRONYMS AND ABBREVIATIONS

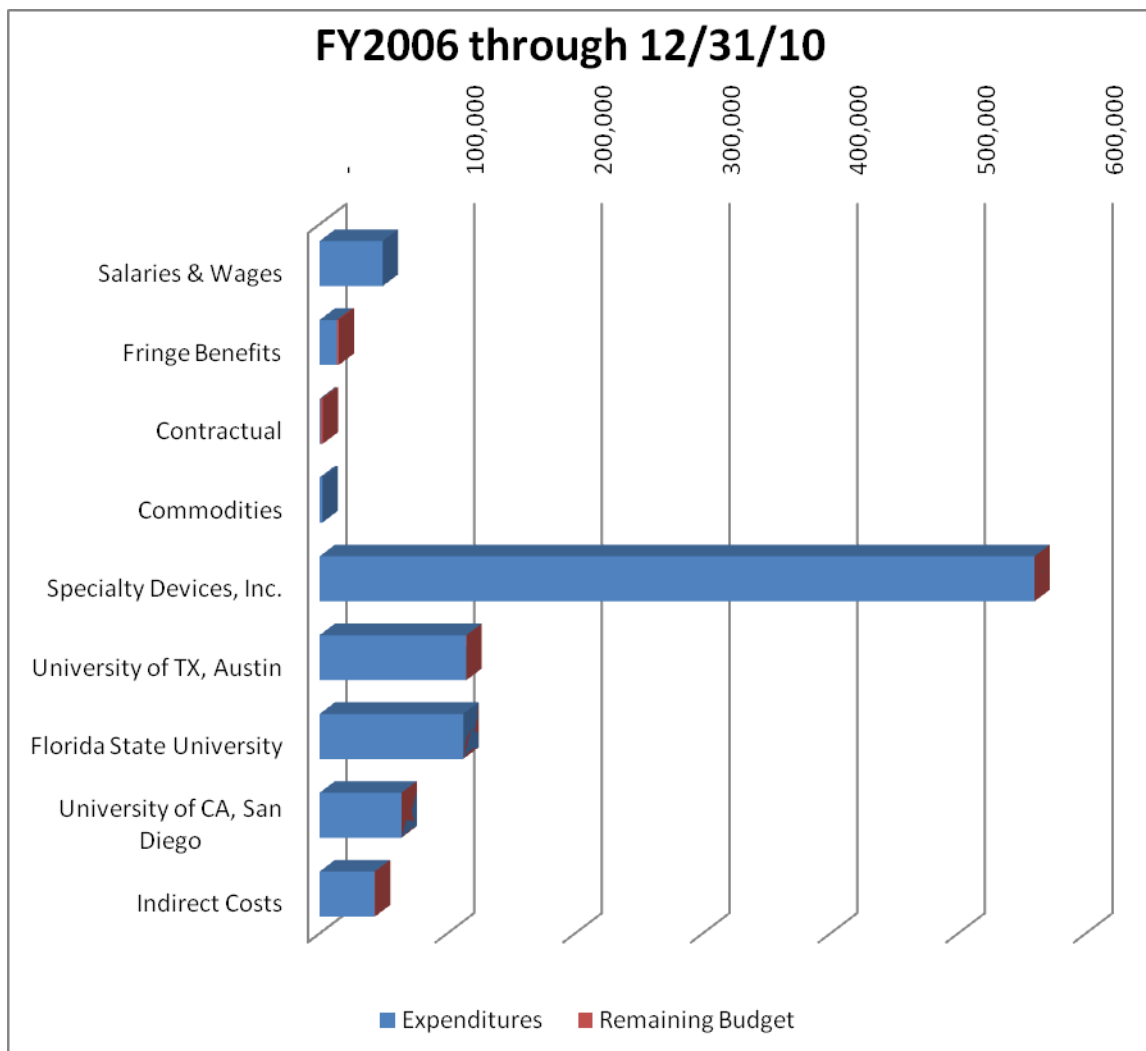
3-D	3-dimensional
4-D	4-dimensional
4-C	four component
ABCMS	Automated Biological Chemical Monitoring System
AGM	Absorption Glass Mat (battery)
AUV	autonomous underwater vehicle
AVO	amplitude vs. offset
BBLA	Benthic Boundary Layer Array
BEG	Bureau of Economic Geology (University of Texas)
BLA	Borehole Line Array
BOEMRE	Bureau of Ocean Energy Management, Regulation, and Enforcement
BSR	bottom-simulating reflector
C&C	Chance and Chance
CDOM	colormetric dissolved organic material

CF	cross-correlation function
CGGVeritas	Compagnie Générale de Géophysique (CGG) and Veritas
CH ₄	methane
CMRET	Center for Marine Resources and Environmental Technology
CMSHYD	stand-alone computer program; Sloan's statistical thermodynamic approach
CSA	Chimney Sampler Array
CTD	Conductivity, Temperature, Depth
DATS	Data Acquisition and Telemetry System
DF	double frequency
DOC	Department of Commerce
DOE	Department of Energy
DOI	Department of the Interior
EGL	Exploration Geophysics Laboratory
EOS	equation-of-state
FY	Fiscal Year
G	shear modulus
GHSZ	Gas Hydrate Stability Zone
GIS	Geoinformatics Systems
GOM	Gulf of Mexico
GOM-HRC	Gulf of Mexico-Hydrates Research Consortium
HLA	horizontal line array
HRC	Hydrates Research Consortium
HSZ	Hydrate Stability Zone
IDP	Integrated Data Power Unit/Interconnection and Data Recovery device
IODP	Integrated Ocean Drilling Program
IP	Internet Protocol
JPC	Jumbo Piston Core/Coring
LUMCON	Louisiana Marine Consortium
MC	Mississippi Canyon
MeOH	Methanol
MIMS	membrane introduction mass spectrometer
MMRI	Mississippi Mineral Resources Institute
MMS	Minerals Management Service
uM	micromolar
MPa	Mega-pascal
MS/SFO	monitoring station/sea-floor observatory
NAGA	N-acetylglucosamine
NB	Nutrient broth
NETL	National Energy Technology Laboratory
NIUST	National Institute for Undersea Science and Technology
NOAA	National Oceanographic and Atmospheric Administration
NRL	Navy Research Laboratory
NURP	National Undersea Research Program
OBS	ocean bottom seismometer
OER	Ocean Exploration and Research

<i>P</i> -wave	compressional wave/pressure wave
P_{eq} ,	equilibrium pressure
PFA (=PCA)	pore-fluid array
PVT	pressure-volume-temperature
ROSSCAN	rotating multibeam sonar scanner
ROV	remotely operated vehicle
ROVARD	ROV Assisted Recovery Device
R/V	Research Vessel
SAIC	Science Applications International Corporation
SDI	Specialty Devices, Inc.
SFO	Sea Floor Observatory
SFP	Sea Floor Probe
SRI	SRI, International
SSD	Station Service Device
SS/DR	Surface-Source Deep Receiver
SSVP	Shallow Sediment Velocity Probe
STAR	SAIC's multidimensional simulator
STAR/HYDCH4	constitutive description
strI	structure I (hydrate)
strII	Structure II (hydrate)
STRC	Seabed Technology Research Center
TA	thermistor array
TGS-NOPEC	geophysical data (2-D, 3-D) acquisition company
THROBS	SAIC's hydrate simulator
TSS	dynamic motion sensor
UCSB	University of California, Santa Barbara
UGA	University of Georgia
UMS	underwater mass spectrometer
USBL	ultra-short baseline navigation system
USB	Universal Serial Bus
USC	University of South Carolina
USF	University of South Florida
USGS	United States Geological Survey
VLA	vertical line array
WesternGeco	Western Geophysical Company
WHOI	Woods Hole Oceanographic Institution
ρ	gaseous-phase mass density

COST STATUS

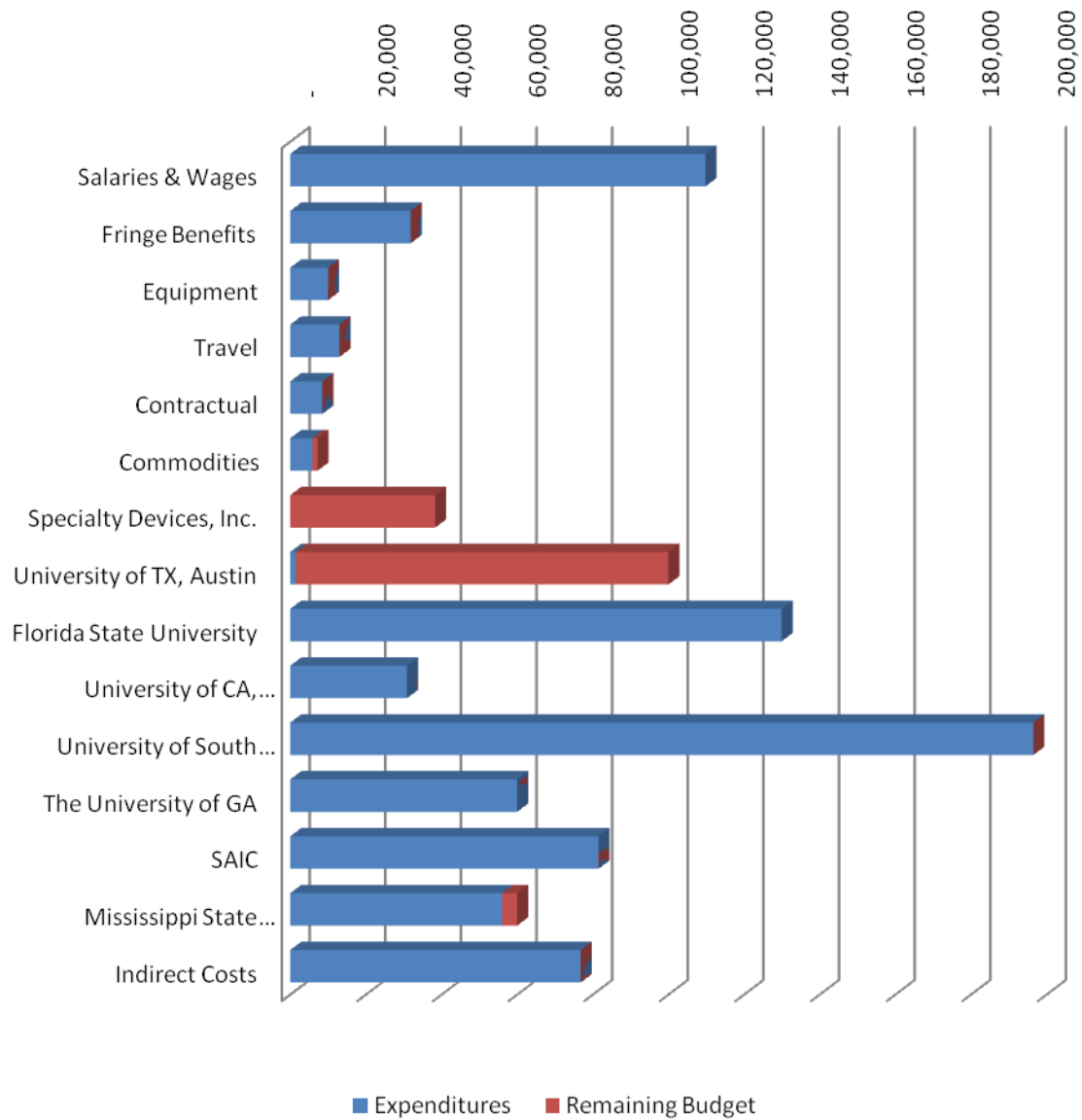
As can be seen in the figures and tables that follow, Phase 1 (FY06) funds are essentially spent. Funds are essentially intact for the Phase 2 (FY08) 4C experiment. These will be transferred to the WHOI subcontract when the change of work is completed. Funds for the speed-of-sound probe will be drawn upon completion of the deployment of the HLAs. Subcontracts for Phase 3 (FY09) are well underway and the subcontracts for Phase 4 (FY10) have just recently been signed so invoicing on them will begin soon..



Mississippi Mineral Resources Institute
DOE DE-FC26-
06NT42877
Funding Status as of 12/31/2010

FY2006	Expenditures	Remaining Budget
Salaries & Wages	49,309	(229)
Fringe Benefits	13,471	1,646
Contractual	1,026	1,474
Commodities	2,176	(2,176)
Specialty Devices, Inc.	559,912	-
University of TX, Austin	114,979	21
Florida State University	112,520	-
University of CA, San Diego	64,113	-
Indirect Costs	43,155	187
Total	960,661	923

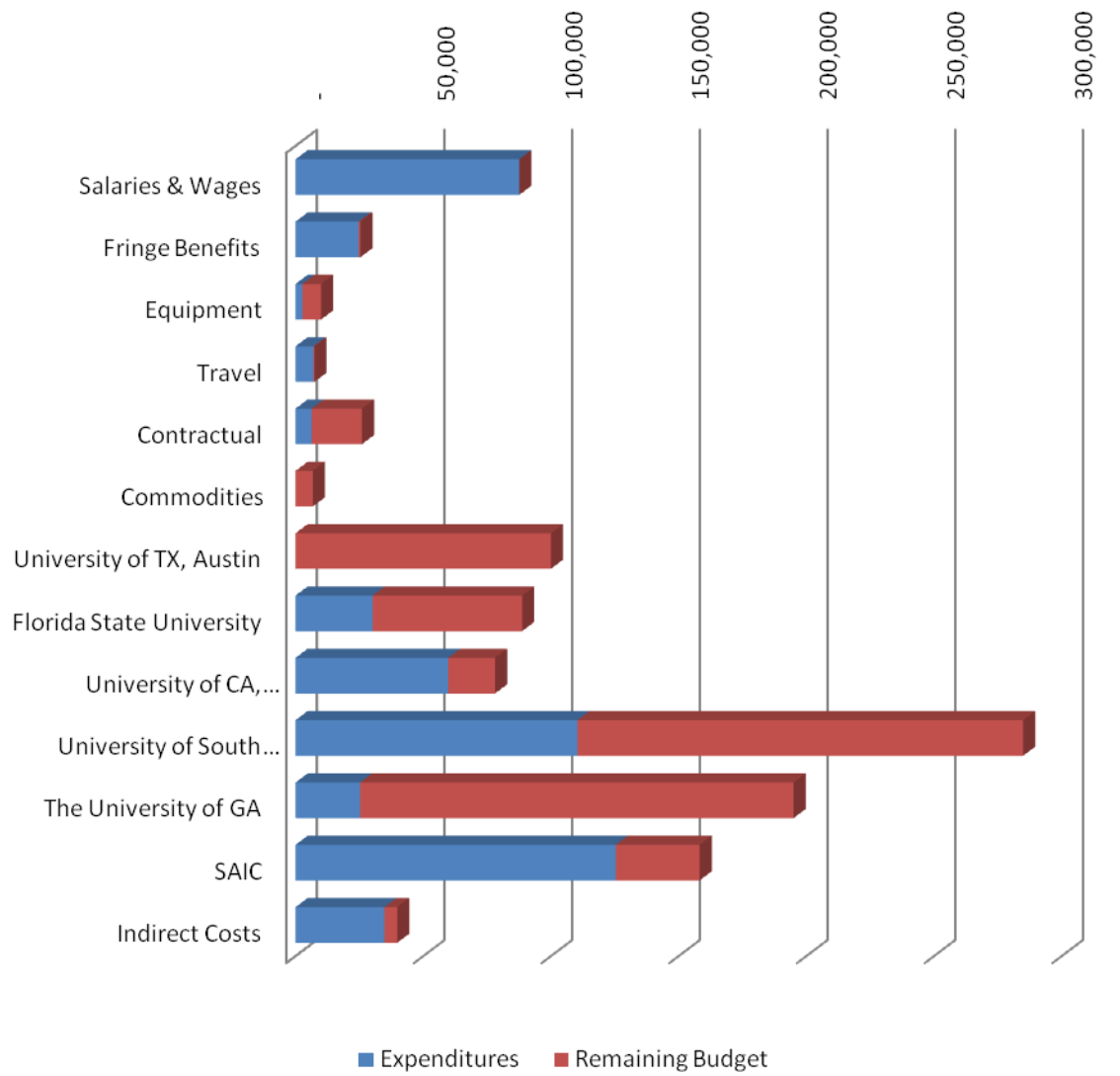
FY2008 through 12/31/10



**Mississippi Mineral Resources Institute
DOE DE-FC26-06NT42877
Funding Status as of
12/31/2010**

FY2008	Expenditures	Remaining Budget
Salaries & Wages	109,809	-
Fringe Benefits	31,845	-
Equipment	10,000	-
Travel	13,000	-
Contractual	8,500	-
Commodities	5,827	1,388
Specialty Devices, Inc.	-	38,336
University of TX, Austin	1,445	98,555
Florida State University	129,972	-
University of CA, Santa Barbara	30,881	-
University of South Carolina	196,517	-
The University of GA	60,000	-
SAIC	81,527	-
Mississippi State University	56,070	3,932
Indirect Costs	76,796	-
Total	812,189	142,211

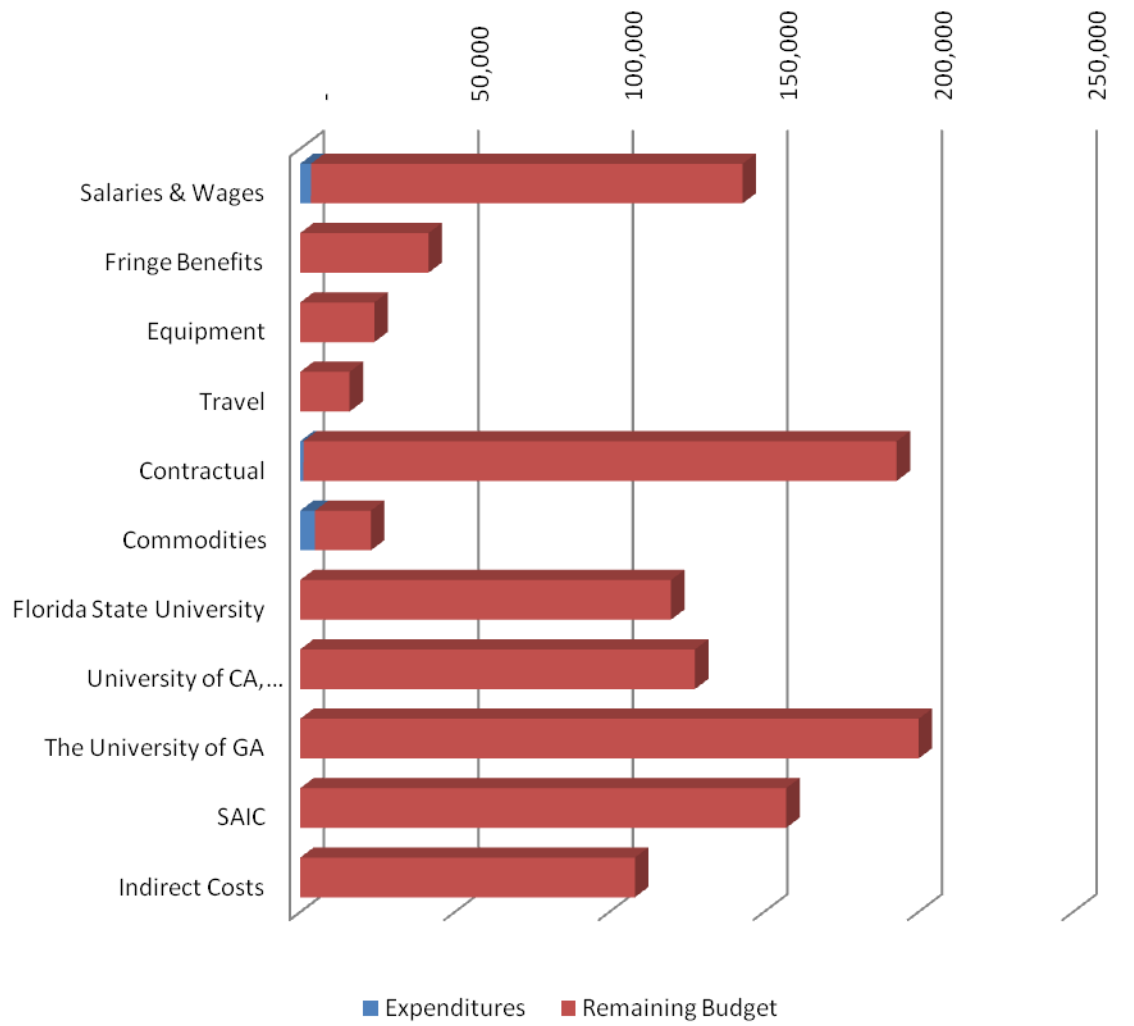
FY2009 through 12/31/10



Mississippi Mineral Resources Institute
DOE DE-FC26-06NT42877
Funding Status as of
12/31/2010

FY2009	Expenditures	Remaining Budget
Salaries & Wages	87,602	-
Fringe Benefits	24,712	693
Equipment	2,692	7,308
Travel	7,082	318
Contractual	6,306	19,694
Commodities	-	6,767
University of TX, Austin	-	100,001
Florida State University	30,186	58,539
University of CA, Santa Barbara	59,796	18,322
University of South Carolina	110,419	174,481
The University of GA	25,261	169,768
SAIC	125,363	32,889
Indirect Costs	34,753	5,072
Total	514,172	593,852

FY2010 through 12/31/10



**Mississippi Mineral Resources Institute
DOE DE-FC26-06NT42877
Funding Status as of
12/31/2010**

FY2010	Expenditures	Remaining Budget
Salaries & Wages	3,486	139,665
Fringe Benefits	-	41,514
Equipment	-	24,000
Travel	-	16,000
Contractual	1,100	191,902
Commodities	4,819	18,099
Florida State University	-	119,981
University of CA, Santa Barbara	-	127,743
The University of GA	-	200,121
SAIC	-	157,259
Indirect Costs	-	108,311
Total	9,405	1,144,595

MILESTONE STATUS

Milestones identified in the Project Management Plan are discussed below and related to their status.

Milestone 1: Complete the baseline characterization of the subsurface at the Observatory site, MC118 for presentation to the panelists at the DOE Merit Review. Complete Seismic Analysis of data from MC118 including defining features that relate to the occurrence of gas hydrates.

Baseline character of the Observatory site at MC118, as revealed in several seismic data sets is continuing to be expanded and refined. TGS-Nopec industry standard data, high resolution data (chirp-sonar and surface-source-deep-receiver) have been tied together and referenced to the ARCO well in the block. However, expansion of the site characterization, including a time element, is moving forward with the analysis of additional industry standard data from WesternGeco. Chemical surveying has added valuable information to the site baseline characterization. The polarity-preserving chirp system has been received and is being installed on the NIUST AUV for survey work at MC118, simultaneously with the debugging and adjustments to the accompanying software. The photo-AUV, Mola Mola is scheduled to survey MC118 in July, 2011.

Milestone 2: Recover instruments from the seafloor and analyze data for baseline geochemistry and microbiology for the model (Task 9).

Most instruments have been recovered from the seafloor at MC118, data recovered and mostly analyzed. However, some instruments remain on the seafloor even after several efforts to retrieve them. Additional attempts to recover instruments – primarily the PFA-2 - are scheduled for 2011.

Milestone 3: Deploy horizontal line arrays, connect them to the data recovery system and collect test data from the data-logger. All components of the deployment have been tested successfully. Deployment cruises for this task failed to get the job done. Two cruises are scheduled for June and August to maximize prospects for good weather and a 2-vessel deployment option added to the schedule. All four arrays are ready for deployment but will likely be deployed in installments as deck-space and maneuvering have turned out to be even more challenging than anticipated.

Milestone 4: Complete installation of all Observatory components and collect geophysical data for input into model (Task 9). Due to deployment logistics, this milestone will necessarily follow the deployment of the horizontal arrays and collection of geochemical sensors. However, time-series pore-fluid, JPC and heat-flow data will be incorporated at the earliest opportunity.

Milestone 5: Complete additional surveys – SSSR, Mass spectrometer (STRC-funded), multibeam (NIUST-funded) to provide important updated baseline seismic data prior to the commencement of true monitoring. The multibeam and mass spectrometer surveys are complete. We will be getting a complementary update in the multibeam as C&C will use our 2005 survey to calibrate a new AUV they are testing for the Navy. The hydrophone array – necessary for the SSSR survey with the AUV-borne receiver - is in Phase 2 of development by NOAA and is due for testing.

Milestone 6: Complete 4C survey and analyze data for new software: This plan to achieve this milestone has necessarily changed. WHOI has offered a contract to collect the 4C data with their ocean bottom seismometers from a CMRET-chartered vessel and CMRET source-guns.

Milestone 7: Establish a “final” model of the observatory site, from which changes can be determined and monitoring established. The initial phases of the modeling effort are complete. A confidential report of the integration of the equation of state into the SAIC model will soon arrive at NETL. Real data are now being incorporated into the final model.

New Milestones – and status - from FY10 Program Management Plan

Milestone 5: Collect and evaluate giant piston cores from the MC118 Sea Floor Observatory. This Phase 4 milestone is tied to Task 2 and is estimated to be complete in June, 2011. This task is scheduled for early 2011.

Milestone 6: Collect heat-flow data from MC118. This Phase 4 milestone is tied to tasks 2 and 3 and is estimated to be complete by August, 2011. This task depends on TDI’s schedule. We will piggy-back on a heat-flow cruise.

Milestone 7: Collect and evaluate additional gravity cores to complete sedimentation model, support geochemical and geophysical (structural) characterization of MC118. This Phase 4 milestone is tied to Tasks 2, 3 and 4 and is estimated to be complete by June, 2011. This task is the primary mission of an 11-day April cruise

Milestone 8: Integrate geophysical datasets with geochemical and biological data. This Phase 4 milestone is tied to tasks 2 and 3 and is estimated to be complete by October, 2011. This task is in progress and results thus far have contributed significantly to numerous evaluations of MC118, most significantly the selection of sites for both the JPC and heat-flow cruises as well as our gravity coring cruise.

Milestone 9: Purchase and learn to operate an Infrared camera for the purpose of distinguishing hydrates in unopened cores. This Phase 4 milestone is tied to tasks 2 and is estimated to be complete by April, 2011. This camera has been ordered and will, be available for use on the coring cruises, helping to determine which sections do and do not contain hydrate.

Milestone 10: Collect and analyze hydrate and “slime”(= protective ? biofilm) at hydrate outcrops in an effort to explain the existence and persistence of hydrate in seawater undersaturated for methane. This Phase 4 milestone is tied to tasks 2 and 4 and is estimated to be complete by September, 2011. We will attempt this on any cruise with ROV capabilities.

Milestone 11: Recover additional pore-fluid time-series via additional instrument (PFAs, osmolander, peepers) deployments and recoveries. This Phase 4 milestone is tied to task 4 and is estimated to be complete by October, 2011. We have deployed several systems of pore-fluid collection and hope to collect peepers in April and the PFA-2 in August.

Milestone 12: Deploy the ABCMS lander in upgraded configuration including

video, lights reduced-size mass spectrometer, and altimeter. This Phase 4 milestone is tied to task 5 and is estimated to be complete by October, 2011. August and October cruises are scheduled to deploy this upgraded system.

ACCOMPLISHMENTS

Major accomplishments of this reporting period include:

- Identification of a chemical hydrate formation inhibitor produced in microbes' cell walls
- Advances in mapping capabilities
- Detailed plan for jumbo piston coring at Woolsey Mound
- Numerous well-received presentations at national meetings
- Successful proof of concepts and recovery of data in support of CH₄ plumes in the water-column near MC118
- Successful recovery of targeted push-cores with the SSD
- Establishment/renewal of important collaborations (Penn State University, Contros, WHOI's OBS group)
- Successful tests and repeat performances of additional functions of the SSD (push-cores, surveying)
- Deployments: peepers, CSA, BBLA
- Innovative deployment method – ROVARD – proven
- New launch and recovery technique for the SSD – replacing the midwater weight (anchor) with weights attached to the cable – proven
- Recovery of geochemical data and sediment samples from the near-seabed and shallow seabed
- Successful at-sea tests of the *Mola Mola* AUV
- Coordination of multiple methods of water-column chemical evaluation
- High-Definition stills and video from MC118
- SSD transferred to MMRI/CMRET/STRC shop

PROBLEMS/DELAYS

The majority of delays in the program derive from one of two sources, or a combination of the two: weather and electronics at 900m water depth. In addition, the Deep Water Horizon spill has complicated our work and hijacked significant portions of our resources – both time and personnel. Ship time remains difficult to schedule but we have 5 Pelican cruises scheduled and hope to participate in at least two TDI-Brooks cruises and as many ROV cruises as possible. The deployment of the HLAs has been rescheduled but the projects that are depending upon this critical achievement remain in “stand-by” mode. The ROVARD has been designed, built and employed in an effort to alleviate some of the back-log. Researchers are working with other or synthetic data until data can be recovered from the HLAs and, in the case of UT-Austin, have nearly all funds remaining to do the work when the data do become available.

Weather dictates cruise scheduling and successes. Although extra cruises have been scheduled for 2011, weather conditions cannot ever be predicted and we face similar delays in the future.

Electronics at depth will always be challenging. The SDI/CMRET team continues to work diligently to overcome many but anticipate additional difficulties in the future as part of working in extremely challenging environments.

PRODUCTS

Important products of this reporting period are:

1. Western Geco dataset and beginning analyses
2. Additional modeling
3. Cruise accomplishments and deployments
4. Progress Report from January – June, 2010
5. Publications and presentations at national meetings
6. Discovery of hydrate inhibitor in microbial cell walls
7. Rovard deployment system
8. Improved surveying and sampling capabilities of the SSD

REFERENCES

References for individual reports follow the appropriate section directly.

RECENT PUBLICATIONS BY CONSORTIUM MEMBERS:

2010:

Bell, R. J., S. K. Toler, R. T. Short, In Situ Chemical Analyses by Underwater Mass Spectrometry (oral), Goldschmidt Conference on Earth, Energy and the Environment in Knoxville, TN (2010).

Bowles, M.W., and S.B. Joye, 2010. High rates of denitrification and nitrate consumption in cold seep sediments. *The ISME Journal*, doi:10.1038/ismej.2010.134.

Bowles, M.W., V. A. Samarkin, K. L. M. Bowles, and S.B. Joye, 2010. Weak coupling between sulfate reduction and the anaerobic oxidation of methane in methane-rich seafloor sediments in *ex situ* incubations. *Geochimica et Cosmochimica Acta*, doi:10.1016/j.gca.2010.09.043.

Bowles, M.W., V.A. Samarkin, and S.B. Joye. Pressure regulation of microbial methane cycling in deep-sea sediments. Goldschmidt 2010 Conference, Knoxville, TN, June.

*Camilli, R.; Bowen, A.; Farr, N., 2010, "Bright Blue: Advanced Technologies for Marine Environmental Monitoring and Offshore Energy" Oceans 2010. pp 1-7.

Chapman, Ross, Mike Morley, Erika Geresi, Tom McGee, Paul Higley, *Characterizing the gas hydrate stability zone using a vertical hydrophone array*, *The Leading Edge*, October 2010, p. 800-804.

Constable S, and Weitemeyer, K., 2009: Applying marine EM methods to gas hydrate mapping, *MARELEC Meeting*, Stockholm, Sweden - July 7-9 2009

Diercks, A.R., V.L. Asper, R. Highsmith, M. Woolsey, S. Lohrenz, K. McLetchie, A. Gossett, M. Lowe, D. Joung, L. McKay, S. Joye, and A. Teske, 2010. The NIUST Deepwater Horizon Oil Spill Response Cruise. OCEANS 10 MTS/IEE Conference, Seattle.

Ingram, W.C., Meyers, S.R., **Brunner, C.A.**, and Martins, C.S., 2010, Evaluation of Late Pleistocene-Holocene sedimentation surrounding an active seafloor gas hydrate and cold seep field on the Northern Gulf of Mexico Slope, *Marine Geology*, v. 278, no. 104, p. 43-53.

Innman, A., Easson, G., Asper, V. L., and Diercks, A. -R., 2010, *The Effectiveness of Using MODIS Products to Map Sea Surface Oil*, OCEANS 2010 MTS/IEEE Seattle, Sept. 20-23, 2010.

Innman, A., Macelloni, L., Easson, G., and Woolsey, M., 2010, *Incorporating Seafloor Data into GIS*, IEEE OES South American International Symposium, Buenos Aires, Argentina, April 12-16, 2010.

Joye, S.B., A. Diercks, A. Teske, and D. Valentine, 2010. Open ocean impacts of the BP Oil Well Blowout. American Geophysical Union, Fall Meeting, AGU, San Francisco, Calif., 13-17 Dec.

Knapp, James H., Camelia C. Knapp, Leonardo Macelloni, Antonello Simonetti, Carol Lutken, 2010, *Subsurface Structure and Stratigraphy of a Transient, Fault-Controlled Thermogenic Hydrate System at MC-118, Gulf of Mexico* AAPG 2010 Annual Convention Oral Presentation, Abstracts Volume, p.134.

Knapp, Camelia C., James H., Knapp, Adrian Addison, Leonardo Macelloni, Michael Waddell, 2010, *Geophysical Baseline Characterization of Subsurface Gas Hydrates at MC-118, Gulf of Mexico*, AAPG 2010 Annual Convention Poster Presentation, Abstracts Volume, p.134.

* Lapham, Laura L., Jeffrey P. Chanton, Ross Chapman, Christopher S. Martens, 2010, *Methane under-saturated fluids in deep-sea sediments: Implications for gas hydrate stability and rates of dissolution*, Earth and Planetary Science Letters (2010), 298 275-285. doi:[10.1016/j.epsl.2010.07.016](https://doi.org/10.1016/j.epsl.2010.07.016)

Lapham, L. R. Wilson, C. Paull, J. Chanton and M. Riedel. Measuring *in situ* dissolved methane concentrations in gas hydrate-rich systems Part 1: Investigating the correlation between tectonics and methane release from sediments. , presented at 2010 Fall Meeting, AGU, San Francisco, Calif., 13-17 Dec.

Lapham, L. R. Wilson, C. Paull, J. Chanton and M. Riedel. Measuring *in situ* dissolved methane concentrations in gas hydrate-rich systems Part 1: Investigating the correlation between tectonics and methane release from sediments. , presented at 2010 Fall Meeting, AGU, San Francisco, Calif., 13-17 Dec.

*Lloyd, K. G., D. Albert, J. F. Biddle, J. Chanton, O. Pizarro, and A. Teske. 2010. Spatial structure and activity of sedimentary microbial communities underlying a *Beggiatoa* spp. mat in a Gulf of Mexico hydrocarbon seep. *PLoS One*, 5(1): e8738.

*Lloyd, K. G., B. J. MacGregor, and A. Teske. 2010. Quantitative PCR methods for RNA and DNA in marine sediments: Maximizing yield while overcoming inhibition. *FEMS Microbiology Ecology*. 72: 143-151.

Lutken, Carol B., Leonardo Macelloni, Laura Lapham, Simona Caruso, Mariangela Lodi, Richard Camilli, Vernon Asper, Arne Diercks, Camelia Knapp, Jim Knapp, 2010, *Monitoring Seafloor Morpho-Geological Evolution of the MC118 Hydrate/Carbonate Mound via Multiple AUV Missions*, AAPG 2010 Annual Convention Poster Presentation, Abstracts Volume, p.155.

*Macelloni, L., S. Caruso, L. Lapham, C. Lutken, C. Brunner, and A. Lowrie, 2010, *Spatial distribution of seafloor biogeological and geochemical processes as proxy to evaluate fluid-flux regime and time evolution of a complex carbonate/hydrates mound, northern Gulf of Mexico*: Gulf Coast Association of Geological Societies Transactions, v. 60, p. 461-480.

McGee, T., 2010, *Geologic Features Associated with a Carbonate/Hydrate Mound in the Northern Gulf of Mexico: Results of Preliminary Studies*, IEEE Oceanic Engineering Society, US-Argentina International Symposium, Buenos Aires, Argentina, 12-14 April 2010

McGee, T. (2010): Geologic characteristics in the vicinity of the Deepwater Horizon oil spill. In *Proceedings of the US/EU Baltic International Symposium*, keynote presentation to the IEEE/ Oceanic Engineering Society, Riga, Latvia, 24-27 August 2010.

Short R. T., R. J. Bell, S. K. Toler, F. H. W. van Amerom, *Recent Developments and In Situ Measurements of Underwater Mass Spectrometers* (poster), 58th ASMS Conference on Mass Spectrometry and Allied Topics in Salt Lake City, UT (2010).

Short, R. T., R. J. Bell, A. M. Cardenas, A. Chaudhary, S. K. Toler, F. H. W. van Amerom, Miniature Ion Trap Mass Spectrometers and Applications for In Situ Analysis of Seawater (invited oral), Annual meeting of the Center for Analytical Instrumentation Development at Purdue University in West Lafayette, (2010).

Short, R. T., R. J. Bell and S. K Toler, 2010, *In situ characterization of distributions of dissolved gases, volatile organics, and light hydrocarbons using underwater membrane introduction mass spectrometry*, American Chemical Society meeting in Boston, MA, oral presentation, August 24.

Simonetti, Antonello, Leonardo Macelloni, James H. Knapp, Camelia C. Knapp, Carol B. Lutken, 2010, Multiple resolution seismic data integration as a tool for the shallow hydrocarbon plumbing system definition. Examples from Mississippi Canyon Block 118 carbonate-hydrate mound (Gulf of Mexico), Gordon Research Conference on Natural Gas Hydrates,

Colby College, Waterville, Maine, June.

Sleeper, K., Bell, R., Short, T., Chanton, J., Wilson, R. D'Emidio, M., Macelloni, L. (2010), The Detection of Elevated Methane Concentration Indicate The Presence of Deep-Water Plumes Northwest of the DWH Site, Abstract OS21G-05 presented at 2010 Fall Meeting, AGU, San Francisco, Calif., 13-17 Dec.

Terry, D. A.; Knapp, C. C.; Knapp, J. H.; 2010. Comparison of Effective-Medium Models for Marine Gas Hydrate Templates. Poster Presentation at the 2010 American Geophysical Union Fall Meeting, 13-17 December 2010 (Poster OS53A-1361).

Teske, A. 2010. *Sulfate-reducing and methanogenic hydrocarbon-oxidizing microbial communities in the marine environment*. Part 21: Microbial Communities based on hydrocarbons, oils and fats: Natural habitats. Pp. 2203-2223. Handbook of Hydrocarbon Microbiology, Edited by Kenneth Timmis. Springer, DOI 10.1007/978-3-540-77587-4_160.

Wade, T.L., Sweet S.T., Sericano, J.L., Guinasso, N.L. Jr., Lohrenz, S.E., Shiller, A.M., S.B. Joye, Dierks, A.R., Asper, V.L. and Highsmith, R.C. . 2010 Documentation of Sub-Surface Oil Plume by Analyses of Toxic PAH in Water Samples from the Deep Water Horizon Oil Spill. SETAC 31th Annual Meeting, November 7-11, 2010, Portland OR.

Weitemeyer, K., and S. Constable, 2010: Mapping shallow seafloor structure with marine CSEM, examples from the Gulf of Mexico gas hydrate experiment. *First Break*. **6** (28), 97-102.

*Weitemeyer, K., G. Gao, S. Constable, and D. Alumbaugh, 2010. The practical application of 2D inversion to marine controlled source electromagnetic data. *Geophysics*, 75(6), doi:10.1190/1.3506004

Weitemeyer, K., and S. Constable, 2010: Preliminary results from the Gulf of Mexico gas hydrate CSEM experiment. *Fire in the Ice Spring 2010*. Methane Hydrate Newsletter US Department of Energy Office of Fossil Energy National Energy Technology Laboratory. p 13-17. http://www.netl.doe.gov/technologies/oil-gas/publications/Hydrates/Newsletter/MHNews_2010_03.pdf

Weitemeyer, K. and S. Constable, 2010: Mapping gas hydrates and shallow sedimentary structure in the Gulf of Mexico using marine controlled source electromagnetics, *20th International Workshop on EM Induction in The Earth*, Giza, Egypt - Sept 18-24 2010.

Wilson, R M., L. L. Lapham, M. Riedel, and J. P. Chanton. Measuring In situ Dissolved Methane Concentrations in Gas Hydrate-Rich Systems. Part 2: Investigating Mechanisms Controlling Hydrate Dissolution. presented at 2010 Fall Meeting, AGU, San Francisco, Calif., 13-17 Dec.

Wood, W. T.; Knapp, C. A.; Knapp, J. H.; 2010. Constraints on Methane and Methane Hydrate Distribution at a Gulf of Mexico Seep Using Waveform Inversion of Seismic Data. Oral Presentation at the 2010 American Geophysical Union Fall Meeting, 13-17 December 2010 (Paper OS44A-04).

Yao, H, P Gouedard, P Gerstoff, J McGuire, J A Collins, R van der Hilst, Analysis of fundamental and higher mode surface waves from noise correlation near Eastern Pacific Rise, AGU fall meeting 2010.

*Zhang, Jian, Peter Gerstoff, and Peter D. Bromirski (2010), Pelagic and coastal sources of P-wave microseisms: Generation under tropical cyclones, *Geophys. Res. Lett.*, 37, L15301, doi:10.1029/2010GL044288.

Zhang, Jian, Peter Gerstoff, Peter M. Shearer (2010), Resolving P-wave travel-time anomalies using seismic array observations of oceanic storms, *Earth and Planetary Science Letters*, 292, 419-427, doi:10.1016/j.epsl.2010.02.014.

Zhang, J., P. Gerstoff, P. M. Shearer, P. D. Bromirski, H. Yao, 2010, Imaging Earth Structure and Microseism Sources Using Seismic Array Observations of Oceanic Storms, AGU fall meeting, 2010.

In Press:

*Battista, B. M., L. Macelloni, Camelia C. Knapp, and T. McGee, A Band-Modulated Empirical Mode Decomposition Operator for use with High-Resolution Seismic Reflection Data, *IEEE Transactions on Geoscience and Remote Sensing (in review)*.

*Dearman, J., W. Wilson, R. Rogers, and G. Zhang, 2009, Gas hydrate promotion by smectite-bioproduction interactions, *Marine Chemistry*, accepted for publication and in press.

*Ingram, W.C, Meyers, S.M., Brunner, C., and Martens, C.S. Late Pleistocene-Holocene sedimentation surrounding an active seafloor gas hydrate and cold seep field on the Northern Gulf of Mexico Slope.

*Luzinova, Y, G. T. Dobbs, L. Lapham, J. Chanton, B. Mizaikoff. Detection of cold seep derived authigenic carbonates with

infrared spectroscopy. *Marine Chemistry*, in press.

In Review:

Bowles, M.W., Samarkin, V.A., and Joye, S.B. Geochemistry, microbial activity, and microbial community composition in gas and oil-rich sediments from the Northern Gulf of Mexico. *Geochimica et Cosmochimica Acta* (in review)

Camilli, R., O. Pizarro, J. Whelan "An in-situ chemical observatory characterizing a naturally occurring gas hydrate formation" for submission to *Deep Sea Research* New paper just accepted by IEEE OCEANS

Joye, S.B., V.A. Samarkin and M.W. Bowles (2009) Microbial activity and abundance in "in tact" structure II gas hydrate incubated at in situ temperature and pressure. *Geobiology* (submission planned in July 2009).

Lapham, LL., R. Y, Wilson, B. Anderson, Samantha Joye, Ian MacDonald, J. P. Chanton, Towards understanding processes controlling naturally forming gas hydrate through both *in situ* and laboratory experiments. *Geochim. Cosmochim Acta*, in preparation.

Leifer, I., and D. Culling (2009), Formation of seep bubble plumes in the Coal Oil Point seep field, *Geo-Marine Letters*, submitted.

Leifer, I., et al. (2009), Geologic control of natural marine seep hydrocarbon emissions, Coal Oil Point seep field, California, *Geo-Marine Letters*, submitted.

Leifer, I., et al. (2009 (in prep)), Spatial and temporal variations in marine seep field emissions on diurnal to decadal time scales and decameter to kilometer length scales, *Geochemistry, Geophysics, Geosystems*.

National Energy Technology Laboratory

626 Cochrans Mill Road
P.O. Box 10940
Pittsburgh, PA 15236-0940

3610 Collins Ferry Road
P.O. Box 880
Morgantown, WV 26507-0880

One West Third Street, Suite 1400
Tulsa, OK 74103-3519

1450 Queen Avenue SW
Albany, OR 97321-2198

2175 University Ave. South
Suite 201
Fairbanks, AK 99709

Visit the NETL website at:
www.netl.doe.gov

Customer Service:
1-800-553-7681

